DEPARTAMENTO DE CIÊNCIAS DA VIDA

FACULDADE DE CIÊNCIAS E TECNOLOGIA
UNIVERSIDADE DE COIMBRA

Validation of Tau aggregation model in HEK cells and cortical rat neurons

Dissertação apresentada à Universidade de Coimbra para cumprimento dos requisitos necessários à obtenção do grau de Mestre em Biologia Celular e Molecular, realizada sob a orientação científica do Doutor Arjan Buist (Janssen Pharmaceutica) e do Doutor Diederik Moechars (Janssen Pharmaceutica

Rita Marisa Gomes Marreiros

2013

The work presented in this thesis resulted from a partnership between the University of Coimbra and Janssen Pharmaceutica NV, Beerse I. All experimental activities were performed at Janssen Pharmaceutica NV, Beerse I, a Johnson & Johnson pharmaceutical research and development facility in Beerse, Belgium.

Beerse, 2013

Acknowledgemets

First, I would first like to express my sincere thanks to everyone who supported me this year, both physically and in thought. For everything I just can say thanks for all the support, teachings, joy and specially for everyone at Janssen for having received me and making me feel like I was at home.

I owe the greatest thanks to the best teacher I could have asked for, even on the days that my English was imperceptible. Thank you Arjan for all the patience with my difficulties in English, for all that you taught me, and for all the advices you gave me, as well as the trust that you had in me. I also want to say thank you for making a difference in the beginning of my scientific career.

This only was possible due to Dieder who gave me the opportunity to belong to this group. Thank you for all the scientific support during this year as well all the enthusiasm in my work.

To all the members of Tau group, thank you for all the scientific support, as well all the help and the availability that you gave me. I would especially like to thank to Kathleen Callaerts for all the support, you were the "Belgian mommy" during this year. I want to say thanks to Ian Charles and James Glasper for all the help with the English. Also to Sara Calafate, for all the help, teaching, support and patience, inside and outside the lab. Thank you for all the great moments you gave me in Belgium, for the weekends, smiles and friendship.

I also want to say thank you to everyone in the neuroscience lab, and I just can say that this lab is a fantastic place to work, and that sometimes I felt I was in Portugal.

Professor Carlos Duarte, and Professor Emilia Duarte, thank you for the fantastic first year of Master and thank you for believing and making me believe that I was able to go to Belgium. I must not forget a thank you to all the professors that in some way contributed to my academic training and personal growing, and gave me my love and knowledge for science.

André, Beli and Sofia thanks a lot for the support, the smiles, for everything. During this year we were liked brothers with all that it implies. Without you guys, this year would not have been the same! For all Janssen students, thanks for all the dinners, all the nights and all the Belgium beers. Thank you for everything!

I appreciate all the support of my friends, being away or standing with me, that fill my life with interesting experiences and enriching moments that contribute to who I am.

I want to say a special thanks to André for everything, for all the emotional support, all the scientific discussions, as well as all the help with my English limitations. Thanks a lot for what you are to me, for their unconditional support and constant companionship!

Gostaria de finalizar com um enorme agradecimento aos meus pais e ao meu irmão, pela forma incansável como apoiam todas as minhas decisões, deixando-me sempre toma-las livremente, bem como por todo o carinho e compressão nas alturas mais difíceis.

Resumo

A proteína Tau esta envolvida no assembly e na estabilização dos microtúbulos (MT) contribuindo para a normal função destes. Alterações na quantidade e na estrutura da Tau, como é o caso da hiperfosforilação, desencadeiam a libertação da Tau que medeia a estabilização dos MT, levando ao sequestro desta, formando agregados. Este processo pode estar envolvido em muitas doenças neurodegenerativas referidas como Tauopatias, como e o caso da doença de Alzheimer. Uma das características mais evidentes da doença de Alzheimer é a formação de tranças neurofibrilares compostas por deposições intracelulares de agregados de Tau hiperfosforilados. Contudo, o mecanismo que está na origem da transformação de Tau solúvel em agregados insolúveis, bem como o mecanismo envolvido na propagação dos agregados, continua sem explicação. Um modelo *in vitro* que reproduza as principais características envolvidas na doença pode ser uma útil ferramenta para estudar as causas e consequências da agregação da Tau.

No presente estudo, foram optimizados dois modelos celulares, um em que foram utilizadas células QBI e outro em que foram utilizados neurónios corticais de rato. As culturas foram expostas a fibrilas pré-agregadas sinteticamente produzidas, a partir de Tau recombinante (K18P301L), que podem recrutar Tau endógena solúvel transformando-a em agregados insolúveis. A vantagem destes modelos é o rápido processo de agregação, uma vez que com o uso das fibrilas o passo limitante, a nucleação, é ultrapassado, e a transformação de Tau de forma monomérica em agregados é acelerada. Foi provado que em culturas neuronais primarias as fibrilas pré-agregadas são absorvidas espontaneamente, não sendo necessário o uso de nenhum reagente de entrega, o que leva a crer que este processo é mediado por endocitose. A indução de agregação endógena através das fibrilas de Tau sintéticas é um processo dependente do tempo de exposição, uma vez que foi detectado um aumento de agregação com um aumento do tempo de exposição às fibrilas, o que representa um ponto de suporte na hipótese de propagação patológica da Tau. No presente estudo foi também descrito que o processo de agregação desencadeado no modelo de agregação neuronal hTauP301L, não é um processo neurotóxico.

Os modelos descritos neste estudo foram utilizados como uma plataforma para testar compostos que têm como finalidade diminuir os níveis de agregação da Tau. Neste estudo, foi também testado um inibidor de Hsp90 que demonstrou um evidente efeito na diminuição da Tau solúvel e insolúvel.

Utilizando os modelos celulares apresentados, no presente estudo foi testado o processo da agregação da Tau em células. Foram desenvolvidos dois ensaios, um ensaio de BRET e um ensaio de *Venus split complementation* para estudar o processo de agregação da Tau no *QBI seeding model*.

Resumidamente, o estudo apresentado tem por objectivo estabelecer uma relevante plataforma que pode ser utilizada para o estudo da patologia da Tau, bem como identificar futuras terapias com base na proteína Tau.

Palavras-chave: Doença de Alzheimer; Tau; Fosforilação; Agregação da Tau; K18P301L; Degradação da Tau

Abstract

Tau protein promotes assembly and stabilization of microtubules (MT), which contributes to proper neuronal function. Alterations in the amount and structure of Tau protein, as hyperphosphorylation, results in detachment from MTs and sequestration into aggregates leading to a loss of Tau-mediated MT stabilization. This process is present in some neurodegenerative disorders referred as Tauopathies, such as Alzheimer Disease (AD). One of the major hallmarks of the AD is the formation of neurofibrillary tangles (NFTs) composed of intracellular deposition of hyperphosphorylated Tau aggregates.

However the mechanisms causal of the conversion of soluble Tau in insoluble Tau aggregates, as well the propagation of Tau aggregates remains inconclusive. An *in vitro* system recapitulating the characteristics of this disease would provide a useful tool to study the causes and consequences of Tau aggregation.

In this study, we optimized two cellular models, in QBI cells and in rat cortical neurons, wherein synthetic pre-aggregated fibrils made from recombinant protein (K18P301L) introduced in cell cultures can recruit soluble endogenous Tau into insoluble fibrillar aggregates. The advantage of these models is a faster aggregation process once the fibrils can overstep the rate limiting nucleation and accelerate the transformation of monomeric Tau into aggregates. We found that pre-aggregated fibrils are spontaneously taken up by primary cortical neurons and that this does not require any delivery reagent. This could mean that the uptake of this material is mediated by endocytosis. The induction of endogenous aggregation by synthetic Tau fibrils is a time-dependent process, since we observed an increase in Tau aggregation with increasing exposure time to fibrils, supporting the hypothesis of propagation of pathological Tau. We also found that the aggregation process triggered in the hTauP301L neuronal aggregation model is not a neurotoxic process to rat cortical neurons.

The models described in this study were used as a platform to test compounds that could potentially decrease the levels of Tau aggregation. In this study an HSP90 inhibitor was test that demonstrated evident effects in decreased of soluble and insoluble Tau.

The cellular models present here, were also used to study Tau aggregation process in life cells. In this study, we developed two assays, a BRET assay and a Venus split complementation assay to study Tau aggregation process in the QBI seeding model.

In summary, we have developed and optimized a platform which can be used to study the pathogenesis of Tauopathies, and indentify new Tau-based therapies.

Keywords: Alzheimer's disease; Tau; Phosphorylation; Tau aggregation; K18P301L; Tau clearance

Index

Abbreviations

17-AAG - 17-N-Allylamino-17-demethoxygeldanamycin

17-DMAG - 17-Dimethyl-amino-ethylamino-17-demethoxygeldanamycin

Aß - ß-Amyloid peptide

ABCA7 - ATP-binding cassette transporter Advanced

AD - Alzheimer's disease

AGE - Glycation end products

AMPA- α-amino-3-hydroxy-5-methyl-4-isoxazolepropionic acid

APH-1 - Anterior Pharynx-defective-1

APOE - Apolipoprotein E

APP - Amyloid precursor protein

ATP- Adenosine triphosphate

AAV6 - Adeno-associated-viral vector serotype 6

BBB - Blood-brain-barrier

BIN1 - Bridging integrator 1

BRET - Bioluminescence resonance energy transfer

BSA - Bovine serum albumin

Bp - Based pairs

C83 - 83-AA C terminal APP fragment

C99 - 99-AA C terminal APP fragment

CAMKII - Calmodulin-dependent protein kinase II

CD2AP- CD2-associated protein

CD33 - Sialic acid binding immunoglobulin-like lectin

CDK5 - Cyclin-dependent kinase 5

CHIP - C-terminus of Hsp70-interacting protein

CLU - Clusterin

CNS – Central Nervous System

CR1 - Complement receptor 1

DAPI - 4', 6-diamidino-2-phenylindole

DIV- Day *in vitro*

DMEM - Dulbecco's modified Eagle's medium -

DNA - Deoxyribonucleic acid

D-PBS - Dulbecco's phosphate-buffered saline -

EOAD - Early-onset AD

EPHA1 - Ephrin receptor A1

EPOD - Epothilone D

ER- Endoplasmic reticulum

FRET – Fluorescence resonance energy transfer

FTDP-17 – Frontotemporal dementia and parkinsonism linked to chromosome 17

FTDL – Frontotemporal lobar degeneration

GA - Geldanamyci

GFP - Green fluorescence protein

GOF - Gain-of-function

GSK3ß - Glycogen synthase kinase

HBSS - Hank's Balanced Salt Solution

HIP - Hsp70-interacting protein

HOP - Hsp70/Hsp90 organizing protein

Hsp - Heat-shock-protein

Hsp70 - Heat-shock-protein 70

Hsp90 - Heat-shock-protein 90

HSF1 - Heat-shock-transcription factor 1

HSR - Heat-shock response

hTauP301L – Human full-length Tau containing P301L mutation

hTauWT – Human full-length Tau

KPI – Kunitz Protease Inhibitor

LOAD - Late-onset AD

LOF - Loss-of-function

LTP- Long term potentiation

LZs - Leucine zippers

MAPs - Microtubule associated protein

MAPKs- Mitogen-activated protein kinases

MBD - Microtubule binding domain

MCI - Mild cognitive impairment

MOI- Multiplicity of infection

MS4A- Membrane-spanning 4-domains subfamily A

MT- Microtubule

NaCl - Sodium chloride

NFDM - Non-fat dry milk

NFTs - Neurofibrillary tangles

NMDA - N-Methyl-D-aspartic acid

NPDPKs - Non-proline directed protein kinases

PCR - Polymerase Chain Reaction

PDPKs - Proline-directed protein kinase

PenStrep - Penicillin-Streptomycin

PICALM - Phosphatidylinositol-binding clathrin

PIN1 – Peptidyl-prolyl cis-trans isomerase NIMA-interacting 1

PHF - Paired helical filaments

PSEN1 - Presenilin-1

PSEN2 - Presenilin-2

PP2A - Protein-phosphatase-2A

QBI - Human kidney-derived 293

RNA - Ribonucleic acid

RT - Room temperature

S or Ser - Serine residues

T - Threonine residues

Tyr or Y - Tyrosine residues

TPR - Tetratricopeptide repeat

UPS - Ubiquitin-proteasome-system

WT - Wild-type

Chapter 1 Introduction

Dementia is a group of symptoms and signs manifested by difficulties in memory, disturbances in language, and changes in behavior. In most cases, aging is the major risk factor to dementia. Meta-analysis studies done in developed countries have established dementia prevalence at around 1-5% at age 65 years, which doubles every 4 years to reach about 30% at 80 years (Ritchie & Lovestone, 2002). However, dementia is not only a burden on the people affected and their carries but also a heavy financial burden to the society. Knapp and colleagues estimated that in UK, 224 000 of the 461 000 people with cognitive impairment live in institutions costing 8.2 billion dollars every year (Ferri et al., 2005). More than 25 million people in the world today are affected by dementia, most suffering from Alzheimer's disease (AD) (Qiu, Kivipelto, & Strauss, 2009).

1.1. Alzheimer's disease

1.1.1. Epidemiology

Population aging is a worldwide universal phenomenon, being that worldwide aged population will increase from 59% to 71%. The incidence of AD is strongly associated with increasing age. In both developed and developing countries, AD has had tremendous impact on the affected individuals, caregivers, and society (Qiu et al., 2009).

According to the world Alzheimer's report, there were 35.6 million people living with dementia in 2010, increasing to 115.4 million by 2050 being 50%-70% AD cases (Jackson, 2009). The prevalence of the disease in Europe, in people older than 65 is 4.4%, whereas in the US people older than 70 shows a prevalence of AD around 9.7%. The age-specific prevalence of AD almost doubles every 4 years after age 65 (Qiu et al., 2009; Ritchie & Lovestone, 2002) [Figure 1].

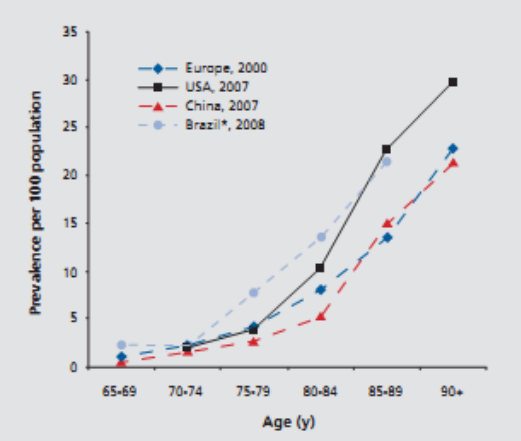

Figure 1 - Age-specific prevalence of Alzheimer's disease (per 100 population) across continents and countries (Qiu et al., 2009).

1.1.2. Risks and protects factors

Various risks factors have been found to be associated with AD, like cerebrovascular disease, diabetes, hypertension, obesity, dyslipidemia and metabolic syndrome driving to pathogenic processes that result in

decreasing the vascular integrity of the blood-brain-barrier (BBB). The BBB breakdown causes increase in neuronal oxidation, adipokines and cytokines, that results in β-amyloid deposition and abnormal phosphorylation of Tau, thereby contributing to the formation of NFTs and amyloid plaques (Reitz C, Brayne C, 2011) and an increased AD risk, and memory impairment. The APOEε4 allele of the apolipoprotein E (APOE) gene is reported as the strongest risk factor for the development of AD and is believed to be involved in β-amyloid (Aβ) aggregation (Qiu et al., 2009).

On the other hand, some evidences suggests that dietary intake of vitamin B12, folate, antioxidants, such vitamin C and E, unsaturated fatty acids and moderate alcohol intake, especially wine, could reduce the risk of AD (Blennow, Leon, & Zetterberg, 2006). In addition, there are psychosocial factors that could be protective to AD, such as high educational attainment, mentally stimulating activities, social activity, enriched social network and physical activity (Qiu et al., 2009).

1.1.3. Alterations in Alzheimer's disease brains and symptoms

Neurodegeneration in AD is estimated to start 20-30 years before clinical onset. During this phase, the hallmarks of disease, senile plaques and NFTs, begin to increase, and when a certain threshold is reached, the first symptoms arise (Blennow et al., 2006). However, the disease often initially manifests as a syndrome termed mild cognitive impairment (MCI), which is usually characterized by a memory complaint and impairments on formal testing, however with intact general cognition, preserved daily activities and absence of overt dementia (Morris et al., 2001; Petersen & Morris, 2005). MCI is an aetiological heterogeneous entity because many patients with MCI have Alzheimer's disease, whereas others patients have a form of MCI as part of the normal ageing process. MCI has been suggested to constitute a transitional stage between normal ageing and AD (Blennow et al., 2006; Petersen & Morris, 2005) [Figure 2].

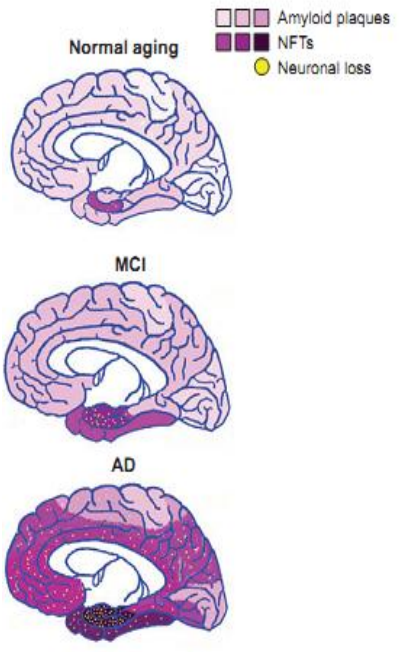

Figure 2 - Progression of neuropathology in aging and Alzheimer's disease. Shown are the neuroanatomical distribution of amyloid plaques and NFTs (Adapted Yankner et al., 2008).

Decrease in white matter density and synaptic loss are associated with aging (Yankner, Lu, & Loerch, 2008) whereas, synaptic loss is one of AD hallmarks and associated with cognitive impairment. However, in some brain areas affected in early AD does not necessary resut in a significative loss of neurons or neuronal connectivity, accoording to some results (Scheff & Price, 2006;

Scheffa, Pricea, Schmitt, Scheff, & Mufson, 2011). Nevertheless different populations of neurons in brain regions critical for memory, learning and cognitive performance is associated with abnormalities in AD. There is a damage in various circuits, as basal forebrain cholinergic system, hippocampus and cortex.

Neurodegeneration in this regions fundamentally results from NFT, related to cytoskeletal abnormalities, and the presence of ß-amyloid peptide, that is involved in cognitive decline present in this disease (J. C. Morris et al., 2001; Siegel, Albers, Brady, & Ph, 2006).

The clinical manifestations of symptomatic AD include increasing difficulties with memory and with other cognitive functions, such as impaired judgment, decision making and orientation. The patients could be presented instrumental signs that include aphasia, apraxia, and agnosia. In later stages, these individuals become profoundly demented and usually die of undercurrent illnesses (Blennow et al., 2006; Siegel et al., 2006)

1.1.4. Genetics of Alzheimer's disease

According to age of onset, two major types of AD are usually distinguished: early-onset form (EOAD) and late-onset form (LOAD). However, an important part of the EOAD form occurs in a familial history context, whereas most forms of LOAD are considered sporadic, without associated with family history (Lambert & Amouyel, 2011; Tanzi & Bertram, 2001).

The EOAD form is often caused by autosomal dominants mutations which accounts for only about 2% - 5% of all Alzheimer patients (Reitz, Brayne, 2011). This form occurs before the age of 65, and is associated with mutations in genes encoding amyloid precursor protein (APP), presenilin-1 (PSEN1) and presenilin-2 (PSEN2) (Lambert & Amouyel, 2011). The APP gene is localized on chromosome 21. APP is a membrane protein cleaved by secretases. This cleavage of APP by secretases leads to both non-amyloidogenic processing, and the amyloidogenic processing, with production of Aß. APP mutations result in privileged processing of APP through the amyloidegenic pathway (Ballard et al., 2011; Yankner et al., 2008). Mutations in highly homologous PSEN1 and PSEN2 account for most cases of familial disease. The PSEN1 gene is on chromosome 14, and the PSEN2 gene is on chromosome 1 and both have homologous functions (Nussbaum & Ellis, 2003). They are both components of γ-secretase, which involved in APP processing into Aß. Familial mutations in this genes can alter production of $Aß_{1-42}$ which form plaques more readily than $Aß_{1-40}$ (Ballard et al., 2011; Blennow et al., 2006).

The genes involved in LOAD, increase disease risk and are not inherited in a Mendelian fashion (Reitz, Brayne, & Mayeux, 2011). LOAD occurs in patients over 65 years old, and it is the most common form of AD. The association of APOEε4 allele with AD was reported in 1993 (Corder et al., 1993). Meta-analyses studies shows that this allele increases the risk of disease by three times in heterozygotes and by 15 times

in homozygotes, and with each allele copy lowering the age at onset by almost 10 years (Blennow et al., 2006). APOE is involved in cholesterol transport, and different isoforms have differing transport efficiencies. APOE also binds Aß in an isoform-specific manner, and these alleles are associated with increased amyloid burden and cholinergic dysfunction (Ballard et al., 2011).

However, there are other candidates genes involved in AD although being their contribution probably minor. Genome-wide associated studies identified news genes involved with LOAD form of disease, these being CLU (clusterin), PICALM (phosphatidylinositol-binding clathrin assembly protein), CR1 (complement receptor 1), BIN1 (bridging integrator 1), ABCA7 (ATP-binding cassette transporter), MS4A cluster (membrane-spanning 4-domains subfamily A), CD2AP (CD2-associated protein), CD33 (sialic acid binding immunoglobulin-like lectin) and EPHA1 (ephrin receptor A1) (Morgan, 2011). Tau haplotype (H1C) is associated with AD, and affects expression levels of Tau splice isoforms (Ballard et al., 2011). Unfortunately, the successful identification of novel AD genes in the sporadic form of AD has several obstacles.

1.1.5. Hallmarks of AD

In AD there are two major pathological hallmarks, the accumulation of extracellular insoluble deposits of an Aß and intracellular tangles consisting of hyperphosphorylated Tau protein.

1.1.5.1. ß-amyloid protein

APP is a type I transmembrane protein and its processing arises through alternative splicing resulting in three different isoforms, APP695, APP751 and APP770 (containing 695,751 and 770 amino acids, respectively) (Y. Zhang, Thompson, Zhang, & Xu, 2011). The isoforms APP751 and APP770 are expressed in most tissues and contain a 56 amino acid Kunitz Protease Inhibitor (KPI) domain within their extracellular regions (Menéndez-González, Pérez-Pinera, Martínez-Rivera, Calatayud, & Blázquez Menes, 2005). Protein levels of KPI-containing APP isoforms are elevated in AD brain, and this is associated with increased Aß deposition.

APP role has been suggested to be involved in neurite outgrowth and synaptogenesis, neuronal protein trafficking along the axon, transmembrane signal transduction, cell adhesion, calcium metabolism and among others (Zheng & Koo, 2006).

APP can be sequentially cleaved by groups of enzymes or enzyme complexes termed α, ß, γ-secretases (LaFerla, Green, & Oddo, 2007). APP can undergo proteolytic processing by one of two pathways

depending on the kind of enzymes and proteolysis sites the non-amyloidogenic pathway or the amyloidogenic pathway (Haass, Kaether, Thinakaran, & Sisodia, 2012).

In the non-amyloidogenic pathway, APP is cleaved approximately in the middle of the Aß region between residues Lys16 and Leu17 by the α-secretase enzyme (Esch et al., 1990). The APP cleveage by α-secretase releases a large soluble ectodomain of APP called sAPPα, which is secreted into extracellular medium. This domain has an important role in neuronal plasticity/survival, protection against excitotoxicity, and also regulation of neuronal stem cell proliferation (Furukawa et al., 1996; Mattson, 1997). Subsequently, the resulting domain, 83-amino-acid C terminal fragment (C83), is retained in the membrane and cleaved by γ-secretase, producing a short fragment termed p3, which apparently is pathologically irrelevant (LaFerla et al., 2007) [Figure 3].

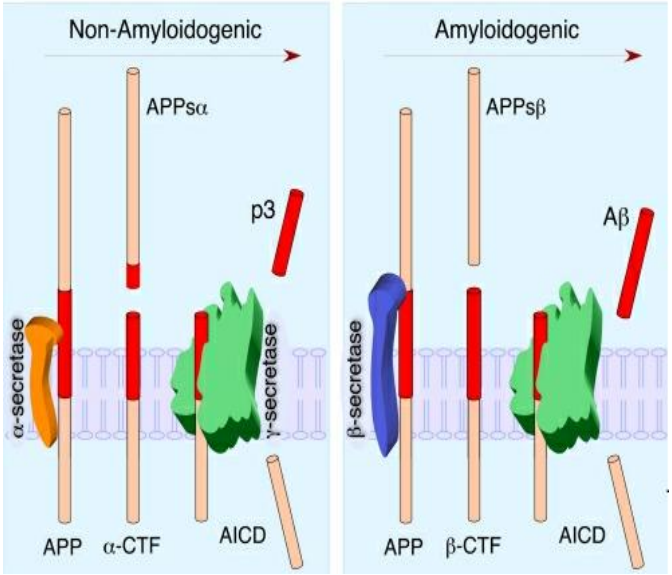

Figure 3 – Proteolytic processing of APP within the anti-amyloidogenic and amyloidogenic pathways (Adapted from Thinakaran & Koo, 2008)

Amyloidogenic pathway is an alternative cleavage pathway for APP which leads to Aß generation (LaFerla et al., 2007). The first step of this pathway is the APP cleavage by BACE1, the major ß-secretase (Zhang et al., 2011). This cut results in release of sAPPß into extracellular space, and leaves the 99-amino-acid from C-terminal stub (known as C99) within the membrane. The subsequent cleavage of this fragment by γ-secretase releases an intact Aß peptide and p83 fragment. Most of full-length Aß peptide produced is 40 residues in length ($Aß_{40}$), whereas a small proportion (approximately 10%) is the 42 residue variant ($Aß_{42}$). This variant is more hydrophobic and more aggregation prone and believed to be the toxic building block of Aß oligomers, which affect memory and cell survival (Haass & Selkoe, 2007; LaFerla et al., 2007)[Figure 3]. In addition to secretases, caspases can directly cleave APP at position Asp664. Studies suggests that caspase cleavage of APP seems to be crucial for Aß-mediated neurotoxicity, since a mutation in this position in transgenic mice negated the synapse, electrophysiology, and behavioral abnormalities, even though Aß plaques were still abundant in the brain (Galvan et al., 2006; Zhang et al., 2011).

The majority of Aß is secreted out of the cell, and this peptide can also be generated in subcellular compartments within the cell, such endoplasmic reticulum, Golgi complex, and in the endosome/lysosome. In addition, extracellular Aß can be internalized for cell degradation. The intracellular existence of Aß implies that it may accumulate within neurons and contribute to AD. Aß internalization can lead to intracellular aggregates, which can lead to vesicular membrane disruption, contributing therefore to the pathological effect (Zhang et al., 2011).

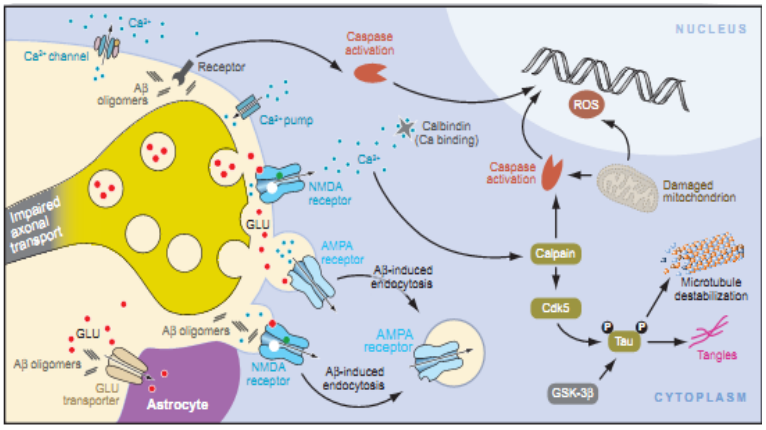

Figure 4 - Representative of neurodegenerative mechanism in Alzheimer's disease (Yankner et al., 2008).

Gradual changes in the levels of Aß toxic species in the brain are thought to initiate the amyloid cascade. The ratio between $Aß_{42}$/ $Aß_{40}$ can be increased by mutations in the three genes involved in familial form of the AD. The relative increase of $Aß_{42}$ enhances oligomer formation, which causes subtle and then increasingly severe and permanent changes of synaptic function, inhibiting hippocampal LTP (Yankner et al., 2008) [Figure 4].

Recent studies suggest that Aß oligomers can also alter glutamatergic neurotransmission by promoting the endocytosis of NMDA and AMPA receptors (Snyder et al., 2005). Consequently, local inflammatory responses arise, due to the activation of microglia and astrocytes [Figure 4]. Over time, these events result in altered neuronal ionic homeostasis, oxidative stress, and formation of NFTs that are induced by altered kinase and phosphatase activities that causes additional defects, as for example alterations in axonal transport. This cascade culminates in extensive synaptic/neuronal dysfunction and cell death, leading to progressive dementia (Blennow et al., 2006; Haass & Selkoe, 2007; Hardy & Selkoe, 2002). Overproduction of Aß results in a neurodegenerative cascade, leading to synaptic dysfunction, formation of intraneuronal fibrillary tangles and eventually neuronal loss in affected areas of the brain (Selkoe, 1998).

1.1.5.2. Tau protein

i. Structure and function of the normal Tau

Microtubule-associated protein Tau was identified as a microtubule-assembly factor in the mid of 1970s (Weingarten, Lockwood, Hwo, & Kirschner, 1975). This protein is associated with promotion of the

assembly and stabilization microtubules, which contributes to the proper function of neurons (Kolarova, García-Sierra, Bartos, Ricny, & Ripova, 2012).

Tau belongs to the microtubule-associated proteins (MAPs) family, and it is highly conserved and exclusively found in higher eukaryotes. This protein is mainly expressed in neurons, but also present in oligodendrocytes, and its primary role, by interacting with microtubules, is to stabilize neuronal cytoskeleton (Neve, Harris, Kosik, Kurnit, & Donlon, 1986). The Human Tau gene is over 100kb and is located on the long arm of chromosome 17 at the position 17q21 and contains 16 exons. The exons 1, 4, 5, 7, 9, 11, 12 and 13 are constitutive exons. Exons 2, 3, and 10 undergo alternative splicing and they are present in the adult brain. In the central nervous system, alternative splicing in these exons results in appearance of six Tau isoforms that are differentially expressed during development of the brain (Sergeant, Delacourte, & Buée, 2005). These isoforms range from 352 to 441 amino acids with an apparent molecular weight between 60 and 74 KDa (Martin, Latypova, & Terro, 2011) [Figure 5].

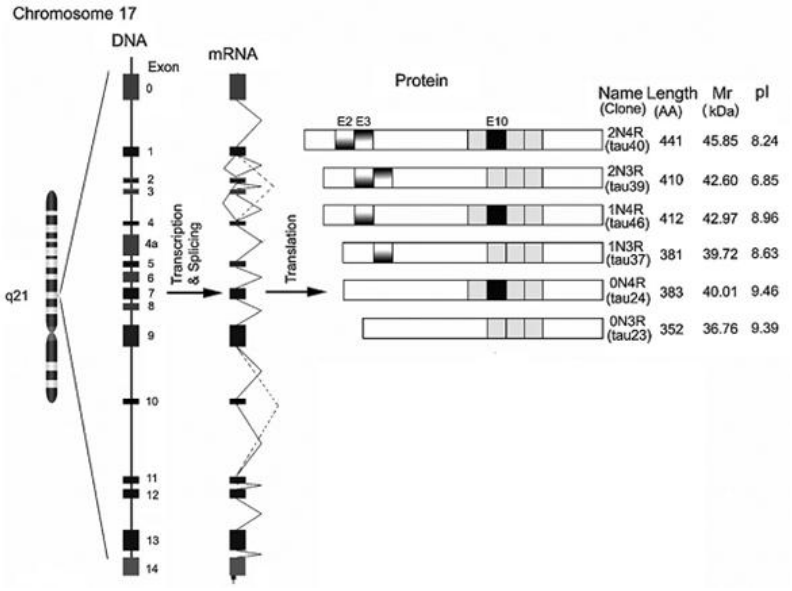

Figure 5 - Schematic representation of transcription and alternative splicing of Tau protein. The diagram indicates the structure of chromosome 17 and the six different Tau isoforms after the Tau transcription, with their length and molecular weight (J.-Z. Wang & Liu, 2008).

The human Tau protein is a product of a single RNA transcript and is subdivided into four regions: 1) An N-terminal region that can associate with the cell membrane and regulate the spacing between microtubules; 2) A Proline-rich region including many phosphorylation sites that can bind to SH3 domains of other proteins, including tyrosine kinase Fyn; 3) The microtubule-binding domain (MBD), a region responsible for Tau binding to microtubules; 4) C-terminal region (Martin et al., 2011; Sergeant et al., 2005). Depending on developmentally controlled alternative mRNA splicing, the repeat domain of Tau can consist of either three or four repeats of 31 of 32 residues each. The 4R variant contains R1=Q244-K274, R2=V275-S3015, R3=V306-Q336 and R4=V337-N368. The 3R variant lacks repeat R2 that is encoded by exon 10. The form without two inserts in N-terminal region called 0N, with one N-terminal insert, 1N, and with two N-terminal inserts 2N. This gives rise to six combinations corresponding to the six Tau isoforms: 2N4R; 1N4R; 2N3R; 0N4R; 1N3R; and 0N3R (Martin et al., 2011; Sergeant et al., 2005) [Figure 5]. However, only the 0N3R Tau isoform is present during fetal stages, while the isoforms with one or two N-terminal inserts and 3R or 4R are expressed during adulthood (Martin et al., 2011; Sergeant et al., 2005).

The major biological function of Tau is to promote microtubule assembly and maintain the stability of the previously formed microtubules, which are essential for the axonal transport of neurons. There is a gradient of Tau along the axon in which highest levels are closest to the synapses (Dixit, Ross, Goldman, & Holzbaur, 2008; Mandell & Banker, 1996). Tau also promotes stabilization of microtubules, because it binds to tubulin and is incorporated into the growing microtubules as an integral structure (Kar, Fan, Smith, Goedert, & Amos, 2003;Wang & Liu, 2008). Additionally, the interaction of Tau with diverse structural and functional proteins suggests that Tau may play crucial roles not only in normal architecture but also in signal transduction of the neurons. Most recently it was discovered that Tau, by the phosphorylation, also participates in the regulation of the cell viability (Li et al., 2007).

ii. Tau post-translational modifications

During normal development, Tau protein undergoes various post-translational modifications, since the regulation of Tau takes place predominantly through these. Tau phosphorylation is the most common post-translational modification, however others post-translational modifications as glycosylation, glycation, poly-isomerization, truncation, nitration, polyamination, ubiquitination, oxidation and aggregation have an important role in maintenance of the structure and conformational state of Tau.

Tau phosphorylation

Tau is a phosphoprotein containing normally 1–3 moles of phosphate per mole of Tau protein. Tau can be phosphorylated at three amino-acid types, serine (S), threonine (T), and tyrosine (Y). 17% of the Tau protein is constituted by these three amino acids (Martin et al., 2011;Wang & Liu, 2008). This protein has among 85 putative phosphorylation sites, of which 45 are serines (53% of the phosphorylation sites on Tau), 35 are threonines (41%) and 5 are tyrosines (6%). A decrease or increase in Tau phosphorylation alters its affinity for microtubules which results in neuronal cytoskeleton modifications (Martin et al., 2011). For example, Tau phosphorylation at residues S262, S293, S324 and S356 has been shown to decrease Tau binding microtubules (Dickey et al., 2007) and decrease the flexibility of the protein (Himmelstein, Ward, Lancia, Patterson, & Binder, 2012).

The expression and phosphorylation of Tau seem also developmentally regulated. In embryonic and early postnatal stages, a single isoform of Tau is expressed with high levels of phosphorylation, while in the brain of the healthy adult, a much lower level of Tau phosphorylation has been detected with a simultaneous appearance of various Tau isoforms (Goedert et al., 1993).

The phosphorylation is regulated by various kinases and phosphatases, and an unbalance between these enzymes families can result in Tau hyperphosphorylation. According to the motif-specificity, Tau kinases can be divided into three major groups: proline-directed protein kinsases (PDPKs); non-proline directed

protein kinases (NPDPKs) and protein kinases specific for tyrosines. Glycogen synthase kinase - 3ß (GSK3ß), cyclin-dependent kinase 5 (CDK5), and mitogen-activated protein kinases (MAPKs) are protein kinases PDPKs (Sergeant et al., 2008). The NPDPKs include calcium- and calmodulin-dependent protein kinase II (CAMKII), PKA, protein kinase C, among others (Wang & Liu, 2008). Alterations in the expression and/or activity of Tau kinases such as PDPKs have been reported in the brains of AD patients, suggesting that one or several of them could be involved in the Tau hyperphosphorylation observed in the AD brain (Martin et al., 2011).

On the other hand, Tau hyperphosphorylation could be a result from phosphatase inhibition. Protein phosphatase-2A (PP2A) accounts for more than 70% of cellular phosphatase activity and is implicated in the regulation of Tau phosphorylation levels (Liu, Grundke-Iqbal, Iqbal, & Gong, 2005; Virshup & Shenolikar, 2009).

Tau glycation

Glycation refers to non-enzymatic linkage of sugars to the amino side chain of polypeptide. This reaction leads to subsequent oxidation and finally formation of heterogeneous products called advanced glycation end products (AGE). Twelve sites of glycation were found on Tau protein, seven of them are located in MBD regions. Glycation might contribute to block Tau degradation and, therefore, promote its pathological accumulation and neuronal cell death (Martin et al., 2011; Yan et al., 1994).

Tau glycosylation

Glycosylation is the covalent reaction that links oligosaccharides to the side chain of proteins with help of glycosyltransferase. According to the nature of glycosidic bond, they are classified into O- and N-linked glycosylation: O-glycosylation results from the attachment of sugar to the hydroxyl group of serine or threonine in the proximity of a proline residue; N-glycosylation results from the attachment of sugar to the amine radical of asparagine side chain of proteins (Gong, Liu, Grundke-Iqbal, & Iqbal, 2005; Robertson, Moya, & Breen, 2004). Tau protein contains 11 putative O-glycosylation sites. Tau glycosylation decreases its phosphorylation by PKA, CDK5 and GSK3ß. Particularly O-glycosylation achieved by the engraftment of N-acetyl-glucosamine (O-GlcNAcylation) has been shown to reduce phosphorylated Tau in rat cortex and hippocampus. This may result from competition between phosphorylation and glycosylation for the same sites on Tau protein (Yu et al., 2008; Yuzwa et al., 2008).

Tau prolyl-isomerization

Prolyl-isomerization is the reaction that allows the rearrangement to disulfide bonds in proteins. This reaction modifies the conformation of the target proteins from *cis* to *trans* conformation. Prolyl-isomerization of Tau is achieved by peptidyl-prolyl *cis-trans* isomerase Pin1 (Martin et al., 2011).

Alteration in Tau conformation from *cis* to *trans* leads to a shift of the peptide chain in space, making them more accessible to phosphatases, and Tau prolyl-isomerization by Pin1 to *trans* conformation facilitates its dephosphorylation by PP2A (Bulbarelli, Lonati, Cazzaniga, Gregori, & Masserini, 2009). Pin1 knock down showed increased Tau aggregation and to influence APP processing towards a decrease in Aß production. This evidences that Pin1 activity interference, either by inhibiton or reduction, misfolded Tau protein presence, or even blocking of Tau protein accessibility might lead to Tau pathology (Martin et al., 2011).

Tau truncation

Truncated Tau proteins are conformationally different from normal healthy Tau. Caspase-3 proteolytic cleveage of Tau leads to the formation of fragments with 46 kDa and 20 kDa, and calpain-mediated Tau cleavage generates a product of 17 kDa (Martin et al., 2011). Tau truncated by caspase at Asp421 exerts stronger microtubule-assembly potency than the full-length Tau molecule a determined by *in vitro* assays (Gamblin et al., 2003). The truncated fragment can cause cell apoptosis (Wang & Liu, 2008). Compared with full-length Tau proteins, the cleavage products of Tau are reportedly more prone to form aggregates (Yin & Kuret, 2006).

Tau nitration

Nitration is the addition of nitrogen dioxide on tyrosine of an organic molecule, and this occurs at 4 sites in Tau: Tyr18, Try29, Tyr197 and Tyr394 (Wang & Liu, 2008). Nitration has been associated with AD since the nitration of Tyr29 was found only in severely affected AD brains, but not in normal aged brains (Reynolds et al., 2006). Nitration was proposed to decrease Tau ability to promote tubulin assembly leading to Tau oligomerization (Martin et al., 2011).

Tau polyamination

The polyamination reaction occurs by transglutaminases involving a glutamine as acyl donor group, and a lysine as acyl acceptor donor. Tau polyamination reaction is observed on the protein before NFT formation, so it might be involved in NFT formation process (Singer, Zainelli, Norlund, Lee, & Muma, 2002).

Tau ubiquitination

Ubiquitination is the specific binding of one or more molecules, of a small protein, ubiquitin, to proteins, that will signal proteins for their degradation in the cytosol by the ubiquitin-proteasome-system (UPS) (Martin et al., 2011). This system participates in defending against misfolded proteins and provides an affective protein quality control system that is essential for cellular survival and functions (Wang & Liu, 2008). Tau normally exists as an unfolded protein and it is degraded *in vitro* by the core (20S) of

proteasome that functions in an ubiquitin-independent manner (David et al., 2002). Proteins after associated with ubiquitin, which is a 76-amino acid protein, are degraded by ubiquitin-proteasome machinery in an ATP-dependent manner (Avila, Lucas, Perez, & Hernandez, 2004). The ubiquitin ligase for Tau is identified as the C terminus of Hsp70-interacting protein (CHIP). This protein works in combination with heat shock proteins, that are induced by the stress derived of the accumulation of misfolded proteins. The combination of the shock proteins and CHIP is important to regulate Tau degradation; a reduction of CHIP levels in AD brains was discovered. The levels of heat shock protein 90 (Hsp90) correlate inversely with levels of soluble Tau and Tau oligomers (Morris, Maeda, Vossel, & Mucke, 2011). As such, in non-pathological conditions Tau has been shown to be ubiquitinated and proteolytically processed by UPS.

1.1.6. Interaction between Aß and Tau in pathological condition

Aβ and Tau, the two main proteins involved in AD, exhibit separate toxicity in this disease. There are however some evidences *in vitro* and *in vivo* of the possibility of interaction between these two proteins. Amyloid oligomers are proposed to precede, and eventually trigger intracellular Tauopathy, likely by increasing phosphorylation of Tau protein.

The first evidence supporting that Aβ drives Tau pathology was given by Götz, et al. They have shown that $A\beta_{42}$ fibrils injected into the brains of P301L mutant Tau transgenic mice caused a significant increased in NFTs formation (Götz, Chen, et al., 2001).

Hurtado et al. developed an AD mouse model generated by crossing PS19 and PDAPP transgenic mice that developed Aß and Tau pathology. They showed that Aβ protein accelerated NFT formation, and enhanced Tau amyloidosis, however the reverse was not found in this model, meaning that Tau protein did not have the same effect on Aβ pathology (Hurtado et al., 2010). There is also evidence of induction of neuronal Tau hyperphosphorylation by Aβ oligomers in rat mature hippocampal cultures (De Felice et al., 2011).

Another piece of evidence for the hypothesis of Aβ and Tau interaction is the fact that Tau can mediate Aβ toxicity. It was found that neurons from Tau knockout mice are protected from Aβ-induced cell death in cell culture (Ittner et al., 2010; Roberson et al., 2007). Tau reduction also prevents Aβ induction defects in axonal transport of mitochondria which may link the Tau hypothesis to other ones, axonal transport impairment hypothesis, according to which Tau induces failure of axonal transport (Stamer, Vogel, Thies, Mandelkow, & Mandelkow, 2002) and also with oxidative stress hypothesis, which suggest that mitochondria are functionally impaired which will result in production of reactive oxidative species (Combadière, Raoul, Guillonneau, & Sennlaub, 2013).

Although scientific research has given an increase in knowledge about the roles of Tau and its interaction with Aβ pathology, many questions about the scaffolding partners for Tau in its interaction with Aβ are still unanswered.

1.2. Pathogenic mechanism associated with Tau

Intraneuronal aggregation of abnormally phosphorylated Tau in NFTs constitutes a major neuropathological hallmark of Tauopathies such as AD. Tau related diseases are considered as a group of more than twenty heterogeneous dementias and movement disorders that are neuropathologically characterized by intracellular accumulations of abnormal filaments formed by the microtubule-associated protein Tau (Lee, Goedert, & Trojanowski, 2001). These disorders are the consequence of abnormal Tau phosphorylation, abnormal levels of Tau, abnormal Tau splicing or mutations in Tau gene. Aggregates consist almost exclusively of Tau protein, albeit as different isoforms in different diseases, that is either Tau 3R or Tau 4R or as a variable mixture (Jaworski, Kügler, & Van Leuven, 2010). However these diseases can be differentiated by the subcellular compartments containing pathologic Tau filaments associated with disease and with specific brain regions affected (Himmelstein et al., 2012) . Table 1 shows the various examples of these diseases.

Table 1 - Summarization of the most frequent disorders associated with Tau pathology.

Tau-related disorder	Characteristics	References
Corticobasal degeneration	- Cognitive disturbance, like aphasia, apraxia and moderate dementia; - Frontoparietal atrophy and glial neuronal Tau inclusions; - Presence of hyperphosphorylated Tau.	(Avila et al., 2004; Jung et al., 2012; Lee et al., 2001; Rana, Ansari, & Siddiqui, 2012)
Down's Syndrome	- Trisomy in chromosome 21; - Results in the defective growth and maturation of the brain, producing a cognitive impairment and dementia; - Tau is hyperphosphorylated similar to AD;	(Avila et al., 2004; Lee et al., 2001)
Frontotemporal dementia with parkinsonism linked to chromosome 17 (FTDP-17)	- Fontotemporal atrophy, with neuronal loss, gliosis and cortical spongiform changes in the lobes; - Tau inclusions in neurons and glial cells; - Tau missense mutations occur preferentially in the microtubule binding region; - Mutations affect the binding of Tau to other proteins that bind to that region of Tau.	(Jesus Avila et al., 2004; (Grover et al., 1999; Hutton, 2001; Lee et al., 2001)
Pick's diesease	- Dementia, with disturbances in language and behavior; - Associated with frontal lobe atrophy; - Presence of cytoplasmic Tau inclusions in neurons of the frontal lobe.	(Jesus Avila et al., 2004; V. M. Lee et al., 2001; Rossor, 2001; Takeda, Kishimoto, & Yokota, 2012)
Progressive supranuclear	- Characterized by supranuclear palsy, prominent postural instability; - Tau inclusions are found in neuronal and glial cells, with astrocytes and oligodendrocytes affected;	(Jesus Avila et al., 2004; de Yébenes, Sarasa, Daniel, & Lees,

palsy	- Tau polymorphism may be a risk factor.	1995; Dickson, Rademakers, & Hutton, 2007; V. M. Lee et al., 2001)
Other Tauopathies	- Tauopathies involving hyperphosphorylated Tau, including parkinsonism with dementia, myotonic dystrophy, prion diseases with tangles, among others.	(Buée, Bussière, Buée-Scherrer, Delacourte, & Hof, 2000; Ingram & Spillantini, 2002)

The causes of Tau aggregation in sporadic Tauopathies are not completely understood. However, abnormalities in post-translational modifications seem to alter the proprieties of Tau (Avila, Santa-María, Pérez, Hernández, & Moreno, 2006).

1.2.1. Tau aggregation and spreading evidences

In many neurodegenerative disorders involved with protein aggregation, like AD, the end-stage aggregated structure is considered a fibrillar amyloid deposit, normally with approximately 10 nm. These deposits are characterized by positive staining with Congo red or thioflavin T and by the signature parallel ß-sheet structure diffraction patterns observed by X-ray fiber diffraction analysis. However, not all protein aggregates in central nervous system (CNS) are of the amyloid fibrillar type. Tau protein forms non structured aggregates intracellularly in neuronal tissues. Although it is a controversial question, because there are some authors that classify Tau protein inclusions as an intracellular amyloid configuration (Pedersen & Heegaard, 2013). The amyloid fibrillation process features characteristic kinetics. Fibril growth is normally preceded by a long lag phase, where monomers try out intermolecular interactions until, a stable oligomeric assembly or a nucleus is formed. After formation of nuclei, fibrils show exponential growth until the reaction reaches an equilibrium phase, where the rate of fibril growth equals that of shrinkage. The addition of pre-aggregated forms eliminates the lag phase, the process known as “seeded” polymerization (S.-J. Lee, Desplats, Sigurdson, Tsigelny, & Masliah, 2010) [Figure 6]. During the course of seeded polymerization, subtle conformational variations in aggregates are propagated through structural conversion of newly added monomers. Fibrillar aggregation typical of amyloid-forming proteins depends on a regular, stacked ß-sheet structure which may be generated through partially unfolded intermediates (Pedersen & Heegaard, 2013).

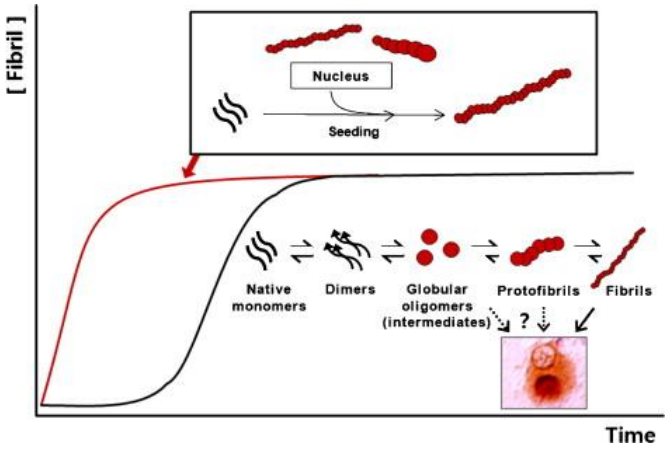

Figure 6 - Scheme of amyloidogenic protein aggregation process. The black trace represents the non-induced amyloidogenesis process, whereas the red trace represents the induced amyloidogenic process. This process is dependent of nucleation, and after this phenomenon there is a rapid elongation phase (SJ, Lee, HS, Lim, E, Masliah, HJ, 2011).

The biological process defined as an aggregation process is that association of two or more non-native protein molecules, that is largely driven by hydrophobic forces and primarily results in the formation of amorphous structures (Hartl & Hayer-Hartl, 2009).

Studies demonstrated that the principal post-translational modifications involved in aggregation are phosphorylation, truncation, glycation, and nitration (Cho & Johnson, 2004; Horiguchi et al., 2003; Ledesma, Medina, & Avila, 1996). Different studies in cells have shown that phosphorylation of Tau influence Tau on least two levels, in Tau-microtubule interactions and Tau-Tau interactions. Phosphorylation tends to decrease the binding of Tau to microtubules of KXGS motifs and Ser214 having particularly pronounced effects (Illenberger et al., 1998). The result is a decrease in microtubule stability, but more significantly an increase in the cytosolic pool of Tau, that could contribute to aggregation into paired helical filaments PHFs (Mandelkow, Von Bergen, Biernat, & Mandelkow, 2007).

The progressive accumulation of specific protein aggregates is a defining feature of many neurodegenerative diseases, including AD. Tau proteins aggregate into intraneuronal filamentous inclusions. In AD, these filaments are called PFH, and their constitutive proteins are referred to as PFH-Tau proteins (Buée et al., 2000) [Figure 7]. The aggregation of Tau is based on short hexapeptide motifs ^{275}VQIINK^{280} and ^{306}VQIVKY^{311} at the beginning of R2 and R3. These aggregation motifs have a partially hydrophobic character and predisposed to interact with cross-β structure, contributing to the core of PHFs (Illenberger et al., 1998).

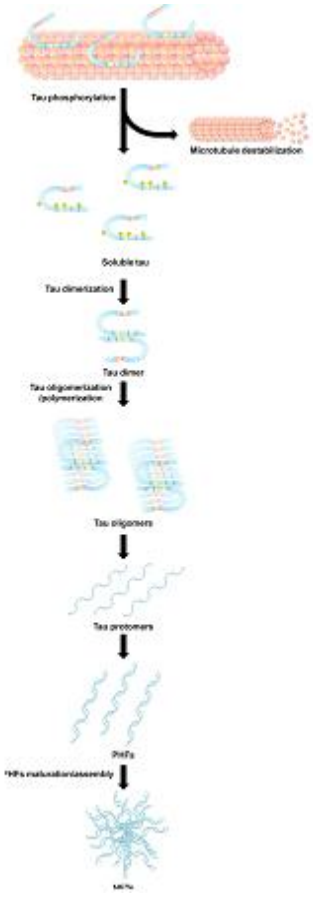

Figure 7- Scheme of the aggregation process in Tau pathology (Martin et al., 2011).

This conformation is also characteristic of prion strains, recently reported to other disease-linked proteins, such as Tau, Aß and α-synuclein (Frost, Ollesch, Wille, & Diamond, 2009). Prion disease belongs to the group of protein misfolding neurodegenerative diseases, and these misfolded proteins are highly ordered in filaments inclusions with core region of cross-ß-conformation (Goedert, Clavaguera, & Tolnay, 2010). However, the diseases related with prions have an important difference with other diseases related with misfolded proteins, since prions disease can be transmitted between individuals across species and can spread from the point of infection, often from peripheral tissue to the central nervous system (Collinge & Clarke, 2007). Prionic diseases are a fatal neurodegenerative disorders, associated with conversion of cellular prionic protein into a scrapie prionic protein. An abnormal conformation state that is predisposed to form an amyloid deposits in brain tissue leading to dementia (Vingtdeux, Sergeant, & Buée, 2012). The propagation of prion aggregates can occur at a relatively fast and efficient step, this propagation is accelerated when aggregates break into smaller seeds that serve to recruit additional monomers (Lee et al., 2010). Nevertheless studies observed that the formation of Tau and α-synuclein inclusions as a function of age has shown to develop in a stereotypical manner in particular brain regions from where they appear to spread (Michel Goedert et al., 2010). Recent research, tissue culture studies and *in vivo* studies describing the induction of protein misfolding and spreading between cells, have shown most convincingly that common neurodegenerative disorders can be driven by cell non-autonomous mechanisms (Clavaguera et al., 2009; Kane et al., 2000; Ren et al., 2009), it can be seen in table 2 for Aβ, Tau, and α-synuclein.

Table 2 - Evidences for speeding of non-protein aggregates in the central nervous system (adapted from (Jellinger & Popescu, 2012)

Inoculum	Host	Propagation effect	References
Aβ			
Brain homogenates from AD or APP transgenic mice	APP transgenic mice (intracerebral injection)	Aβ deposition at injection site and in adjacent brain structures	(Eisele et al., 2009; Meyer-Luehmann et al., 2006)
Tau			
Tau fibrils	Cultured neuronal cells	Endocytic uptake of exogenous Tau fibrils and induction of cytoplasmic endogenous Tau proteins. Cell-to-cell transmission of Tau taken up by cultured cells	(Frost, Jacks, & Diamond, 2009; Guo & Lee, 2011; Nonaka, Watanabe, Iwatsubo, & Hasegawa, 2010)
Brain extracts from Tau transgenic mice	Transgenic mice expressing human wild-type (WT) Tau (intracerebral injection)	Spreading of Tau from site of injection to other brain structures	(Clavaguera et al., 2010; Piao et al., 2001)

α-Synuclein			
Aggregate-producing neuronal cell cultures	Neuronal cells	Endocytic uptake of α-Syn aggregates	(Desplats et al., 2009)
Introduction of α-Syn aggregates by preformed fibrils generated from truncated recombinant human WT α- Syn	Primary hippocampal neurons	Adsorptive-mediated endocytosis promoting soluble α-Syn into insoluble PD-like Lew bodies and Lewy neurites	(Volpicelli-daley et al., 2012)
Transgenic mice overexpressing human α-Syn	Mouse neuronal progenitor cells grafted into mouse brains	Interneuronal transmission of human α-Syn	(Desplats et al., 2009)
Brains of patients with Parkinson disease	Foetal stem cells grafted into the brains of patients with Parkinson disease	Interneuronal transmission of Lewy inclusions	(Luk et al., 2009; Mendez et al., 2008; Ren et al., 2009)

Diamond and colleagues demonstrated by the first time that in cell cultures there is an uptake of Tau fibrils added to culture medium and the fibrils can induced fibrillation of cytoplasmatic Tau (Frost, Jacks, et al., 2009).

There is also another study that reported the evidence of cell-to-cell transference of Tau proteins, the Calvaguera et al. study, where they reported the propagation of Tau in transgenic mice. Brain extracts of transgenic mice (P301S) with filamentous of Tau, were injected into the hippocampus and cerebral cortex of ALZ17, a transgenic line over expressing the WT Tau protein. Tau deposition was found not only within the injection sites but also in neighboring brain regions, being severely diminished with the increasing distance from the injection site, and they could see an increase in brain lesions over time (Clavaguera et al., 2009). This could mean however that this was due to perfusion of the injected material throughout the brain.

Different research in this area have demonstrated that Tau aggregates can propagate a misfolded state inside cells and provided also an experimental system where molecular mechanisms underlying the intracellular transfer of inclusions can be identified (Goedert et al., 2010). The major fundamental question in this subject is what is the mechanism of the prion-like spreading of Tau pathology to selective regions of the brain. One of the possibilities would be that the selectivity of the propagation could follow neuronal circuits through synaptic transmission. That could be possible by exossomes, small specialized membranous vesicles that can be secreted by many cell types including neuronal cells. Synaptic activity could enhance exossomal production and secretion by neurons (Lachenal et al., 2011). Another explanation could be the existence of tunneling nanotubes, the fine membrane channels that have recently been described in mammalian cells for communication between cells, but also for cell-cell propagation of misfolded prion protein (Vingtdeux et al., 2012). Zhang et al. described that tunneling nanotubes are induced in rodent hippocampal neurons and astrocytes by oxidative stress. We also know that cell-to-cell connection and communication of intracellular organelles or Aβ could be triggeredd by

cellular stress. The stressed cells, like degenerating neurons, would connect via tunneling nanotubes to closely surrounding or connected neurons to delivery pathogenic proteins. So, these mechanisms of cell-to-cell communication under stress conditions could contribute to neurodegenerative diseases and explain the spreading that occurs in neurons in these cases (Wang, Cui, Sun, & Zhang, 2011). It also has been shown that Tau protein aggregates present in extracellular space can be internalized into cells through endocytosis. Internalized Tau aggregates showed partial co-localization with dextran, a feature indicative of involvement of the endocytic pathway (Frost, Jacks, et al., 2009). Aggregates are packaged into endocytic vesicles, and therefore, require another mechanisms by which they can gain access to the cytosol (Frost, Jacks, et al., 2009).

1.2.2. Pathological species associated with Tau aggregation

Over the last few years, researchers have been describing toxic species of Tau protein associated with AD. One of the hallmarks of AD is the accumulation of NFTs in the brain; however these are not the exclusive pathological form of Tau protein that exist in AD patients brain. Thus, some investigators have shifted their focus to not just to study NFTs, but also to study pre-filament Tau species such as Tau oligomers and hyperphosphorylated Tau monomers.

1.2.2.1. Tau oligomers

Non-fibrillar Tau aggregates of different sizes have been reported by various research groups, as possibly the most toxic and pathologically significant forms of Tau aggregates (Francisco, 2007; Lasagna-Reeves et al., 2011). This toxic species is considered to be intermediates between soluble Tau monomers and insoluble Tau filaments.

Tau oligomer is the term used to describe any complex of two or more Tau molecules in a multimeric structure. They can be formed both by hyperphosphorylated and by non-phosphorylated Tau proteins and they have been shown to be both soluble (they are made up a small number of Tau proteins), or insoluble (when they include a large number of Tau molecules) (Cowan, Quraishe, & Mudher, 2012).

Different research groups identified small soluble oligomers of approximately 140 and 170 kDa in brain homogenates of P301L transgenic mice (mice used as Tauopathy model with Frontotemporal lobar degeneration (FTLD) mutation) (Berger et al., 2007; Sahara et al., 2007). The oligomers detected by Berger and colleagues appeared at early stages of disease when memory deficits were evident in the absence of tangle formation or neuronal loss. The majority of the 140 kDa oligomers appeared to be soluble and did

not contain hyperphosphorylated Tau proteins, however the 170 kDa oligomers detected in sarkosyl-insoluble fraction showed Tau proteins hyperphosphorylated at the residues (Ser202/Thr205, Ser396 and Ser422) (Berger et al., 2007).The effect of this kind of Tau oligomers on physiological processes has been investigated. The oligomers that Lasagna-Reves and colleagues developed, have been shown to be toxic *in vitro* (Lasagna-Reeves, Castillo-Carranza, Guerrero-Muoz, Jackson, & Kayed, 2010) and *in vivo* (Lasagna-Reeves et al., 2011). When SH-SY5Y cells were treated with soluble oligomers, these oligomers cause significantly more cell death than Tau monomers or filaments (Flach et al., 2012; Lasagna-Reeves et al., 2010)

The large insoluble oligomers were first described by Takashima group and were described as granular Tau oligomers. This species consist of an average of 40 molecules of Tau, which normal size of 180 kDa and with 20 nm of diameter. The granular oligomers were identified in early Braak stages in human brain and can also form from recombinant non-phosphorylated Tau *in vitro*. However, with advance of pathology by Braak stages the levels of granular oligomers decreased, when tangle formation is higher, meaning that they could be pre-tangle structures (Maeda et al., 2006).

Concluding, the precise composition and pathological significance of oligomers has yet to be fully understood.

1.2.2.2. NFTs

NFTs are toxic species characterized by intraneuronal accumulation of fibrillar material named PHF. This term was introduced by Kidd in 1963 to describe filaments in AD neurons (Kidd, 1963). PHF is produced by a double helical stack of morphological units, each with a C-shaped cross-section displaying three domains. By electron microscopy, PHF was determined to have between 8 nm and 20 nm of width with a cross-over spacing of 80nm (Crowther, 1991). A higher level of organization will be the arrangement of protofibrils within a PHF. Their number of interactions is currently unknown, but there are several constrains for possible arrangements. One of them described that the mass per-length of the PHF core, determined by scanning transmission electron microscopy is about 60-70 KDa/nm, equivalent to approximately 3.5-4.5 repeat domain molecules per nm (von Bergen et al., 2006).

With aging, NFT spread from the transentorhinal cortex to the hippocampal formation. Neuropathological as well biochemical studies show that Tau spreads progressively, invariably from the transetorhinal cortex to the whole neocortex, along the cortical-cortical connections (Vingtdeux et al., 2012). However, recently Braak and Del Tredici describe locus coeruleus as the initiating region of NFT formation (Braak & Del Tredici, 2011)

Hyman and colleagues defined 3 majorly stages of NFTs, pre-tangle phospho-Tau aggregates, intraneuronal NFTs, and extraneuronal NFTs. Pre-tangles showed granular cytoplasmatic phospho-Tau staining, with a detectable nucleus and the normal cell morphology. This was observed especially with phosphor-Tau antibodies, which recognize phosphorylation at T231, S262 and T153.

Intraneuronal NFTs includes aggregated filamentous structures within cytoplasm and the cell nucleus, but these often eccentric or pyknotic. These fibrillar structures of Tau were most preeminently stained with phosphorylation dependent antibodies that recognize T175, T185 and S262, S356, S422, S46, S214. Extraneuronal aggregates show extracellular phospho-Tau filaments, but these are not related with to the neuronal soma or nucleus. This prominent filamentous form of Tau is most significantly recognized by antibodies recognizing the phosphorylation at S199, S202, S205, S214 and T212. However, in intracellular and extracellular NFT there are common phosphorylated sites S396 and S404 (Augustinack, Schneider, Mandelkow, & Hyman, 2002; Lu, 2005).

1.2.3. The role of Tau in pathogenic mechanism

In pre-clinical stages of AD, Tau pathology is distributed in the hippocampal formation and temporal cortex. However, Braak et al, described that when Tau pathology is found in other brains areas, it is constantly along stereotyped, sequential pathways categorized into six stages according to the brain regions successively affected. Initially there is the occurrence of pretangles in axons and dendrites of noradregenic cells. After this, pretangles also appear in non-thalamic brainstem nuclei with diffuse cortical projections. Stage I, includes the formation of pre-tangles in the cerebral cortex. The cell-to-cell propagation of abnormal Tau molecules could utilize synaptic contacts between subcortical terminal axons and pyramidal cells of the transentorhinal region. The pathological process progresses to mesocortical areas of the media temporal lobe and to neocortical high-order association areas as been defined by Braak as NFT stage II, III, and IV. The stage V-VI is defines as when NFT reach secondary and primary fields of the neocortex. This hypothesis suggested by Braak propose that the spreading process is a process likely transmitted through cortical-cortical connections, in an organized manner and not randomly and most likely not by diffusion (Braak & Braak, 1991; Braak & Del Tredici, 2011).

Evidence that Tau mutations and hyperphosphorylation can affect microtubule binding proposes that impairment of microtubule function and axonal transport contributes to neurodegeneration in AD (Brunden, Trojanowski, & Lee, 2009a). Alterations in the expression and the activity of Tau kinases such as GSK3ß, CDK5, and CK1 have been reported in the brains of AD, suggesting that one or several of them could be involved in the Tau hyperphosphorylation (Chung, 2009). GSK3ß phosphorylates Tau at T231

residue, which makes the C-terminus of Tau an easier substrate for hyperphosphorylation, promoting NFT formation (Martin et al., 2011)[Figure 8].

On the other hand, PP2A activity is reduced in 50% of AD brains, and in *in vitro* studies, incubation of Tau aggregates with this phosphatase restores Tau binding to microtubules to a level similar to that of controls. The endogenous inhibitors of PP2A, I_1^{PP2A} and I_2^{PP2A}, have been shown to be increased by 20% in neurons of AD brains and to co-localize with PP2A and hyperphosphorylated Tau (Chen, Li, Grundke-Iqbal, & Iqbal, 2008).

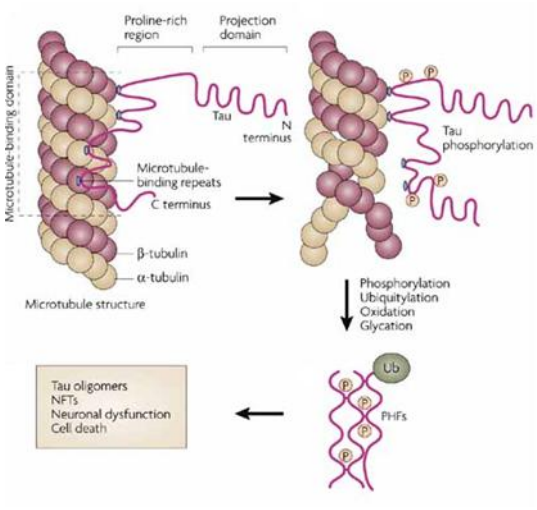

Figure 8 - Representation of the hyperphosphorylation of Tau that occurs in in AD (Mazanetz & Fischer, 2007).

Recent results may indicate that abnormal phosphorylation is a key event that triggers the pathological aggregation of Tau in AD (Mondragón-Rodríguez et al., 2008). The other post-translational modification, glycation, is also involved in promotion of Tau polymerization and stabilization of aggregated Tau proteins, but it does not induce Tau aggregation by itself (Martin et al., 2011). Nitration may also promote aggregation, since Tau nitration at Y29 was found in AD brains, is proposed that nitration decreases Tau ability to promote tubulin assembly leading to Tau oligomerization (Martin et al., 2011). Another post-translational event that may facilitate Tau aggregation is proteolytic cleavage, as it seems that both calpain and caspases, can act on Tau producing fragments that may have an increase propensity to aggregate (Brunden et al., 2009a)

It is possible that changes in protein kinase and/or phosphatase activities could enhance Tau phosphorylation resulting in loss-of-function (LOF) and/or gain-of-function (GOF) toxicities. However, additional post-translational modifications may also contribute to Tau dysfunction (Alonso, Zaidi, Grundke-Iqbal, & Iqbal, 1994).

The hypothesis that Tau LOF contributes to neuronal dysfunction shows that disease phenotype were caused by loss of Tau function due to hyperphosphorylation and sequestration of soluble Tau (Zhang et al., 2005). In other words, neurodegeneration is due to the loss of Tau caused either by a decrease in Tau microtubule binding capabilities or by a decrease of the available pool of Tau protein as a result of aggregation and/or phosphorylation (Dawson et al., 2010). However, there are data that contradict the viewpoint that Tau LOF contributes to neurodegeneration, because some recent studies demonstrated that loss of Tau function is an unlikely cause of neurodegeneration and neuronal dysfunction. Studies suggest that the complete depletion of Tau in Tau knockout mice does not cause premature mortality or major abnormal deficits (Dawson et al., 2010; Yuan, Kumar, Peterhoff, Duff, & Nixon, 2008). Based in electrophysiological recordings in acute hippocampal slices, Tau knockout mice and WT controls have

similar NMDA/AMPA receptors currents, synaptic transmission strength and short-term as well long-term synaptic plasticity (Roberson et al., 2011; Shipton et al., 2011).

On the other hand, the other hypothesis predicts that misfolded and aggregated Tau protein causes a gain of toxic function by delaying normal axonal processes. This argument is supported by *in vitro* experiments demonstrating that mutations in Tau gene either decrease the binding of Tau to microtubules or increase aggregation of the mutant Tau proteins (Barghorn et al., 2000;Gamblin et al., 2000). It is hypothesized that the decreased ability of mutated Tau to bind to microtubules would allow for more free Tau and therefore increase Tau aggregation (Dawson et al., 2010). Being mutated Tau more prone to aggregate, and taking in account that Tau aggregates are toxic, it is possible to affirm that Tau gains a toxic function.

1.2.4. Cellular model to study the effect of Tau in Tauopathies

Cellular models have also been used in AD research. Guo et al. established a cellular system that robustly develops NFT-like Tau aggregate which provides mechanistic insights into NFT pathogenesis. The induction of formation of intracellular aggregates in this model is different to the models described previous since (i) intracellular aggregates are morphologically different to the previous studies; (ii) the intracellular aggregates exhibits a diversity of morphologies, which probably represent different stages of aggregation similar to Tau tangles detected in Tauopathies; (iii) Use of protein delivery reagent to augment introduction of performed fibrils into cells provides better efficiency of Tau performed fibrils entry as compared to previous studies.

In this study, Tau aggregation could be rapidly induced within hours after the introduction of small quantities of misfolded Tau preformed fibrils and result in accumulation of large amounts of insoluble Tau fibrils.

In summary, the authors of this paper established a reproducible and robust, cellular model of Tau aggregation in which the key features of Tauopathies are present. This model is a potential system for the identifying therapeutic strategies against Tauopathies.

Until now the present model to test aggregation *in vitro* proposed by Guo and the colleagues seems to be the best model to test the Tau aggregation.

1.2.5. Animal models to study the effect of Tau in Tauopathies

Several approaches have been adopted in an attempt to model Tauopathies in vertebrates, to elucidate their pathogenic mechanisms and to investigate potential therapeutics interventions. Transgenic animals for genomic human Tau, as well as mice carrying cDNAs encoding either the largest or the smallest CNS isoform of human Tau have been generated (Avila et al., 2004).

In the field of the Tauopathies, there are several models of transgenic mice expressing either the longest Tau isoform (4R-Tau), that may favor fiber formation, or the shortest one (3R-Tau) (Buée et al., 2000). The first transgenic mice to be published that carried cDNA encoding the largest human brain Tau isoform showed low levels of overexpression. The transgenic human Tau protein was present in nerve cell bodies, axons and dendrites (Götz et al., 1995). Two studies reported the generation of transgenic mice expressing mutant human Tau containing the P301L mutation that is located in the tubulin-binding domain, and that reduces the affinity of Tau microtubules (Götz, Tolnay, et al., 2001; Lewis et al., 2000). These transgenic mouse lines expressing human MAPT with a proline to leucine mutation at amino acid 301 (P301L) recapitulate aspects of familial FTLD (Orr, Pitstick, Canine, Ashe, & Carlson, 2012), having developed NFTs mainly in the spinal cord, and like the previous transgenic models, some neuropathological symptoms encouragingly reminiscent of the human disease (Götz et al., 2001). In this model it was verified that extensive axonal and myelin degeneration also occurred in peripheral nerves, and that neuronal loss is similar of what occurs in FTLD and the other Tauopathies. This model also shows a behavioral deficit (Lewis et al., 2000).

A significant body of data demonstrates that a large excess of normal or mutant human Tau can promote some of the cellular changes observed in Tauopathies, however that this may also be insufficient for the formation of the mature neurofibrillary aggregates observed in the human disease (Avila et al., 2004). Thus, transgenic mice models of Tauopathies exhibit similarities which the pathological mechanisms involved in AD, especially in regard to the aberrant intracellular targeting of Tau proteins (Buée et al., 2000).

1.3. Tau focused AD treatments

Treatments of various aspects of Tau biology are under intense investigation. Therapies targeting Tau phosphorylation, aggregation and microtubule stabilizers are already in clinical trials for people with MCI, AD and different Tauopathies. However more research in this field is necessary.

Tau phosphorylation inhibitors

Normal Tau is phosphorylated at many residues, and the extent of this phosphorylation is considerably increased in the brains of patients with AD (Matsuo et al., 1994). Inhibiting Tau hyperphosphorylation requires an understanding of the specific enzymes that are involved in these modifications (Brunden, Trojanowski, & Lee, 2009). Numerous Tau kinases have been implicated in AD pathogenesis, but the most widely studied are GSK-3ß, CDK5, MARK and MAPK.

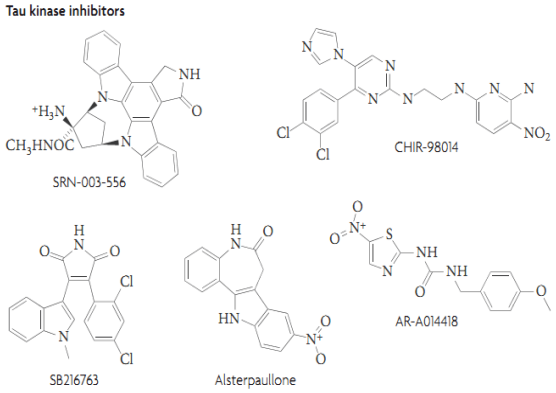

Figure 9 - Structures of the compounds that inhibits Tau kinases (Brunden et al., 2009)**.**

There is indeed substantial evidence to suggest that CDK5 and GSK-3ß are relevant kinases in Tauopathies. Interestingly, both kinases have been implicated in the upregulation of Aß synthesis, so inhibition of these kinases leads to a decrease in Aß levels (Phiel, Wilson, Lee, & Klein, 2003). Recent animal studies demonstrated that Lithium, a potent inhibitor of GSK-3ß, decreases levels of phosphorylated Tau and the expression of this kinase in the cortex and hippocampus, suggests that GSK-3ß is one of the key targets for future disease-modifying therapies for AD (Mendes et al., 2009; Selenica et al., 2007). MARK1, another important kinase present in Tau fibrils in AD brain, could be a most promising candidate to reduce Tau hyperphosphorylation. Cells that overexpress this kinases showed increased Tau phosphorylation, and enhanced neurotoxicity (Brunden et al., 2009).

Although kinase inhibitors have been used successfully in oncology, it remains to be determined whether these molecules can be usefully administrated on a chronic basis for the treatment of Tauopathies.

Tau aggregation inhibitors

Conversion of soluble Tau into oligomeric and fibrillar species could result in Tau GOF and LOF toxicities. Inhibiting Tau assembly into multimeric structures might therefore prevent the formation of toxic species and increase the levels of monomeric Tau, which could contribute to the microtubules stabilization (Brunden et al., 2009).

The first compound that was reported to inhibit Tau interactions was the phenothiazine methylene blue, which was shown to alter the structure of existing PHFs that were isolated from the brains of patients with AD (Wischik, Edwards, Lai, Roth, & Harrington, 1996) [Figure 10]. Results of the Phase II data presented at 2008 international conference on Alzheimer suggests that this compound had a positive therapeutic effect, even though larger Phase III studies are required (Brunden et al., 2009).

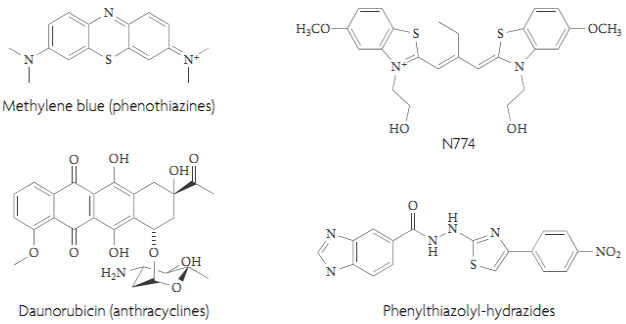

Figure 10 - Structures of the compounds that inhibits Tau fibrillation (Brunden et al., 2009)

Another dye-like molecule, N744, has also been identified as an inhibitor of full-length Tau fibrillation and, like methylene blue, this compound could disaggregate existing filaments (Chirita, Necula, & Kuret, 2004).

However, many of the drugs that block aggregation of the Tau also block the pathological aggregation of others proteins under cell free conditions, including Aß and α-synuclein, suggesting that therapies might be of benefit in diverse disorders correlated with protein aggregation (Morris et al., 2011).

Many of the existing Tau assembly inhibitors have chemical or biological properties that will probably make them unsuitable for the generation of reactive species that increase the potential for off-target effects (Brunden et al., 2009). Therefore preferred compounds are likely to be those that prevent the initial stages of Tau-Tau interaction, so they lead to an increase of Tau monomers and not uncharacterized intermediate multimeric structures, which could have a biological activity (Brunden, Trojanowski, & Lee, 2008) [Figure 13].

Enhancing intracellular Tau degradation

There are two pathways involved in degradation of the misfolded cytosolic proteins, UPS and macroautophagy. There is evidence that both of these systems may be affected in AD brain and, although normal Tau has not been shown to use these systems, there are reports which suggests that hyperphosphorylated and misfolded Tau can undergo degradation through both of these pathways (Keller, Hanni, & Markesbery, 2000; Nixon et al., 2005).

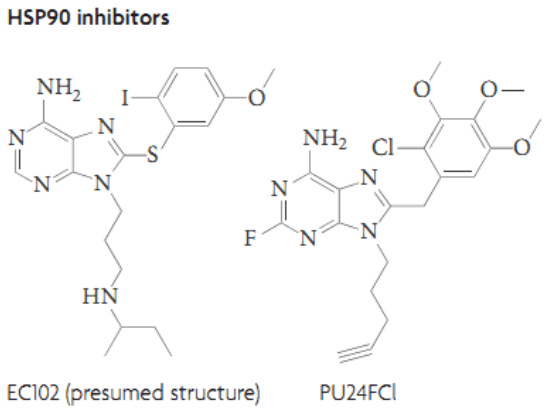

Figure 11 - Structures of the compounds that inhibits HSP90 (Brunden et al., 2009).

The ubiquitin ligase for Tau was recognized as the C-terminus of heat-shock-protein 70 (Hsp70) interacting protein CHIP (Hatakeyama et al., 2004). Recent studies suggest that CHIP works in combination with heat shock proteins to regulate Tau degradation. Levels of Hsp90 correlate inversely with the levels of soluble Tau and Tau oligomers, (Dickey et al., 2007; Sahara et al., 2007) however Hsp inhibitors, molecules that inhibit refolding but stimulate degradation, in this case Hsp90 inhibitors, seem to hold promise in reducing phosphorylation and misfolding of monomeric Tau through the UPS, it is unlikely that this strategy would

affect larger Tau oligomers and fibrils (Brunden et al., 2009)[Figure 13]. Immunosuppressant FK506 that reduces microgliosis and Tau aggregation in transgenic mice overexpressing P301S human 4R1N could be used as treatment by forming complexes with Hsps (Yoshiyama et al., 2007). Since this compound affects diverse signaling pathways in many cell types, it may act directly on neurons or influence the neuronal environment by modulating glial activation. Inhibition of Tau aggregation may also be mediated by direct binding of Tau to the FK506 binding protein (Morris et al., 2011)

Larger aggregates of Tau are not likely to be accessible to the proteasome but degraded by the autophagy system. Studies demonstrated that addition of the autophagy inhibitor 3-methyladenine lead to enhanced Tau accumulation and Tau aggregation (Hamano et al., 2008). Consequently, this is a great evidence that aggregated Tau can be degraded by autophagy system and the upregulation of this system with drugs such as rapamycin, and nilvadipine, that blocks the calcium channel, might be a potential strategy for the treatments of Tauopathies (Tung et al., 2012).

Increasing the activity of one or both of these catabolic systems may therefore lead to reduction of pathological Tau in AD and in the others Tauopathies (Brunden et al., 2009)

Microtubule stabilization treatment

As referenced before, Tau plays an important role in stabilizing microtubules within neuronal cell populations. In AD patient's brains we can find a decrease in the number and length of microtubules and a reduction in the levels of MT-binding can be clearly linked to a disruption in Tau function (Himmelstein et al., 2012). In an attempt to compensate for the loss of Tau function, different research groups are testing different microtubule stabilizing compounds, like taxane, already used in cancer therapies. This has been deemed however unsuitable for Tauopathies, as it does not effectively penetrate the BBB and its side effects render it ineffective for long term use (Brunden et al., 2011).

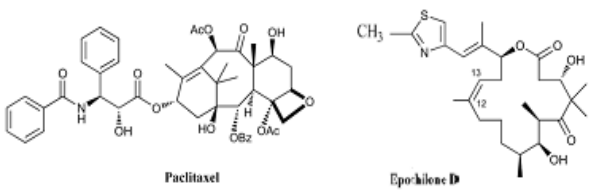

Figure 12 - The structures of the compounds that are involved in microtubule stabilization (Brunden et al., 2011).

Nevertheless microtubule stabilization drugs currently in use for cancer treatments seem to be a good way to developed new treatments in Tau related disorders, as their metabolism and toxicity effects are already well established. Epothilone D (EpoD) it is one of most promising candidates, since it has been suggested that this compound can cross the BBB (Andrieux et al., 2006; Brunden et al., 2010). In one of the studies with transgenic mice expressing the human Tau containing a PS19 mutation, EpoD treatment showed an improvement in microtubule density, in axonal integrity and what seems to be a reduction in cognitive decline (Brunden et al., 2010). Additional analysis of EpoD and other brain-penetrate MT-

stabilizing agents are nevertheless necessary to provide more information about safety and efficacy before these compounds could be used for therapeutically approaches in Tau related disorders.

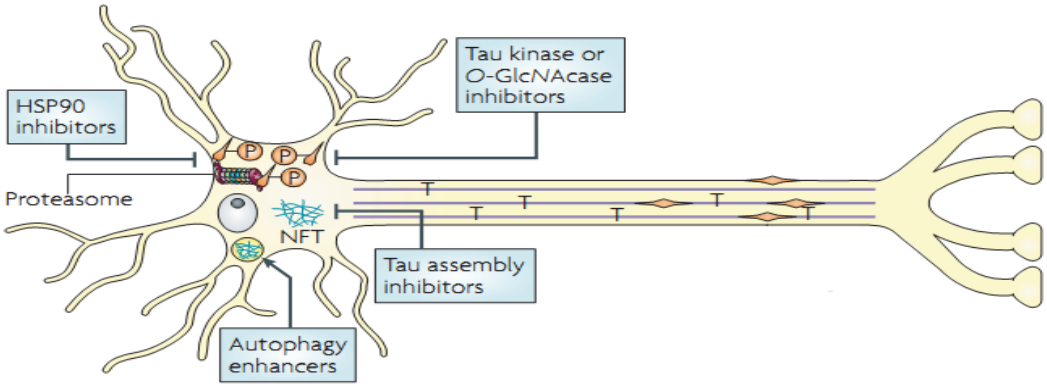

Figure 13 - Summary of therapeutic strategies focused in Tau pathology (Adapted Brunden et al., 2009).

1.4. Tau clearance by intracellular degradation

The trigger of Tau aggregation and Tau-induced neurodegeneration is still elusive. The impairment of protein-degradation systems might play a role in pathways that normally keep Tau levels at a low level which may prevent aggregation. The two major pathways that are associated with degradation of proteins are UPS and autophagy-lysosome-system. UPS system is the intracellular mechanism mostly responsible for degradation of short-lived proteins, whereas autophagy is associated with degradation of many long-lived proteins and damage organelles. The Hsp70/Hsp90 systems play also a critical role in the regulation of Tau degradation through proteasome system, and chaperones could also be involved in Tau degradation mediated by autophagy.

In a initially stage of AD, UPS is the primary clearance system of pathological Tau, however the importance of autophagy-lysosome-system mediated Tau degradation is increased particularly in late stage of NFT formation.

1.4.1. Contribution of UPS and autophagy in Tau degradation

The UPS is a major cellular mechanism that regulates intracellular protein levels and eliminates damaged, misfolded and mutant proteins for protein quality control in cytoplasm and in nucleus (Lee, Lee, & Rubinsztein, 2013). The proteasome is a protein complex consisting of at least 33 distinct subunits. Structurally and functionally, proteasomes comprise the 28-subunit core particle, also known as 20S

catalytic core, and the 19-subunit regulatory particle, also known as 19S particle (Kisselev, Callard, & Goldberg, 2006). The 20S catalytic core contains three types of subunits that execute trypsin-like, chymotrypsin-like and peptidylglutamyl-peptide hydrolyzing activities (Yipeng Wang & Mandelkow, 2012). The conical ubiquitin-proteasome pathway involves two steps: (i) UPS substrates are covalently conjugated with ubiquitin, a highly conserved 76-residue protein, that is involved in a cascade mechanism involving ubiquitin-activating enzyme E1, ubiquitin conjugated enzyme E2 and ubiquitin ligase E3; and (ii) degradation of the ubiquitinated protein by the 26S proteasome with the release of free and reusable ubiquitin (Shang & Taylor, 2011).

The downregulation of enzymes E1 and E2 have been reported in AD (Shang & Taylor, 2011). The initial clue for the pathological link between Tau and UPS was derived from the frequent co-localization and accumulation of ubiquitin in PHFs and NFTs, since Tau ubiquitination occurs both in monoubiquitinated and polyubiquitinated forms (De Vrij, Fischer, Van Leeuwen, & Hol, 2004). Another study, reported a significantly decrease of trypsin-like activity in post-mortem AD brains (López Salon, Morelli, Castaño, Soto, & Pasquini, 2000),and this subunit seemed the most critical for the degradation of full-length Tau and its truncated forms. Another unclear area is how unfolded Tau proteins are recognized by proteasome and translocated in the active sites. One of the options is that Tau is slowly but constantly degraded through ubiquitin-independent process under normal conditions, as in stress conditions, Tau proteins are actively ubiquitinated by CHIP and removed by 26S proteasomes. Therefore, if we consider that most of the natively unfolded proteins are short-lived, and since Tau is relatively stable, ubiquitin-independent proteasomal degradation may be more responsible for Tau turnover than ubiquitin-dependent degradation. Some studies suggest that proteasomal dysfunction could be associated with beginning or facilitation of Tau aggregation process, however there is a reciprocal process between abnormal UPS activity and PHF formation, being the impairment of the proteasome function as a consequence of AD, instead of the cause of Tauopathies (Lee et al., 2013).

Higher ordered oligomers and aggregates are more likely to be inaccessible to the narrow proteasome opening and these species are expected to have much higher dependency on autophagy for degradation. There are three type of autophagy: 1) macroautophagy that is the main pathway for eukaryotic cells to degrade long-lived proteins and organelles; 2). microautophagy where the lysosomal membrane directly engulfs part of the cytosol; and 3).chaperone-mediated autophagy, a type of selective autophagy targeting soluble cytosolic proteins containing a motif biochemically related to the pentapeptide KFERQ (Lys-Phe-Glu-Arg-Gln) (Wang & Mandelkow, 2012) .

Autophagy involves the formation of a double-membrane vesicle termed the autophagossome and its sequestration of a portion of the cytoplasm. The completed autophagosome has a diameter of 300-900 nm and matures by fusing with lysosomes to form autolysosomes, allowing hydrolysis of target substrates or organelles (Yorimitsu & Klionsky, 2005). In pathological AD brains an accumulation of autophagosomes

and autolysosomes was reported, suggesting that the basal autophagy process in neurons is abnormal in AD (Lee et al., 2013).

Several studies, using neuronal ATG gene knockout mice, a gene essential for autophagy, revealed that autophagy is critical for normal neuronal health. They proved that with loss of either ATg5 or ATg7 autophagy genes in CNS, an age-dependent accumulation of intraneuronal aggregates with polyubiquitination, inclusion formation and neurodegeneration occurred (Hara et al., 2006; Komatsu et al., 2006). In a transgenic mice with overexpression of P301L Tau mutation, autophagy vacuoles were found to accumulate in neurons (Lin, Lewis, Yen, Hutton, & Dickson, 2003). An increase in the number of lysosomal complexes was also detected in neurons in transgenic mice expressing Tau with G272V, P301L and R406W mutations (Lim et al., 2001).

Numerous experiments confirmed that the chemical inhibition of lysosomal degradation could delay Tau clearance, enhance Tau aggregation, and evoke cytotoxicity (Hamano et al., 2008),

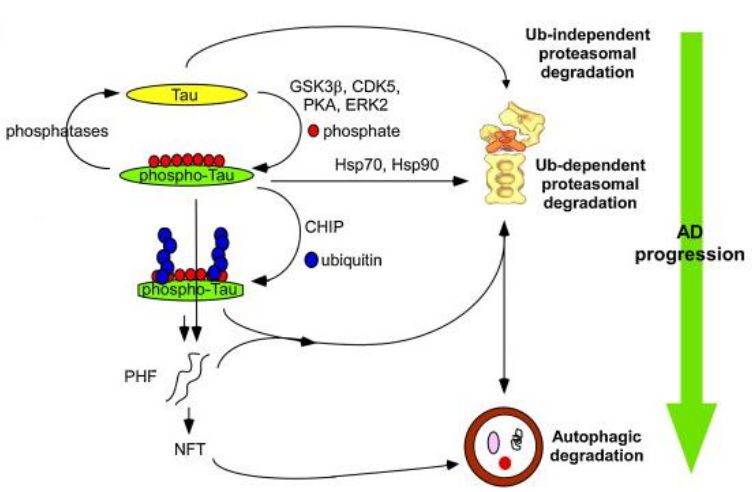

Figure 14 - Illustration of pathways involved in clearance of Tau protein. In early stage, the soluble Tau could be degraded by UPS ubiquitin dependent or independent mechanisms, however the Tau oligomers is inaccessible to UPS and are degraded by autophagy-lysosome system (Adapted from (Lee et al., 2013)).

1.4.2. Chaperone complexes action on Tau protein to increase intracellular degradation

In all cells, there are a large group of unrelated proteins which assist protein folding by reversible binding to unfolded and misfolded proteins and thus prevent their aggregation and facilitate formation of a correct conformation of a non-native protein. This group is called chaperones, and they can augment the functional activity of proteins, direct the cellular trafficking and also induce their degradation (Hartl, 1996). The chaperones only transiently interact with their substrate proteins and are not present in the final folded product (Turturici, Sconzo, & Geraci, 2011). One of the principal functions of molecular chaperones

is to retain protein quality during stressful insults (Salminen, Ojala, Kaarniranta, Hiltunen, & Soininen, 2011).

Heat shock proteins (Hsp) are protectors of cells against different kinds of stress. In mammalians, Hsp groups can be classified according to their proprieties into several families, Hsp70, Hsp90, Hsp60, Hsp40 and small Hsps (Morimoto, Kline, Bimston, & Cotto, 1997). The transcriptional factor responsible for Hsp transcriptional activation is the heat shock transcription factor 1 (HSF1). According to the chaperone based model, HSF1 in unstressed cells is maintained is an inactive complex with Hsp90, Hsp40, and Hsp70. When increased Hsp levels are necessary in response to cellular stress, HSF1 is released from the complex and migrates to the nucleus, and leads to their upregulation (Pirkkala, Nykänen, & Sistonen, 2001)[Figure 15].

Hsps complexes can bind a large variety of client proteins, called clientele. The versatile chaperones complexes facilitates the maintenance of protein dynamics in cellular environment (Salminen, Ojala, Kaarniranta, Hiltunen, & Soininen, 2011). Hsps also exhibit a variety of cytoprotective functions, in addition to all other functions of this complexes by inhibiting the apoptosis cascade (Beere, 2004). In the nervous system, Hsp are induced in a variety of pathological states, including cerebral ischemia, neurodegenerative diseases, epilepsy and trauma. Their expression has been detected in multiples cells types, including neurons, glia and endothelial cells (Foster & Brown, 1997).

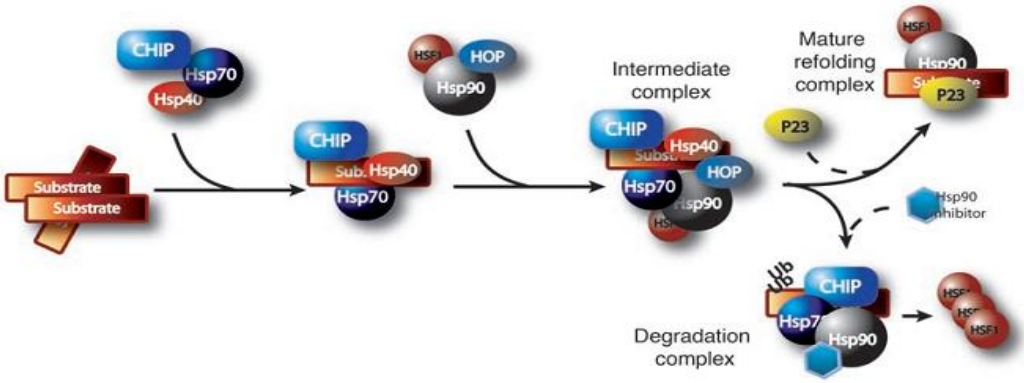

Figure 15 - Mechanism suggested of chaperone/client pathway. A substrate may initially be recognized by the Hsp40/Hsp70 complex with CHIP as the cochaperone/E3 ubiquitin (Ub) ligase. Transfer of the substrate to the Hsp90 complex is facilitated by Hop. There remain 2 fates for the substrate: dephosphorylation and refolding or ubiquitin-dependent proteasomal degradation. The mechanisms dictating which pathway is taken remain undefined. Hsp90 expression inhibits HSF1 activity by direct binding, which prevents HSF1 phosphorylation and trimerization. When Hsp90 is inhibited, Hsp90 levels are decreased, releasing HSF1, which in turn promotes de novo transcription of HSPs and stimulates the degradation pathway (Dickey et al., 2007).

1.4.2.1. Chaperone – assisted Tau degradation

Defective proteins will be initially labeled with ubiquitin tags in Hsp90 complexes. The co-chaperones Hsp70-interacting protein (Hip) and Hsp70/Hsp90-organizing protein (Hop) both interact with Hsp70 via their tetratricopeptide repeat (TPR) domains. In a screen for additional TPR-containing proteins, a protein named CHIP was identified. It was found that CHIP interacts with Hsp70 and inhibits its ATPase activity suggesting that CHIP might be involved in an Hsp70-mediated process distinct from refolding. CHIP can interact with either Hsp70 or Hsp90 through the same TPR, displacing them from Hop or other TPR-containing proteins (Goryunov & Liem, 2007). This needs the recruitment of CHIP into the complex. CHIP is a co-chaperone with E3 ligase activity, highly expressed in the brain, cardiac and skeletal muscles.(Murata, Minami, Minami, Chiba, & Tanaka, 2001). These conjugating enzymes, linked to K48 ubiquitination, controls whether the protein will be directed to proteasomes. CHIP is associated with the MBD of Tau, and especially ubiquitinates the four-repeat Tau rather than the three-repeat counterpart. Later studies, revealed that the up-regulation of CHIP expression can attenuate Tau aggregation (Salminen et al., 2011). Previous studies in mice showed that a CHIP deficiency in this animal causes the accumulation of Tau protein, but does not causes Tau aggregation (Dickey, Yue, et al., 2006). This deficiency in mice also induces a decline in proteasome activity (Min et al., 2008).

Several studies demonstrate that CHIP works in combination with Hsps to regulate Tau degradation, and levels of Hsp90 correlate inversely with the levels of soluble Tau and Tau oligomers (Morris et al., 2011)

The chaperone mediated autophagy is a selective, chaperone-assisted uptake pathway for cytoplasmic proteins, guiding them to lysosomal degradation. Nevertheless, the uptake for this pathway needs a specific motif, KFERG-like sequence, in the protein and the uptake process requires a chaperone complex involving Hsp90, Hsp70 and Hsp40 (Bandyopadhyay, Kaushik, Varticovski, & Cuervo, 2008). Tau protein contains two pentapeptide motifs eligible for degradation by this pathway, the WT Tau has no affinity to chaperone-mediated autophagy uptake but instead, could be degraded via macroautophagy (Wang et al., 2009). This indicate that aggregation-prone Tau protein can be degraded via macroautophagy which is a typical clearance pathway in multiple neuronal disorders involving proteins (Menzies, Ravikumar, & Rubinsztein, 2006).

1.4.2.2. Hsp70 in aggregation

In contrast with other Hsps, Hsp70 proteins are found in almost all intracellular compartments. In humans, the Hsp70 multigene family includes the cytosolic and nuclear localization tag. Similar to the others chaperones, Hsp70 adopts three different conformations, one in the absence of a nucleotide, one with

ADP bound, and one with ATP bound (Turturici, Sconzo, & Geraci, 2011). This protein is involved in different chaperoning processes, such as refolding of misfolded or aggregated proteins, preventing protein aggregation, folding and assembly of nascent polypeptides, and promoting the ubiquitination and degradation of misfolded proteins (Young, Barral, & Ulrich Hartl, 2003). The role of Hsp70 in folding of non-native proteins can be separated into three activities: prevention of aggregation; promotion of folding the native state; and solubilization and refolding of aggregated proteins (Mayer & Bukau, 2005). Molecular chaperones and components of the proteasome can also be found in aggregates formed in transgenic animal models and transfected cell cultures by various polypeptides, as intracellular Tau tangles. In various cellular models, increased levels of Hsp70 promote Tau solubility and Tau binding to microtubules, reduce insoluble Tau and cause reduced Tau phosphorylation (Dou et al., 2003; Jinwal et al., 2010).

Several studies, in recent years, have demonstrated that activation of the heat-shock response (HSR), and in particular elevation of Hsp70 levels, has a neuroprotective effect that is believed to be related mainly to its chaperone role.

1.4.2.3. Heat shock protein 90

The 90-KDa Hsps are ATP-dependent molecular chaperones that interact with many co-chaperones to fold proteins or targets misfolded proteins for degradation (Lu, Ansar, & Michaelis, 2009). This protein contain three domains; (i) N-terminal domain contains the binding site for adenine nucleotides and displays a low inherent ATPase activity; (ii) intermediate segment that interacts with client proteins; (iii) C-terminal domain mediates the dimerization of Hsp90 proteins and co-chaperone binding (Pearl & Prodromou, 2006).

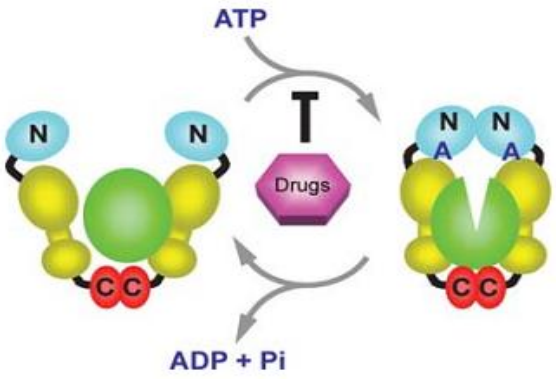

Figure 16 - Representation of the current model for the conformational changes that accompany binding and hydrolysis of ATP by Hsp90 on the basis of structural and biochemical evidence. Inhibition of ATP binding by drugs, such as geldanamycin, blocks client protein activation (Pearl & Prodromou, 2006).

The ATPase domain is an important therapeutic target, since geldanamycin (GA), radicicol and their derivates, modulates at least two different conformational states, and can bind to and inhibit the action of Hsp90 chaperone complexes (Pearl, Prodromou, & Workman, 2008) [Figure 16]. In general, Hsp90 complexes can assist in the folding process of proteins, stabilize them and even activate their clients. The most important regulators of this chaperone machinery are the co-chaperones and, the post-translational modifications of

the Hsp90 protein itself, for example acetylation, where this can inhibit the binding of clients to Hsp90, nitrosylation and phosphorylation (Wandinger, Richter, & Buchner, 2008).

1.4.2.4. Hsp90-CHIP complexes

Different studies have demonstrated that CHIP protein, with the Hsp90 chaperone complex, has a key role in the removal of phosphorylated Tau protein. The same studies showed that CHIP does not recognize Tau proteins which are phosphorylated at normal Ser residues but binds only to mutant proteins and those which are phosphorylated at proline-directed Ser/Tyr sites. Therefore, the authors of this paper demonstrated that high-affinity Hsp90 binding complexes are present in the affected regions of AD brain but not in control samples (Dickey et al., 2007;Dickey, Dunmore, et al., 2006). Evidences suggested that Hsp90 forms a complex with mutated or distinctively phosphorylated Tau species and consequently recruit protein phosphatases, to facilitate dephosphorylating and refolding process (Goryunov & Liem, 2007). There is a kind of phosphorylation code in Tau which determines whether the Hsp90 complexes dephosphorylate the Tau protein and enhance its binding to microtubules or recruit CHIP and mark the Tau with ubiquitin for degradation or in some contexts for aggregation. This evidence indicates that the effects of CHIP are neuroprotective rather than toxic (Dickey,Patterson, Dickson, Petrucelli, 2007). Minor perturbations in the chaperone system with aging may reduce the turnover of Tau, leading to aggregation and subsequent neurodegeneration (Dickey et al., 2007).

1.4.2.5. Hsp90 complexes and Tau aggregation

The functional role of Hsp90 chaperone in the aggregation of aberrant Tau protein is still largely unknown. However, this chaperone is associated with maintenance of the functional stability of neuronal proteins of aberrant capacity, thus allowing and sustaining the accumulation of toxic aggregates (Luo, Sun, Taldone, Rodina, & Chiosis, 2010). It is know that Hsp90 increase the stability of the oncoproteins and in that way can enhance cancerous growth (Luo, Rodina, & Chiosis, 2008). In neurodegenerative disorders associated with protein aggregation, the rationale has been that inhibition of Hsp90 activates HSF-1 to induce production of Hsp70 and Hsp40, as well as of other chaperones, which in turn, promote disaggregation and protein degradation (Muchowski & Wacker, 2005). Previous studies also demonstrated that Hsp90 inhibition selectively reduced the level of Tau phosphorylated at proline-directed Ser/Tyr sites (Dickey, Dunmore, et al., 2006).

When the cells are exposed to conditions of stress, the cells normally respond by activation of the HSR accompanied by increased synthesis of a number of Hsp which reduce cytotoxicity, such as caused by misfolded and denatured proteins (Muchowski & Wacker, 2005). In mammals, protein damaging stress is regulated by activating of HSF-1, which binds to upstream regulatory sequences in the promoters of heat shock genes, and the function of HSF-1 is regulated by Hsp90 (Anckar & Sistonen, 2007).

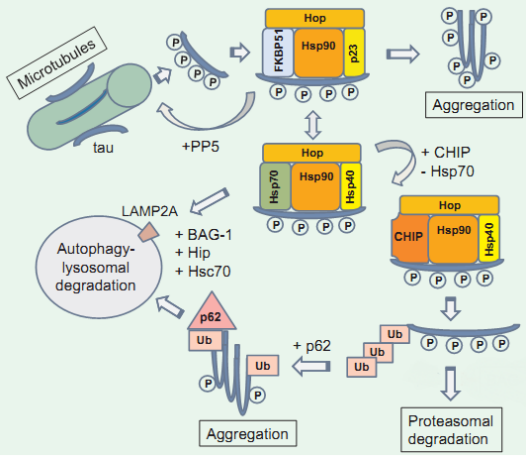

Figure 17 - Representation the role of Hsp90 chaperone complexes in the regulation of, client protein of Hsp90, Tau protein modifications and trafficking (Salminen et al., 2011).

However, under non-stress conditions, Hsp90 binds to HSF-1 and maintains the transcription factor in a monomeric state. In other words, stress, heat shock, or inhibition of Hsp90 release HSF-1 from the Hsp90 complex, which results in its trimerization, activation and translocation to the nucleus where it induce a heat shock response manifested in the production of Hsps such as the chaperones Hsp70 and its activator, Hsp40 (Brown, 2007). The function of Hsp90 can be inhibited by acetylation and subsequently blocks the binding of ATP to Hsp90 protein. This inhibits Hsp90 and the clients are degraded in the same way as with drugs targeting directly the ATP binding motif (Bali et al., 2005).

1.4.2.6. Hsp90 inhibitors

As mentioned before Hsp90 assists in protein folding, it stabilizes various proteins including oncoproteins, it assists in protein degradation and it regulates HSF-1. Inhibition of ATP binding to Hsp90 with molecules such as GA enhances degradation of Hsp90 client proteins and results in the activation of HSF1 (Dickey et al., 2007).

Previous studies identified that Hsp90 inhibitors promoted selective proteasome dependent degradation of aberrant p-Tau species *in vitro*, as well as induction of a significant reduction in the levels of both hyperphosphorylated and insoluble, aggregated mutant Tau in mouse brain (Dickey et al., 2007; Luo et al., 2007). Treatments with Hsp90 inhibitors induce a time-dependent reduction in p35 levels and a clear decline in Tau phosphorylation, meaning that inhibition of Hsp90 can reduce Tau phosphorylation through the inhibition of p35-CDK5 (Salminen et al., 2011). Another Tau kinase, GSK-3ß, is also a client protein of the Hsp90 protein, and this chaperone regulates the autoactivation of GSK-3ß kinase. Diverse studies demonstrated that Hsp90 inhibitors can trigger the degradation of this kinase and thus inhibit it is activity (Banz et al., 2009).

The first identified Hsp90 inhibitors used *in vitro* are GA, and radicicol, two natural products that were developed as antifungal agents, however this compounds are hepatotoxic for clinical use. Another class of Hsp90 inhibitors is Novobiocin analogues. These compounds do not compete for ATP binding, but have been found to be a novel promising class of C-terminal Hsp90 inhibitors (Lu et al., 2009).

Developed from GA, 17-allylaminogeldanamycin (17-AAG), is a less toxic inhibitor than GA, however, this compound has a very low brain exposure, making them not useful (Kamal, Boehm, & Burrows, 2004; Waza et al., 2006). This compound currently is in phase III clinical trial for cancer therapies (Salminen et al., 2011). Hsp90 inhibitors, as GA, disturb the interaction between Hsp90 and HSF-1 and subsequently HSF-1 triggers a heat shock response involving an increase in the levels of several chaperones, as Hsp70 and Hsp40. In cancer therapy, these have a protective role, exerting potent anti-apoptotic activity by inhibiting the assembly of the caspase-9-Apaf-1-cytochrome C apoptosome (Waza et al., 2006). However Dickey and colleagues demonstrated in neurodegenerative disorders, that Hsp90 inhibitors enhance Hsp90/CHIP – mediated p-Tau degradation helps to clarify the mechanisms of Tau metabolism and provides a possible therapeutic strategy for management of Tauopathies [Figure 18]. All these observations indicates that chaperone-mediated therapy could provide therapeutic benefits in AD, either by activating Hsp70, inhibiting other Hsps other than Hsp70, or stimulating HSF1 without Hsp90 inhibition.

In summary, it has been shown that Hsp90 inhibitors seem to hold promise for reducing phosphorylation and misfolded monomeric Tau through the UPS (Brunden et al., 2009).

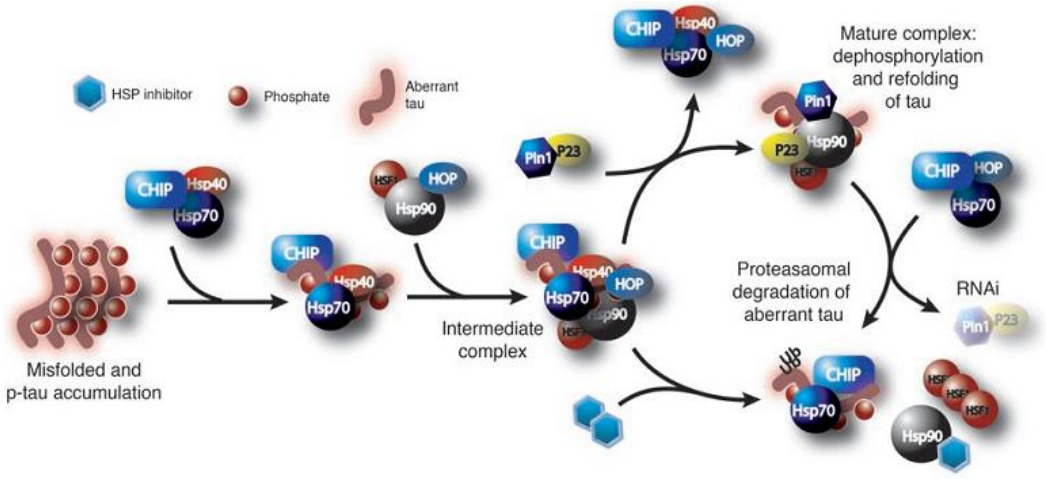

Figure 18 - Components of the constitute chaperones system are required to facilitate degradation of aberrant Tau species by Hsp90 inhibitors, in turn refolding machinery prevents p-Tau degradation (Dickey et al., 2007).

1.5. Objectives

The spreading and clearance of Tau are relevant processes in AD, so in an attempt to study these processes, validate possible targets and initiate drug discovery, it is extremely important to have relevant models as similar as possible to the pathological condition. In an attempt to identify a robust model to study pathological mechanisms that occur in AD, the main goal of this experimental project was to try to develop a seeding and aggregation model *in vitro.*

Of all the existing models already described for Tau pathology, we directed our focus to a model developed by Guo and Lee who reproduced aggregation of Tau in a cellular context, similar to the pathological condition, making this a robust model to study aggregation process.

In this project we optimized Tau aggregation seeding model in primary cortical neurons, with induction of aggregation by seeding with a synthesized and *in vitro* aggregated Tau fragment. Establishing a model related as much as possible to Tauopathy conditions could give us the possibility of studying alterations that occur in neuronal cells, such as post-translational modifications in presence of pathology, spreading of Tau protein in pathological case, pathways involved in endocitosis of pathological forms of Tau, as well as mechanisms involved in degradation of Tau. The strategy used in primary neuronal cultures was extrapolated from QBI cell seeding model, an already optimized model, with some adaptations, for example in neuronal cells we used an adeno-associated-viral vector serotype 6 (AAV6) to deliver hTauP301L gene in cultures instead of transient transfection of plasmid DNA. Our objective was then to optimize this model in primary cortical neurons, so that it can be a reproducible model to study Tau aggregation.

In order to identify a compound that inhibits and/or delay Tau aggregation in QBI seeding model and in neuronal Tau aggregation model, we performed various tests in this model used an Hsp90 inhibitor, 17-AAG, to evaluate its capacity of altering the process of Tau aggregation and contribute to Tau clearance.

Identifying Tau-Tau interactions could be an essential way to understand AD mechanisms, as well other Tauopathies. Therefore, in an attempt to detect the interaction of Tau-Tau proteins in aggregation process in living cells, we used a bioluminescence resonance energy transfer (BRET) and Venus split complementation assay. This kind of strategies could be extremely useful to study different mechanisms that occur in cells in presence of Tau aggregated species. QBI seeding model was used for these assays, since this can reflect what physiologically happens in cells in Tau aggregation conditions.

Chapter 2 Materials and Methods

2.1 Materials

Table 3 - Materials used in this project.

Company	Product
BD Falcon	Tissue culture flasks (353028)
	Conical Tubes Screw Caps of 50mL(358206), 15mL(352097)
Beckman Coulter	Beckman centrifuge tubes (243775)
	Optima MAX-XP ultracentrifuge
Bio-Rad	Trans-Blot® Turbo™ Midi 0.2µM Nitrocellulose Transfer (170-4159)
	Trans-Blot® Turbo™ Transfer System #170-4150
Santa Cruz	Non-fat dry milk (NFDM) (sc-2325)
Eppendorf	Electroporation cuvettes, gap width 1mm, 100ml (4307 000.569)
	Eppendorf tubes of 0.5mL (022363719); 1.5mL (022363212) and 2 mL (022363344)
Eurogentec	SmartLadder (MW-1700-10)
Falcon	Multiwell plates of 96 (655946), 24 (354414) and 6 (354515) wells
Genlantis	BioPORTER Reagent QuikEase Single-Use Tubes (BP509696)
HyClone	Research Grade Fetal Bovine Serum(FBS) (SV30160.03)
Life technologies	B27 supplement (0080085SA)
	DMEM - Dulbecco's modified Eagle's medium (1956)
	Dulbecco's phosphate-buffered saline (D-PBS) (1X) (-/- $CaCl_2$; -/- $MgCl_2$) (14190-094)
	E-Gel® Single Comb (G5018-08)
	HBSS - Hank's Balanced Salt Solution (14025076)
	Gibco® HEPES (15630-122)
	Horse Serum (26050088)
	iBlot® (IB3010-01)
	L-glutamine (25030)
	MagicMark™ XP Western Protein Standard (LC5602)
	MEM (31095)
	Neurobasal® Medium (21103-049)
	NuPAGE® LDS Sample Buffer (4X) (NP0007)
	NuPAGE® MOPS SDS Running Buffer (20X) (NP0001)
	NuPAGE® Novex® 4-12% Bis-Tris Gels, 1.0-mm thick, 12-well (NP322BOX)
	NuPAGE® Novex Bis-Tris Gels, 1.0-mm thick, 12-well (WG14003BOX)
	NuPAGE® Reducing Agent (10X) (NP0009)
	One Shot® TOP10 Chemically Competent *E. coli* (C4040-10)
	One Shot® TOP10 Electrocomp™ *E. coli* (C4040-50)
	Opti-MEM® Reduced-Serum Medium (11058-021)
	Penicillin-Streptomycin antibiotic solution (15140-122)
	S.O.C. Medium (15544-034)

	UltraPure™ 5 M Sodium chloride (NaCl) (24740)
	Sodium Pyruvate 100 mM Solution (11360-039)
	UltraPure™ 1M Tris-HCl, pH 8.0 (15568-025)
	0.05% Trypsin-EDTA (1X) (25300-054)
Merck	Glucose (104074.1000)
New England BioLabs	BsgI Restriction Enzyme (R0559S)
	S-adenosylmethionine (B9003)
Promega	FuGENE® 6 Transfection Reagent (E2691)
	HaloTag® TMR Ligand (G825A)
	Nano-Glo® Luciferase (N1130)
QIAGEN	QIAGEN Plasmid Maxi Kit (12162)
	QIAprep Spin Miniprep Kit (27104)
Roche	cOmplete mini EDTA-free Mini Protease Inhibitor Cocktail Tablets (0469319001)
	PhosphoSTOP Phosphatase Inhibitor Cocktail Tablets (04906837001)
Sigma-Aldrich	Bicinchoninic Acid Kit for Protein Determination (BCA1-1KT)
	Goat serum (G9023)
	Heparin (H-5284)
	LB Broth-Liquid Medium (L2542)
	Sodium acetate –anhydrous (S2889)
	Lithium dodecyl sulfate (L2274)
	TWEEN® 20 (P1379)
	Triton™ X-100 (T8787)
Thermo Scientific	10X FastDigest Green Buffer (B72)
	FastDigest ® Eco91I (BstEII) (ER0391)
	FastDigest ® KpnI (ER0521)
	FastDigest ® NotI (ER0595)
	FastDigest ® XbaI (FD0684)
	SuperSignal* West Dura Chemiluminescent Substrate (34076)
	Restore ™ Plus Western Blot Stripping Buffer (46430)

2.2 Antibodies and Dyes

Table 4 - Antibodies and dyes used in this project.

Antibody/Dye	Target	Host Specie	Company	Application	Dilution/ concentration
Anti-Actin Antibody, clone C4 (MAB1501)	Actin	Mouse	Milipore	Western Blot	1:10000
Alexa Fluor® 555 Goat Anti-Mouse IgG (H+L) (A-21424)	Mouse IgG	Goat	Life technologies	Immunocytochemistry	1:10000
Alexa Fluor® 488 Goat Anti-Rabbit IgG (H+L) (A-11008)	Rabbit IgG	Goat	Life technologies	Immunocytochemistry	1:10000
Anti-HaloTag® Monoclonal Antibody (G921A)	HaloTag fusion protein	Rabbit	Promega	Western Blot	1:1000
Anti-NeuN, clone A60 (MAB377)	IgG	Mouse	Milipore	Immunocytochemistry	1:100
AT8	Phosphorylated Tau on ser202/tre205	Mouse	Produced in house	Western Blot and Immunocytochemistry	1 µg/ml
AT120	Human Tau	Mouse	Produced in house	Western blot	1 µg/ml
Dako antibody (A0024)	Tau	Rabbit	Dako cytomation	Western Blot	1:5000
DAPI (62247)	Double-stranded DNA	Not applicable	Thermo Scientific	Immunocytochemistry	1:5000
ECL Mouse IgG, HRP-linked whole Ab (NA931V)	IgG	Sheep	GE Healthcare Life Sciences	Western Blot	1:10000
ECL Rabbit IgG, HRP-linked whole Ab (NA934V)	IgG	Donkey	GE Healthcare Life Sciences	Western Blot	1:20000
Hsp70/72 (AF1663)	Hsp70	Rabbit	R&D system	Western Blot	1:10000
HT7 (MN1000)	Human Tau	Mouse	Pierce	Western Blot	1:10000
				Immunocytochemistry	0.1 µg/ml
Neuronal class III β-Tubulin (MNS-435P)	Tubulin beta-3 chain	Mouse	Covance	Immunocytochemistry	1:1000

2.3 Mammalian cell culture and Plasmid transfection

Human kidney-derived QBI-293 (QBiogene) were grown in Dulbecco's modified Eagle's medium (DMEM) supplemented with 10% (v/v) heat inactivated FBS, 1% Pyruvate (10 mM), 1% Penicillin-Streptomycin (PenStrep) and L-glutamine (20 mM). Cells were maintained at 37ºC, in humidified atmosphere containing 5% CO_2.

One day prior to transfection, fully confluent cells were trypsinized and then seeded in 24 well plates at density of $5x10^4$ cells per well. After 24 hours of growth, transfection was carried out using 3 µl FuGENE® 6 reagent in 97 µl Opti-MEM medium with 5 minutes of incubation time at room temperature (RT). The nonliposomal-DNA complexes were obtained by mixing the transfection reagent with 1 µg of plasmidic DNA followed with incubation for 15 minutes at RT. This mix was added to the cells with 400 µl of antibiotic free medium. In case of co-transfections, the nonliposomal-DNA complexes were generated using 1 µg in total of desired plasmids.

2.4 Primary neuronal culture and AAV transductions

Primary neuronal cultures were prepared from E17-E18 Wistar WT rat embryos. Brains from embryos were dissected and kept in pre-warmed HBSS/Hepes solution (7 mM Hepes in HBSS and PenStrep) at 37ºC. Cortices were dissociated by trypsinization (4.5 ml HBSS/Hepes plus 500 µl of trypsin) for 10-15 minutes at 37ºC. After removing trypsin, cortices were washed 3 times with pre-equilibrated MEM-Horse medium, supplemented with 10% (v/v) horse serum and 0.6% (v/v) glucose. Mechanical dissociation of biological material was made with pasteur pipettes of normal and small diameter in 3-5 ml of MEM-Horse medium. The cells were spun for 5 minutes at 1000 rpm, and ressuspended in 3 ml of MEM-Horse medium. The neurons were plated at a density of 6×10^5 cells/well in 6 well-plates coated with poly-D-Lysine or 1×10^4 cells/well in 96 well-plates coated also with poly-D-lysine. After 4 hours the medium was changed to Neurobasal serum-free medium supplemented with 2% (v/v) B-27 and 10 mM L-glutamine. Neurons were maintained at 37ºC in 5% CO_2 in humidified incubator.

After 3 days of plating (day in vitro (DIV) 3) neurons were transduced with AAV6-hTauWT or AAV6-hTauP301L at a multiplicity of infection (MOI) of 100. Virus was diluted in Neurobasal medium with B-27 straightaway before adding into the primary cultures.

2.5 *In vitro* fibrillization of recombinant Tau and fibril seeding

A recombinant fragment of Myc tagged human Tau protein containing only the four MT-binding repeats designated K18, containing a P301L mutation (K18P301L) which is associated with Frontotemporal dementia and FTDP-17, was expressed in bacteria and purified using a fast protein liquid chromatography.
In vitro fibrillization was stimulated by mixing 40 µM recombinant Tau protein (Myc-K18Tau-P301L) with 40 µM of low molecular weight heparin and 2 mM DTT in 100 mM sodium acetate buffer (pH=7.0), incubated 3 days at 37ºC. Before seeding in cell lines and in neurons, the fibrilization mixture was centrifuged at 100000g for 30 min at 4ºC, and the resulting pellet was resuspended in an equal volume of 100 mM sodium acetate buffer (pH=7.0) without heparin and DTT. Myc-K18Tau-P301L fibrils were stored as single-use aliquots at -80ºc.
At the day of seeding K18P301L fibrils were diluted to 25 nM using 100 mM sodium acetate buffer (pH=7.0) and sonicated with 25 pulses of 2 seconds pulses, continuously on ice. Fibril seeding was performed in QBI cell line 24 hours after plasmid transfection, using BioPORTER reagent. 80 µl of K18P301L fibrils were added to one tube of BioPORTER reagent, gently vortexed for 5 seconds and allowed to stand at RT for 10 minutes. During the formation of the fibrils-BioPORTER complex, cells were washed once with 200 µl OptiMEM. The fibril-BioPORTER complex was diluted with 1920 µl OptiMEM and 200 µl of the mixture were to each well. After 4 hours of incubation at 37ºC, QBI cells were trypsinated with 100 µl and 900 µl of DMEM was added to each well. The cells were re-plated in 96 well-plates at a cell density of $5x10^3$ per well.
In the experiments where BioPORTER reagent was used to seed primary neurons, the protocol used was the same as described with QBI cell line with Neurobasal medium instead of OptiMEM. In primary cortical neurons fibril seeding was done at DIV8 by adding the mixture of fibrils and Neurobasal medium supplemented with B27 directly to the neurons in the medium unless indicated otherwise.

2.6 Sequential protein extraction

QBI 293 cells were washed three times with D-PBS 48 hours after fibril seeding, while neurons were washed with D-PBS normally at DIV17 (unless indicated otherwise). In each well 160 µl triton lysis buffer were added (1% TritonX-100 in 50 mM Tris, 150 mM NaCl, pH 7.6) containing protease and phosphatase inhibitors and incubated 15 minutes at RT. After sonication in a water bath, cells were scraped and 60 µl of the total lysate was kept (total fraction) while the rest of the lysate material was centrifuged at 100 000 g for 30 minutes at 4ºC. Supernatants were kept (soluble fraction) and the pellets were washed two times

with Triton lysis buffer, resuspended and metal tip sonicated in 100 µl LDS lysis buffer (1% LDS in 50 mM Tris, 150 mM LiCl, pH=7.6) until dissolved. One last centrifugation with the same speed was performed, and the supernatants were kept (insoluble fraction).

2.7 Western Blot analysis

After protein extraction of total, soluble and insoluble fractions, the soluble fraction was used to determinate protein concentration by a Bicinchoninic acid assay. 3 or 5 µg protein of each sample, relative to the protein concentration of the triton fractions, were loaded on NuPage Novex Bis-Tris 4-12% and run in MOPS SDS running buffer. The polyacrylamide gel was transferred to a 0.22 µm nitrocellulose membrane by Trans-Blot® Turbo™ Transfer System. Before probing membranes with primary antibodies, the membranes were blocked with 5% NFDM in TBS-T (1M Tris, 150nM NaCl and 0.05% (v/v) Tween-20, pH 8.5). After 1 hour of incubation at RT, membranes were incubated overnight with primary antibody in 5% NFDM in TBS-T. Membranes were washed 3 times for 5 minutes with TBS-T followed by incubation with sheep anti-mouse IgG-horseradish peroxidase or donkey anti-rabbit IgG-horseradish peroxidase in TBS-T for 1 hour, at RT. Before signal detection, membranes were washed 4 times 5 minutes with TBS-T. Membranes were incubated with SuperSignal®West Dura Extended Duration Substrate and exposed for various times on the Lumi-Imager. To detect with different antibodies after exposing, the membrane was washed 3 times with TBS-T and incubated with 10 ml Restore™ Plus Western Blot Stripping Buffer, during 15 minutes with shaking. After the membrane incubation with this buffer, the membranes were reprobed with different antibodies.

2.8 Immunocytochemistry

Immunocytochemistry was performed in primary cortical neurons plated in 96 well-plates 9 days after fibril seeding. Cells were fixated in 4% (v/v) of pre-warmed paraformaldehyde in D-PBS for 15 minutes and permeabilized with 0.1% (v/v) triton X-100 buffer in D-PBS for 10 minutes. Cells were rinsed 3 times for 5 minutes with D-PBS, and incubated with blocking solution (5% (v/v) normal goat serum and 0.1% bovine serum albumin (BSA) (v/v) in D-PBS) for at least 30 minutes at RT. After blocking, cells were incubated overnight at 4ºC with specific primary antibody diluted in 0.1% (v/v) BSA in D-PBS. The next day neurons were washed 3 times for 5 minutes with 0.1% (v/v) BSA in D-PBS. Appropriated secondary antibodies diluted in 0.1% (v/v) BSA were added to neurons during 30 minutes. For nuclear staining DAPI diluted in D-

PBS was added for 30 minutes and then washed with D-PBS. Fluorescent images were acquired using a Zeiss Axiovert 135 fluorescence microscope equipped with Zeiss Axiocam ICc1 camera and Zeiss Axiovison 4.8 software using 20x objectives. The images were background corrected by ImageJ software.

For cell viability quantification 4 images per well were captured using a multimode microscope reader MIAS-2 with 20x amplification. Cortical neurons fixed at different time points were quantified by manual counting using ImageJ software. At DIV8, 14, 16, 20, 22 in neurons transduced with AAV6 expressing P301L 30 repetitions were performed for each condition with and without seeding with pre-aggregated K18P301L. In neurons non transduced with AAV6 containing P301L 8 repetitions per condition were performed (with or without seeding with pre-aggregated K18P301L) in each day of fixating.

The antibodies designated as A, B, C and D are confidential antibodies, therefore their characteristics cannot be mentioned.

2.9 Cloning of Tau expression plasmids

Nano-Luc, an ATP-independent luciferase, or HaloTag from Promega were cloned in-frame to the N-terminal or C-terminal side of full-length Tau containing the two alternatively spliced N-terminal exons and four MT binding domains (2N4R Tau) with P301L mutation.

Constructs were cloned into BstEII and XbaI sites of TauP301L-pcDNA4-TO vector. *E.coli* TOP10 cells were transformed with pcDNA4-TO plasmids encoding TauP301L-NanoLuc, NanoLuc-TauP301L, TauP301L-HaloTag, and HaloTag-TauP301L through electroporation and plated overnight at 37ºC.

TauP301L was also cloned in-frame with either the N-terminal (aa 1-155) or C-terminal parts of Venus fluorescence protein (aa 156-239) (Nagai et al., 2002). Also expression constructs for N-terminal and C-terminal fusion proteins of both Venus fluorescent protein fragments with the mutant form of Tau, K18-P301L, with only the MT-binding region, were generated by PCR.

Similar constructs made with substitutions of two isoleucine residues at the positions of 277 and 308 to prolines were generated from K18-P301L. *E.coli* TOP10 cells were used to transform the plasmids encoding Venus constructs through electroporation and plated overnight at 37ºC.

In all conditions previously described, Nano-Luc/HaloTag Tau constructs and Tau Venus constructs, a single colony was picked from a selected plate and inoculated in a culture of 5 ml Luria Broth medium with 100 µg/ml concentration of ampicillin (selective condition). The bacteria were incubated for 12–16 h at 37°C with vigorous shaking. To isolate and purify up to 20 µg of high-copy plasmid DNA from overnight cultures of *E.Coli* QIAprep Spin Miniprep Kit was used according to the manufactures protocol.

Isolated plasmids were digested with BsgI and samples were analyzed on a 0.8 or 2% e-gel. The sequence of the clones that showed the expected pattern of DNA bands was confirmed by sequencing.

To have a larger amount of DNA to work with, 1 ml of bacterial cell culture was inoculated in 100 ml of Luria Broth medium with 100 µg/ml ampicillin. The plasmid was purified from these bacteria using the QIAGEN Maxi Kit. To determine the yield, DNA concentration and purity was determined with NanoDrop® 1000, by the absorbance of coefficient between 260 nm and 280 nm.

2.10 BRET assay

QBI 293 cells were co-transfected with plasmids of interest as described earlier, with HaloTag fusion proteins in molar excess to Nano-Luc fusion proteins. The HaloTag™ TMR ligand was used as BRET acceptor and NanoLuc™ Luciferase was used as BRET donor. 24 hours after fibril seeding, QBI cells were treated with 100 nM of HaloTag™ TMR ligand and incubated overnight at 37ºC in 5% CO_2. On the day after, NanoLuc™ Luciferase substrate was diluted 1:250 in Opti-MEM, added to the cells, and HaloTag fluorescence and Nano-Luc luminescence signal was measured and BRET efficiency was calculated based on that.

The Nano-Luc luminescence signal was detected using a 450 nm emission filter and HaloTag fluorescence was measured with second 585 nm emission filter using a Perkin Elmer EnVision 2102 Multilabel Reader. BRET ratio is calculated using the quotient between the average of the readout at 585 nm and the readout at 450 nm in wells treated and not loaded with HaloTag™ TMR ligand. Statistical analysis was made by GraphPad Prism®5 software.

Equations shown below correspond to the way we calculated BRET assay ratio. The reading at 585 nm corresponds to HaloTag measurement wavelength, whereas 450 nm correspond to Nano-Luc measurement wavelength. Conditions 1 and 2 correspond to the different conditions of each experiment.

Equation 1

$$A = \frac{Reading\ 585nm}{Reading\ 450nm}\ \text{Background}$$

Equation 2

$$B = \frac{Reading\ 585nm}{Reading\ 450nm}\ \text{HaloTag TMR ligand}$$

Equation 3

$$BRET\ signal = \frac{[(average\ B) - (averageA)]_{\text{Condition 1}}}{[(average\ B) - (averageA)]_{\text{Condition 2}}}$$

2.11 Venus split complementation assay

QBI 293 WT cells were co-transfected with plasmids of interest as described early, with different combinations of Tau-Venus fusion expression constructs. Cells were seeded with pre-aggregated fibrils (as previously described) 24 hours after the co-transfection with indicated constructs.

Venus fluorescence signal was detected using an excitation filter of 515 nm and an emission filter of 528 nm, by a fluorescence microscope. Fluorescent images were acquired using a Zeiss Axiovert 135 fluorescence microscope equipped with Zeiss Axiocam ICc1 camera and Zeiss Axiovison 4.8 software using 20 x objectives.

Chapter 3 Results

3.1 Optimization of the cellular Tau aggregation model in cortical primary neurons

3.1.1. hTauP301L aggregation model

The first goal of this project was to optimize the aggregation model in cortical primary neurons. Previously a Tau aggregation model was developed in a QBI 293 cell line, but since the objective of the model was to mimic as closely as possible the Tau pathology that occurs in the brain of AD patients, an effort was made to optimize the Tau aggregation model in rat cortical primary neurons.

The same strategy used in the QBI cell model was applied to cortical primary cultures. Neurons were transduced with AAV6 containing WT Tau or P301L-Tau that will be express under the neuron specific SYN1 promoter 3 days after plating of the neurons (Figure 19). Tau aggregation, like in the QBI aggregation model, is a process that is not spontaneous just with the presence of protein hTauP301L. To overcome the rate limiting step of the initial aggregation it is necessary to treat the neurons with *in vitro* pre-aggregated K18P301L that can function as an aggregation seed. For this studied we used, K18P301L a synthetic fragment of Tau containing only the four MT-binding repeats with a mutation where a proline is changed to a leucine at position 301 (position in the longest isoform of Tau). Previous experiments in our group showed that the best time point to add K18P301L fibrils was 8 days after neuronal plating. Tau aggregation in this model was studied either by biochemical analysis or by immunocytochemistry analysis generally 17 days after neuronal plating (Figure 19).

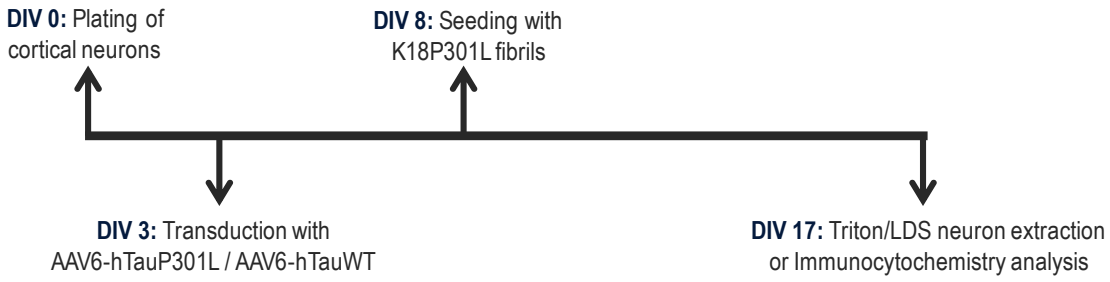

Figure 19 – Schematic representation of strategy used in Tau aggregation model in cortical primary neurons. DIV represents the days that neurons are in culture after plating.

The capacity of *in vitro* pre-aggregated K18P301L to induce intracellular aggregation of hTauP301L was visualized by immunocytochemistry. Neurons transduced with AAV6 containing hTauP301L were seeded with or without pre-aggregated fibrils (Figure 20). Human total Tau present in neurons was labeled with the HT7 monoclonal antibody which recognizes epitopes of human Tau between residues 159-163, whereas the induced aggregated Tau was detected with the antibodies A, B, C, D, and AT8. No signal was

detected with HT7 in cells not transduced with hTauP301L and no seeded with pre-aggregated K18P301L, since HT7 is a human specific antibody that does not detect rat Tau (Figure 20A). A similar result was obtained with specific antibodies to pathological forms of Tau (Figure 20D, G, J, M, P). When neurons were transduced with hTauP301L we were able to see human Tau in neuronal cultures, by HT7 staining (Figure 20B). To discriminate between neurons and astrocytes all samples were co-stained with ß3-tubulin and a nuclear strain. The HT7 staining was only observed in cells positive for ß3-tubulin expression. In conclusion, we found a clear expression of Tau specifically in the neurons when they were transduced with AAV6-hTauP301L.

Augustinack et al. showed that the immunoreactivity of AT8 antibody is associated with different stages of NFT formation in AD human brains (Augustinack et al., 2002). In the conditions where neurons were not seeded with pre-aggregated K18P301L no signal with antibodies against pathological forms of Tau was observed suggesting that Tau does not aggregate under this condition (Figure 20E, H, K, N). However, under these conditions we did observed a weak immunoreactivity for AT8, a monoclonal antibody specific to double phosphorylated Tau epitopes at Ser202 and Tyr205 (Figure 20Q). This suggests that hTauP301L is at least partially phosphorylated at the AT8 epitope in neurons upon overexpression. On the other hand, in neurons transduced with hTauP301L and seeded with 25nM of in *vitro* pre-aggregated K18P301L a strong increase in staining was observed with the aggregation specific antibodies A, B, C, and D and with AT8 suggesting the induction of Tau aggregation in these cells (Figures 20F, I, L, O, R). The staining of aggregated Tau was observed as green dots along dendrites. The induction of a dotted staining pattern of Tau after seeded with pre-aggregated K18P301L was also observed with AT8 suggesting that this treatment produced AT8 positive dots, correspondent with pathological cases of Tau pathology. In Figure 20I the presence of a structure similar to NFT is evident, which is found in pathological human brain, meaning that the Tau aggregation model that we are using could be a promising model to study the aggregation occurring in AD patients brains. With all these observations we can conclude that for inducing a pathological conformation in Tau, the presence of pre-aggregated fibrils is necessary to induce aggregation of unfolded hP301L-Tau.

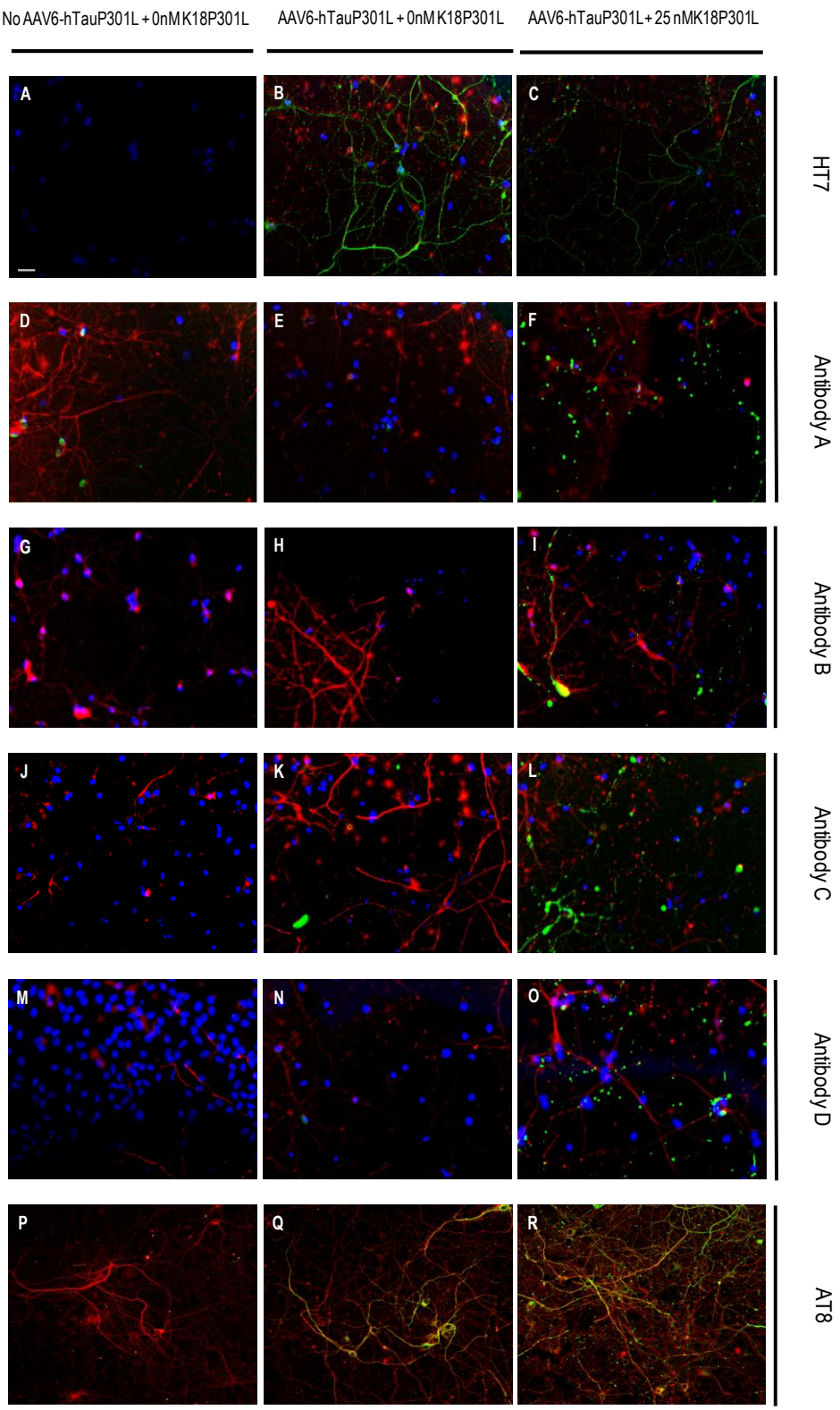

Figure 20 - Immunocytochemistry analysis of cortical primary neurons transduced with or without AAV6 containing P301L-Tau and with or without seeded with pre-aggregated K18P301L. Immunocytochemistry analysis of paraformaldehyde fixed cells. Red staining corresponds to ß3-tubulin, blue to DAPI staining and green to specific antibody stain (antibody used stated in the Figure). HT7 staining shows the presence of total human tau; Antibodies A, B, C, D and AT8 show specific staining for pathological Tau in cortical neurons induced by K18P310L fibrils. Images were acquired by a fluorescence microscopy with magnification of 20x. In contrast images P, Q and R were not stained with DAPI, and these images were acquired by confocal microscopy with magnification of 20x. Scale bar: 219 µm. (Note: Antibodies A, B, C and D were designated by this way due the confidentiality reasons.)

3.1.2. Spontaneous uptake of *in vitro* pre-aggregated K18P301L in cortical primary cultures

As a first approach to optimize the Tau aggregation model in cortical primary neurons, we tested the effect of the use of BioPORTER delivery reagent with K18P301L seeds. BioPORTER reagent interacts non-covalently with the molecule of interest and delivers it into the cells using a lipid-based carrier system.

In the previous model developed in QBI 293 cell line, BioPORTER reagent is crucial to delivery *in vitro* of pre-aggregated K18P301L to the cells. Based on this fact the introduction in neurons of pre-aggregated fibrils was performed using this reagent as well. This reagent however was highly toxic to neurons, since neurons showed a visible damage in presence of the BioPORTER (data not shown). Taking this fact into account we tested the requirement of this reagent for the delivery of K18P301L fibrils. Therefore, we added 10 µM of pre-aggregated K18P301L to one tube with or without of BioPORTER delivery reagent and diluted this in 920 µl of neurobasal medium without B27 supplement. Different amounts of these fibrils complexed with or with BioPORTER were added to neurons plated in 6-well-plate that were previously transduced with AAV6 containing P301L-Tau (Figure 21). 8 days after K18P301L seeding, cells were lyzed and proteins were separated in soluble and insoluble fractions by ultracentrifugation. Samples were analyzed by western blotting using the anti-Tau antibody HT7, which detects human Tau in the residues between 159-163 (absent in the *in vitro* synthetic K18P301L). hTauP301L was only detected in the insoluble fraction after seeding with pre-aggregated K18P301L fibrils. In the total fraction a shift in the apparent molecular weight of the Tau band was observed after seeding with the fibrils. This may be due to an increase in phosphorylation of aggregated Tau causing the protein to migrate significantly slower in the SDS-PAGE gel compared with non-phosphorylated Tau. After separating soluble and insoluble proteins we found that the slower migrating form of Tau was insoluble and the faster migration was soluble. Induction of Tau aggregation after fibril transduction was also observed in the conditions where BioPORTER delivery reagent was not used. Curiously, lower concentrations of *in vitro* pre-aggregated K18P301L in absence of BioPORTER, seemed to show the higher levels of hTauP301L aggregation than higher concentrations of pre-aggregated K18P301L. However, we cannot extrapolate this conclusion, since there is a lot of variation in this western blot. Tau aggregation relative quantification was performed to have a more quantitative view on the western blot results (Figure 21B) confirming what is seen in the western blot.

These results suggest that fibril uptake in primary neurons is different than in QBI cells, there seems to be a spontaneous uptake of fibrilar Tau, leading to an induction of pathological aggregates in neuronal cultures. These data suggests that we do not need to use BioPORTER delivery reagent to induce hTauP301L aggregation in cortical primary neurons. Therefore, in future experiments BioPORTER will no longer be used, because of its toxicity to neurons, and without its use, it is possibly to study the uptake of seeds as a step in the Tau aggregation cascade.

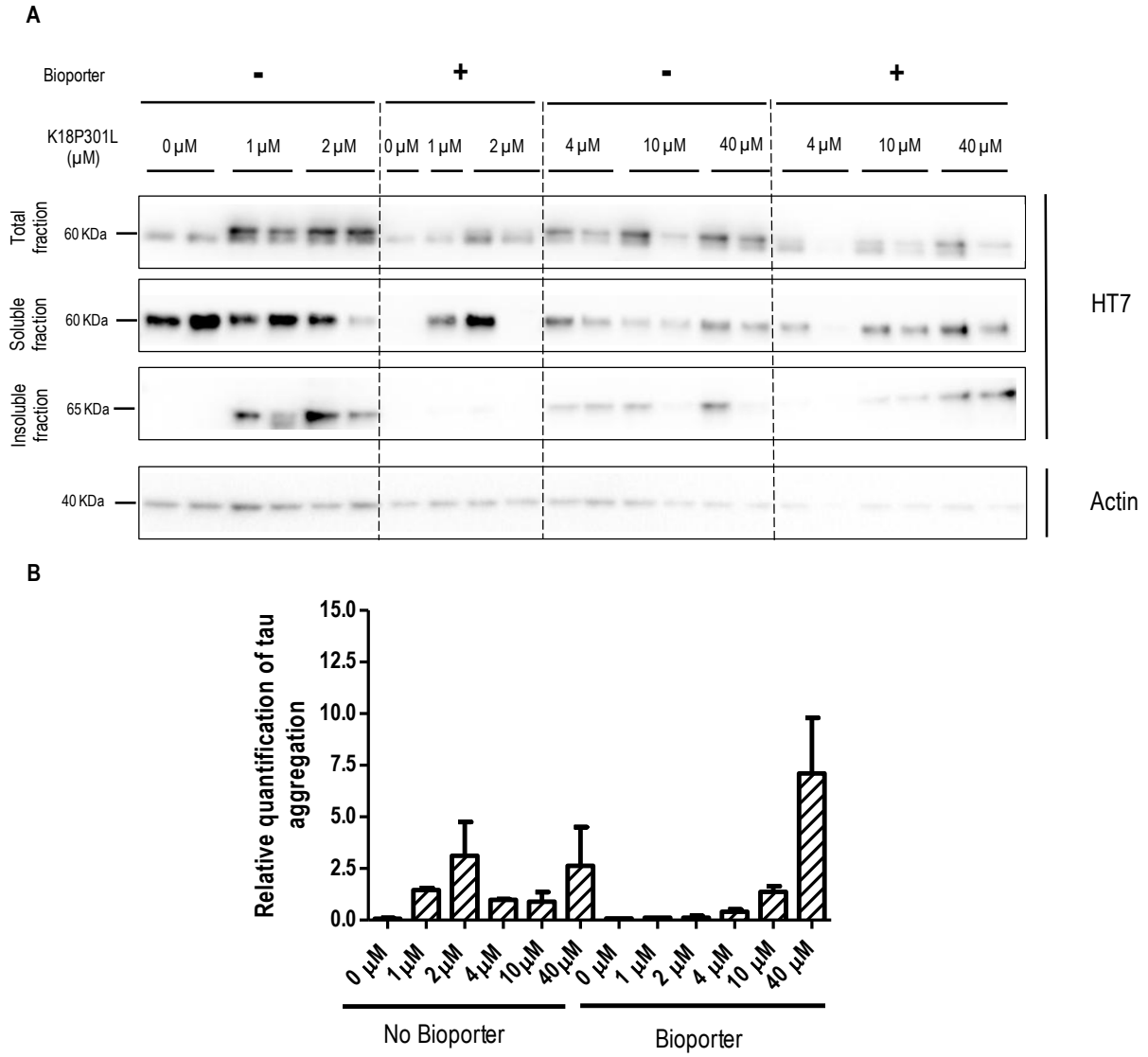

Figure 21 – Analysis of sequentially extraction of proteins from cortical primary neurons seeded with different concentrations of pre-aggregated K18P301L with or without BioPORTER delivery reagent. (A) Western blot analysis of cortical primary neurons with transduction with P301L-Tau and seeded at DIV8 with 1µM, 2µM, 4µM, 10µM or 40µM of K18P301L fibrils with or without BioPORTER reagent. Equal portions of extracted protein were loaded on SDS-polyacrylamide gels. Monoclonal antibody HT7 against human total Tau was used and actin antibody was used as control of protein amounts. (B) Quantification of Tau in insoluble fraction band (normalized to actin), in 0.22 µm nitrocellulose membrane. N=2, average ± SD.

Next we tested the effect of B27 supplementation in the neuronal culture medium on hTauP301L aggregation, without BioPORTER presence. B27 is a protein-rich supplement for long-term cultures. Previous experiments had shown that B27 supplementation greatly reduces uptake of Fibril/BioPORTER complexes.

Therefore the medium on the cortical primary neurons was replaced with new medium with or without B27 supplement before seeding with 1 µM of synthetic pre-aggregated K18P301L fibrils. The medium was changed again to neurobasal medium supplemented with B27 4 hours after the K18P301L fibril seeding.

The effect of B27 supplement on Tau aggregation induction was analyzed by western blot (Figure 22). hTauP301L was observed in the insoluble fraction only in samples from neurons transduced with AAV6-hTauP301L and seeded with K18P301L fibrils. This was independent of the presence of the B27 supplement. In conclusion there was no need to remove B27 supplement from the medium during fibril seeding in neurons. This way, the management of the neurons is easier and they are less exposed to possible ambient damages, since manipulation is reduced by one step.

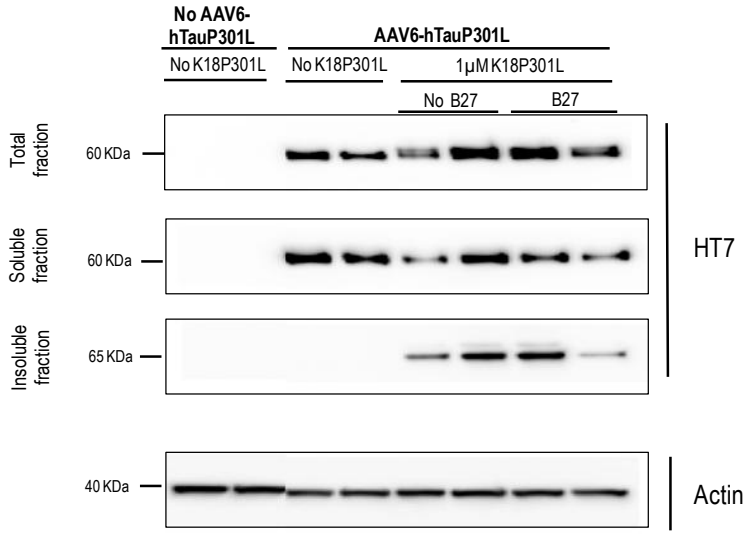

Figure 22 - Western Blot analysis of the effect of B27 supplement during fibril seeding on efficiency of aggregation induction in neurons. Cortical primary neurons were transduced with or without P301L-Tau at DIV3 and also seeded with 1 µM pre-aggregated K18P301L at DIV8 in the presence or absence of B27. In neuronal samples where K18P301L fibrils were added to neurons in the absence of B27, the medium was changed 4 hours later to Neurobasal medium supplemented with B27. Equal portions of extracted protein were loaded on SDS-polyacrylamide gels. The human total Tau was detected used HT7 monoclonal antibody, equal protein loading was confirmed by actin antibody.

3.1.3. Cellular viability of hTauP301L neuronal aggregation model

In conformity with our main objective, the optimization of hTauP301L aggregation model in cortical primary neurons, we tested the effect of hTauP301L expression and aggregation on cellular viability in this model at different time points, during 22 days in culture. Therefore, cortical neurons with or without transduction with AAV6 containing P301L-Tau and with or without seeding with pre-aggregated K18P301L were fixed at different time points. Samples were stained with a NeuN antibody which recognizes DNA-binding neuron-specific protein NeuN and DAPI, a nuclear acid stain that binds preferentially to double-stranded DNA (Figure 23A).

In Figure 23A the morphology of neurons after different days of culture is shown, where DIV0 corresponds to the day that the neurons were plated. The DIV0 neurons were fixed with paraformaldehyde 19 hours after plating (Figure 23A, panel A).

We noticed that with an increase in culture days the density of NeuN positive cells decreased as well the total number of the cells. This suggests a decrease over time in the neuron density as well the number of non-neuronal cells, although with a slower rate since we observed a higher relative amount of non-neuronal cell compared with neurons overtime.

Viability of the neurons was quantified by manual counting of the NeuN positive cells after different days of fixation (Figure 23B). We observed (Figure 23) an increase in the number of NeuN positive cells of about 30% between DIV0 and DIV3, likely due to a fixation artifact, since it will be expected that on DIV0 all neurons present in culture are already expressed NeuN protein. Between DIV3 and DIV16 around 65% of the neurons in culture died. From DIV16 until DIV22 there was not an obvious further decrease in cell viability. Transduction with AAV6-hTauP301L or seeded with pre-aggregated K18P301L did not affect neuronal survival (Figure 23A and 23B). Also the combined transduction with AAV6-hTauP301L and seeded with pre-aggregated K18P301L showed no effect on neuronal survival rate. Even at higher concentrations of pre-aggregated K18P301L (100 nM and 50 nM) no noticeable difference in mortality of neurons was observed (data not shown).

These data suggests that transduction with AAV6-hTauP301L by itself, seeded with pre-aggregated K18P301L, and induction of intracellular Tau aggregation does not have a neurotoxic effect in hTauP301L neuronal aggregation model, and it was not observed a dotted staining pattern indicative of damage to dendritic structures.

A

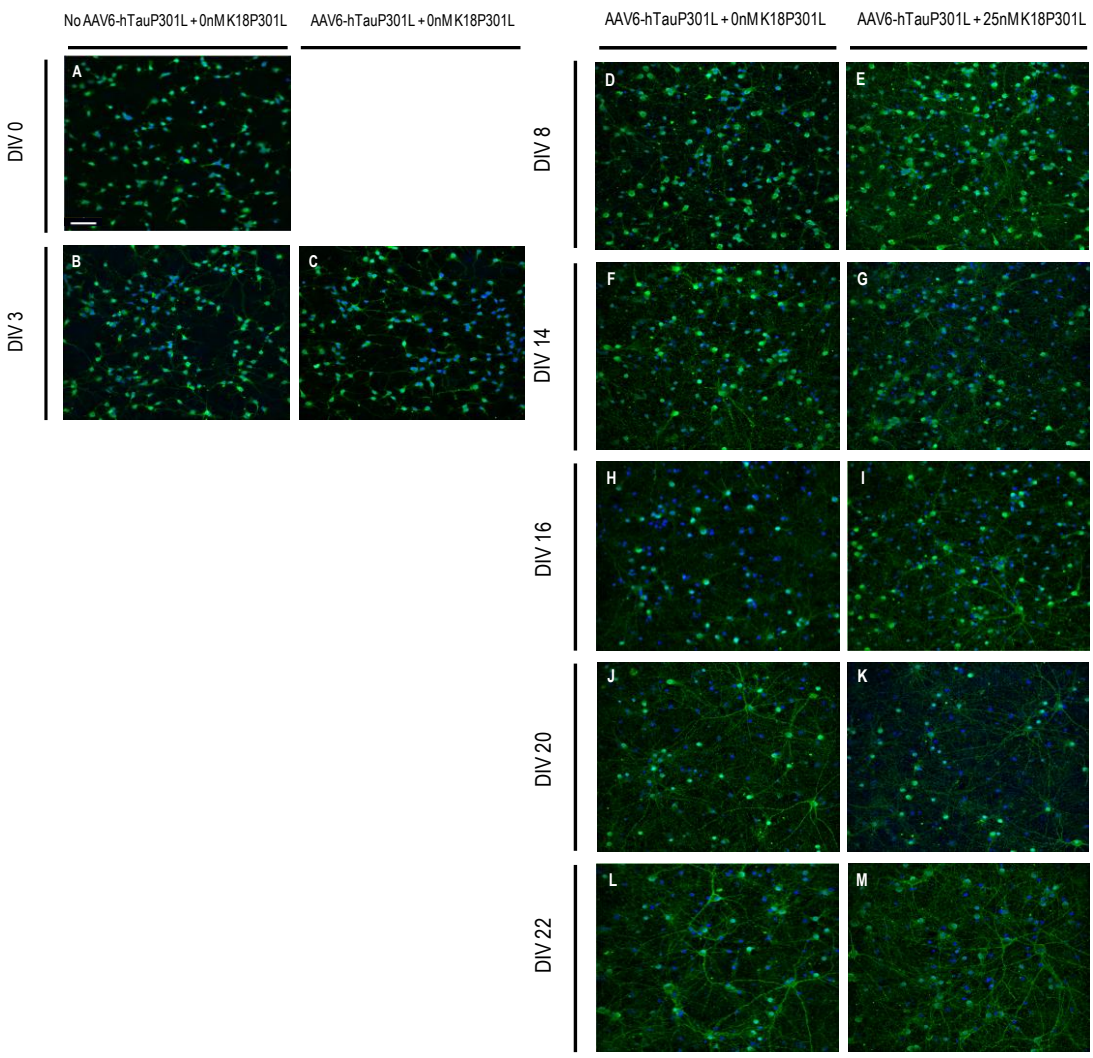

B

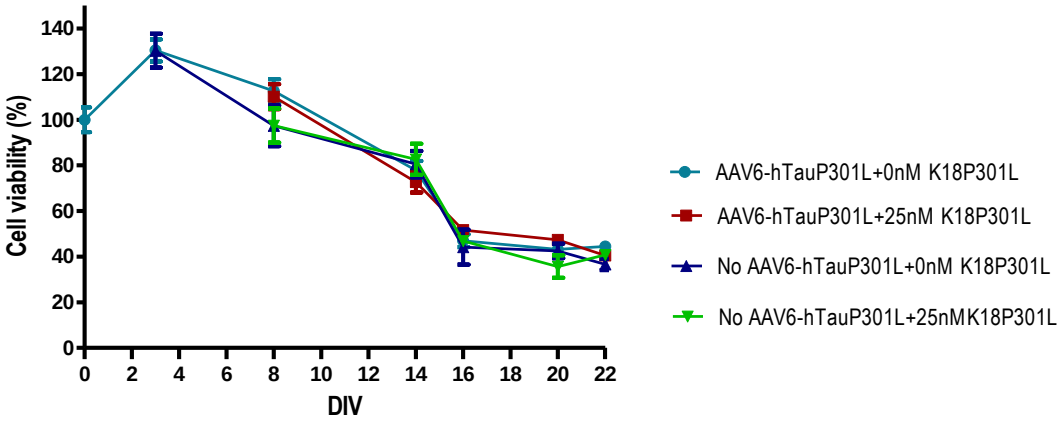

Figure 23 – Effect of AAV6 P301L-Tau transduction and pre-aggregated K18P301L seeding on cell viability of cortical neurons. Cortical primary neurons with or without transduction with AAV6 on DIV3 were seeded with or without 25 nM K18P301L. Cells were fixed at different time points DIV0, 3, 8, 14, 16, 20, 22. (A) Immunocytochemistry analysis of paraformaldehyde fixed cells. Blue staining corresponds to DAPI staining all cells, and green to the neuron specific NeuN antibody staining. Images were acquired by a multimode microscopy reader MIAS-2 with magnification of 20x. Scale bar: 422 µM. (B) Quantification of neuronal cell viability (%) was assessed by manual counting using Image J software. 8 replicates were counted for cells not seeded with K18P301L fibrils, and 30 for cells seeded with K18P301L fibrils. Depicted is the average ±SEM

3.1.4. Effect of K18P301L on hTauP301L and hTauWT aggregation kinetics in cortical primary neurons

Next we wanted to test the effect of the P301L mutation on Tau aggregation kinetics in primary neurons. Therefore, we compared the efficiency of aggregation of hTauP301L and hTauWT. At DIV3 cortical neurons were transduced with AAV6-contaning either P301L-Tau or WT Tau that will be express under the neuron and were seeded with different concentrations of *in vitro* pre-aggregated K18P301L at DIV8. Evaluation of efficiency of the procedure was done by western blot analysis, through the observation of the presence of Tau aggregation in both transduction conditions (observed in the insoluble fraction). We used two different antibodies to detect total Tau, AT120 which detects total Tau in an epitope between residues 215 and 227, and HT7 antibody, and Tau phosphorylation was studied with AT8.

Upon AAV transduction hTauP301L and hTauWT protein was detected in total lysate with both total Tau antibodies (Figure 24). Upon seeding with fibrils, different forms of hTauP301L were detected with HT7 one of which was AT8 positive and insoluble. In contrast, fibril transduction did not induce aggregation on hTauWT, and the presence of phosphorylation in AT8 epitope was not detected and caused no change in gel mobility. In addition, no insoluble hTauWT could be detected under these conditions. We did not observe (Figure 24) hTauP301L protein in insoluble fraction in neurons seeded with 10nM of fibrils with AT120. We can conclude that *in vitro* pre-aggregated K18P301L can induce Tau aggregation of hTauP301L but not of hTauWT in this cortical neuronal model.

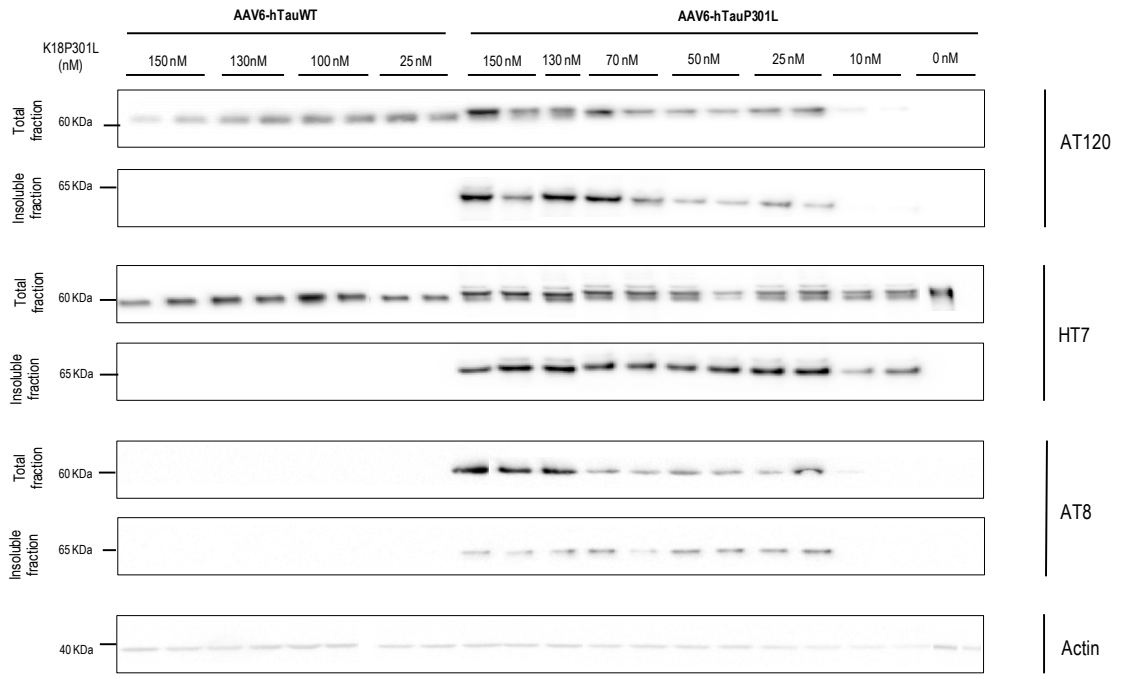

Figure 24 - Analysis of sequential extraction of proteins from cortical primary neurons transduced with AAV6 containing wild-type Tau or P301L Tau. WB analysis of total and insoluble fractions of cortical primary neurons transduced with P301L Tau or with WT Tau and seeded with different concentrations of pre-aggregated K18P301L at DIV8. Equal portions of extracted protein were loaded on SDS-polyacrylamide gels. Monoclonal antibodies HT7 and AT120 against human total Tau were used, as well as the phosphorylation-dependent anti-Tau antibody AT8. Actin antibody was used as control for protein amounts.

3.1.5. Effect of extracellular fibril concentration in cortical primary neurons

We aim to develop the Tau aggregation model to identify compounds, genes, and pathways that may modulate the Tau aggregate uptake, build-up and degradation. To optimize the sensitivity of the model we investigated the minimal concentration of fibrils needed to induce intracellular Tau aggregation.

Previous results showed that without using any delivery regent it was possible to induce hTauP301L aggregation in neurons already with 1 µM K18P301L fibrils (see Figure 21). Therefore, we examined the level of hTauP301L aggregation in neurons seeded with 1-100 nM pre-aggregated K18P301L fibrils (Figure 25). We observed a strong hTauP301L aggregation in neurons seeded with 100 nM, 50 nM, and 25 nM of pre-aggregated K18P301L, since we saw a strong signal with HT7 antibody in the insoluble fraction (Figure 25A). However, compared to the data show above, we could not detect similar results with 10 nM and 3 nM of K18P301L fibrils, with these amounts only a weak Tau signal was observed in the insoluble fraction (Figure 25A). Tau aggregation relative quantification was performed to have a more quantitative view on the western blot results, and it clear that there is more hTauP301L aggregation in neurons treated with 50 nM of pre-aggregated fibrils compared with neurons treated with a higher amount of fibrils (100 nM). There is however a clear variation between repetitions within the same condition (Figure 25). However,

we could not detect hTauP301L in the insoluble fraction from cortical neurons seeded with 1 nM of pre-aggregated K18P301L fibrils (Figure 25B). Taking this into account, we can presume that this concentration of K18P301L is not enough to induce Tau aggregation.

Considering the data shown, we chose to use in further experiments 25 nM of fibrils, not being however the concentration that showed stronger aggregation levels but this concentration showed an adequate induction of hTauP301L aggregation.

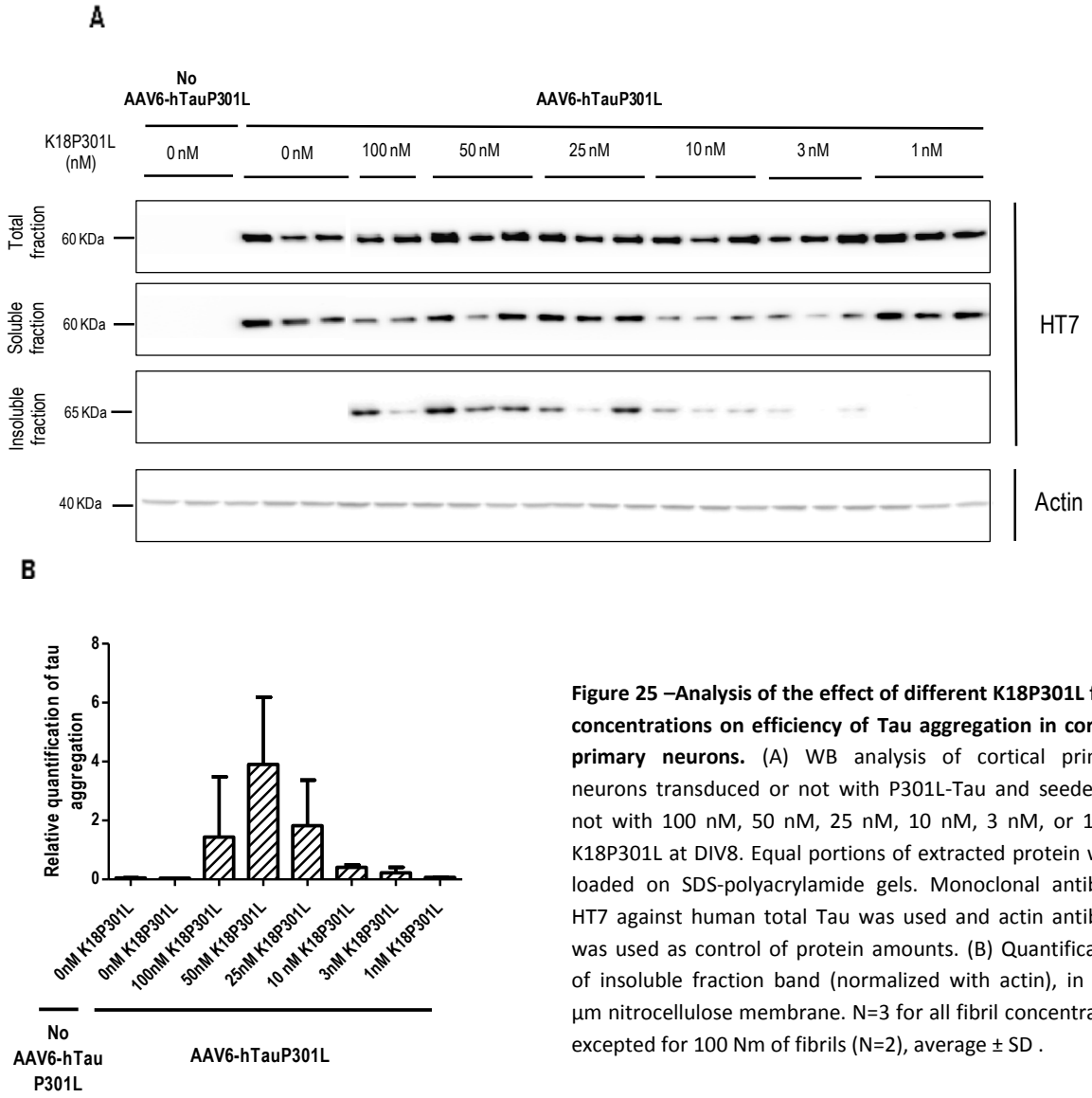

Figure 25 –Analysis of the effect of different K18P301L fibril concentrations on efficiency of Tau aggregation in cortical primary neurons. (A) WB analysis of cortical primary neurons transduced or not with P301L-Tau and seeded or not with 100 nM, 50 nM, 25 nM, 10 nM, 3 nM, or 1 nM K18P301L at DIV8. Equal portions of extracted protein were loaded on SDS-polyacrylamide gels. Monoclonal antibody HT7 against human total Tau was used and actin antibody was used as control of protein amounts. (B) Quantification of insoluble fraction band (normalized with actin), in 0.22 µm nitrocellulose membrane. N=3 for all fibril concentration excepted for 100 Nm of fibrils (N=2), average ± SD .

3.1.6. Kinetics of Tau aggregation in primary neuronal model

With the objective to continue the optimization of the Tau aggregation model in cortical primary neurons, the variation of kinectics of Tau amyloidogenic aggregation process with different exposure time to *in*

vitro pre-aggregated K18P301L was analyzed. Primary cultures were seeded with the same quantity of fibrils (25nM), and then we did protein extraction at different time points, 14, 17, 20 and 22 days after neuronal plating (Figure 26). For aggregated Tau detection we used HT7 antibody (human total Tau) and AT8 antibody (human phosphorylated Tau) in western blot analysis.

Aggregated Tau species with a molecular weight of ~ 65 KDa were observed in the insoluble fraction from cortical neurons after 14 days in culture. An increased in amount of aggregated Tau was seen in neurons after 3 more days of culture (17 days) (Figure 26). We observed (Figure 26B) a small increase in Tau aggregation detected with HT7 antibody, over the next 3 day in culture (20 days), which reaches a plateau between DIV20 and 22. These results could be confirmed, with quantification of Tau aggregation on 2 different experiments however these kinetics could not confirmed with the AT8 antibody. The high degree of variation in this assay requires multiple replications to reach a conclusion with statistical significance.

These results suggest that hTauP301L aggregation increases with time however we could not conclude that an increase in Tau aggregation is a consequence of a propagation of toxic Tau fragments, which could be occurring in neurons. Considering the data shown, we should choose the DIV14 to perform the sequentially protein extraction instead of DIV17 as we had been using. The difference in Tau aggregation between DIV14 and 17 was small but the increase in neuronal death was significant (as shown in Figure 23).

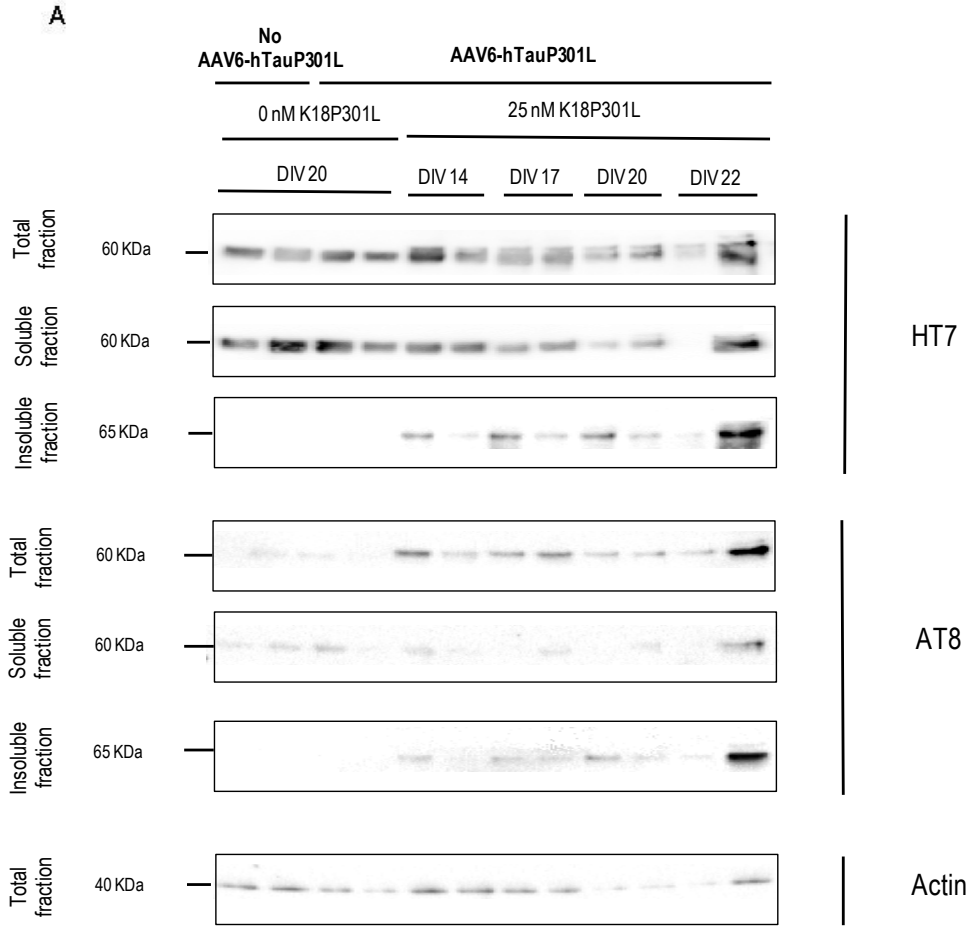

B

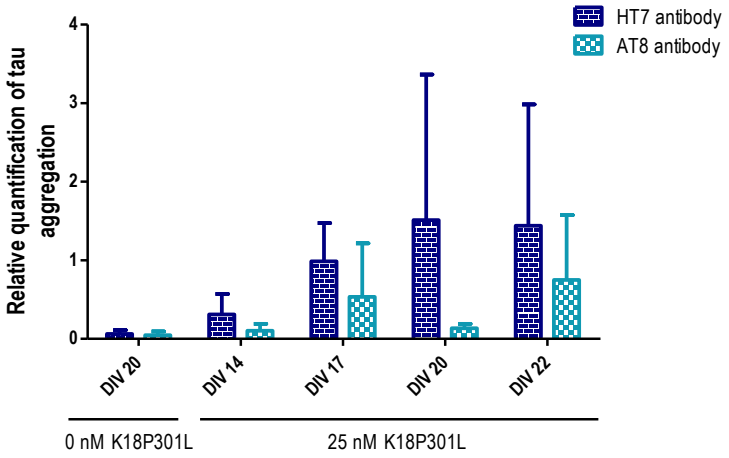

Figure 26 - Sequential analysis of protein extracted from cortical primary neurons at different times after fibril seeding. (A) WB analysis of cortical primary neurons transduced with AAV6 containing P301L-Tau and seeded with or without pre-aggregated K18P301L. Cortical neurons were extracted at different time points after K18P301L seeding. Equal portions of extracted protein were loaded on SDS-polyacrylamide gels. Monoclonal antibody HT7 against human total Tau was used, as well AT8 - phosphorylation-dependent anti-Tau antibody, and actin antibody was used as control for protein amounts (B) Quantification of insoluble fraction band of the 2 WB gels (normalized to actin), in 0.22 µm nitrocellulose membrane. N=4, average± SD.

3.2. Testing Hsp90 inhibitors to decrease Tau aggregation

3.2.1. Effects of 17-AAG on Tau aggregation in the neuronal aggregation model

As described in the introduction (see section 1.4.2) the Hsp90 complex is involved in the clearance of misfolded Tau, leading to a decrease in phosphorylated Tau levels. Hsp90 inhibitors have been extensively studied as possible cancer therapies, and are also being explored as treatment for neurodegenerative diseases. Hsp90 inhibitors seem to hold promise for reducing phosphorylated and misfolded monomeric Tau through the UPS (Brunden, Trojanowski, & Lee, 2009;Wang & Liu, 2008).

With this information, our group has studied the effects of Hsp90 inhibitors on the development and clearance of Tau aggregates. Therefore we used 17-AAG, an Hsp90 inhibitor derived from GA that was reported to be less toxicity than GA in *in vivo* studies, using mice and dogs (Supko, Hickman, Grever, & Malspeis, 1995).

The potential of 17-AAG to clear Tau was evaluated in the Tau aggregation model in cortical primary neurons. Previous work in our group with 17-DMAG, another Hsp90 inhibitor, showed that there was an active inhibition of the Hsp90 activity and an evident decrease in hTauP301L aggregation in neurons treated with this compound. Based in this data we also tested the role of 17-AAG compound in neurons. 17-AAG was the chosen compound to test instead of 17-DMAG since the former in previous results

presented high toxicity levels for neurons in our Tau aggregation neuronal model, and thus possibly compromising the results obtained.

Cortical primary neurons were treated with different concentrations of 17-AAG, and the aggregation of hTauP301L was induced by 1 µM of pre-aggregated K18P301L. The toxicity of this compound for the neurons was shown in Figure 27A, where we can see a morphological alteration in the neurons treated with this compound. With exposure over time to the compound vacuolization started to appear and later, neurites disappeared (Figure 27AII).

To detect the presence of human Tau we used HT7 antibody, and an Hsp70 antibody was used to verify the activity of 17-AAG since Hsp90 inhibition releases a transcription factor that activates the transcription of various Hsps including Hsp70 in western blot analysis. We can see (Figure 27B) that the HT7 signal decreased with an increased 17-AAG concentration. That means that we can detect a decrease in hTauP301L aggregation signal with 1 µM, 3 µM and in 10 µM of 17-AAG. With lower concentrations of this compound (0.1 µM and 0.3 µM) we could not detect an effect of this compound on Tau aggregation, since in this case the levels of protein present in insoluble fraction in conditions treated and not treated with 17-AAG seemed be the same (Figure 27B). However in all of conditions some variation occurred between the triplicates, although the decrease in hTauP301L aggregated levels was consistent. With Hsp70 antibody we identified that levels of hTauP301L aggregation are inversely correlated with Hsp70 expression (Figure 27B), as we expected. However, the effect of Hsp90 inhibitors on soluble and insoluble Tau levels are directly correlated with toxicity levels of these compounds which mean that we could not confirm Hsp90 inhibition to be a viable drug target for AD.

A

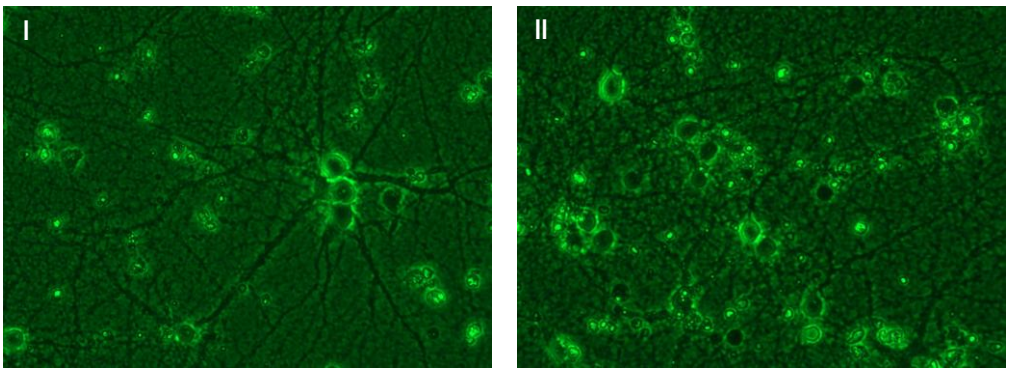

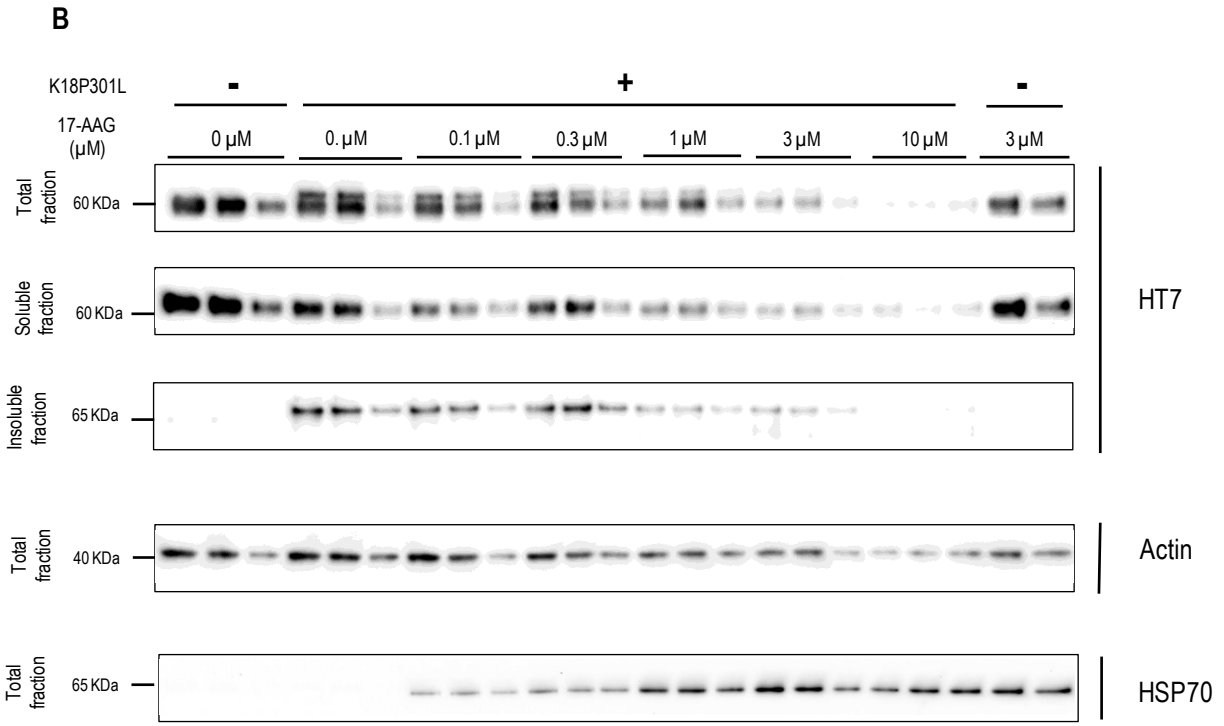

Figure 27 – Analysis of cortical primary neurons treated 48 hours before extraction with different concentrations of 17-AAG. (A) Microscopy images of cortical primary neurons at DIV 17 (I) untreated neurons and (II) 48 hours after neurons treated with 1µM of 17-AAG. (B) WB analysis of cortical primary neurons seeded or not with 1 µM of pre-aggregated K18P301L at DIV8, and treated or not treated with 0.1 µM, 0.3 µM, 1 µM, 3 µM and 10 µM of 17-AAG compound. The human total Tau was detected using HT7 monoclonal antibody, and anti-HSP70 detects endogenous levels of total heat inducible 70kDa protein HSPs. Expression level of Tau was normalized to actin.

3.2.2. Effect of 17-AAG in QBI seeding model

To test the effects of Hsp90 inhibitors on the development and clearance of Tau aggregates we evaluated the role of 17-AAG in the QBI seeding model. QBI cells were treated with different concentrations of 17-AAG 6 hours after seeding with 10 µM pre-aggregated K18P301L with BioPORTER reagent and the effects of the treatment on Tau aggregation was detected by western blot analysis (Figure 28). To detect the presence of human Tau we used HT7 antibody, and an Hsp70 antibody was used to verify the activity of 17-AAG in a western blot analysis. We could detect a clear hTauP301L aggregation in cells not treated with Hsp90 inhibitor, as well in cells treated with lower concentrations of the compound (0.1 µM and 0.3 µM) (Figure 28). However, when cells were treated with higher concentrations (3 µM and 10 µM) of 17-AAG, Tau aggregated signal was highly reduced, since we could not detected presence of protein in insoluble fraction (Figure 28A). Tau aggregation relative quantification was performed to have a more quantitative view on the western blot results (Figure 28B) and it we clearly observed a decrease in Tau aggregated protein with an increase in 17-AAG concentration.

Hsp90 inhibitors simultaneously stimulate degradation of misfolded client proteins and increase the expression levels of several Hsps, so the levels of hTauP301L aggregation are supposedly inversely correlated with Hsp70 expression. However, we did not see alteration in Hsp70 levels with the used of Hsp70 antibody, which was expected, in the presence of different concentrations of the compound.

Taking into account the data shown, we can conclude that 3 µM and 10 µM 17-AAG had a clear effect on insoluble Tau at 48 hours after treatment. This indicates that we had a reduction in the levels of Tau aggregation, just in the presence of higher compound concentrations.

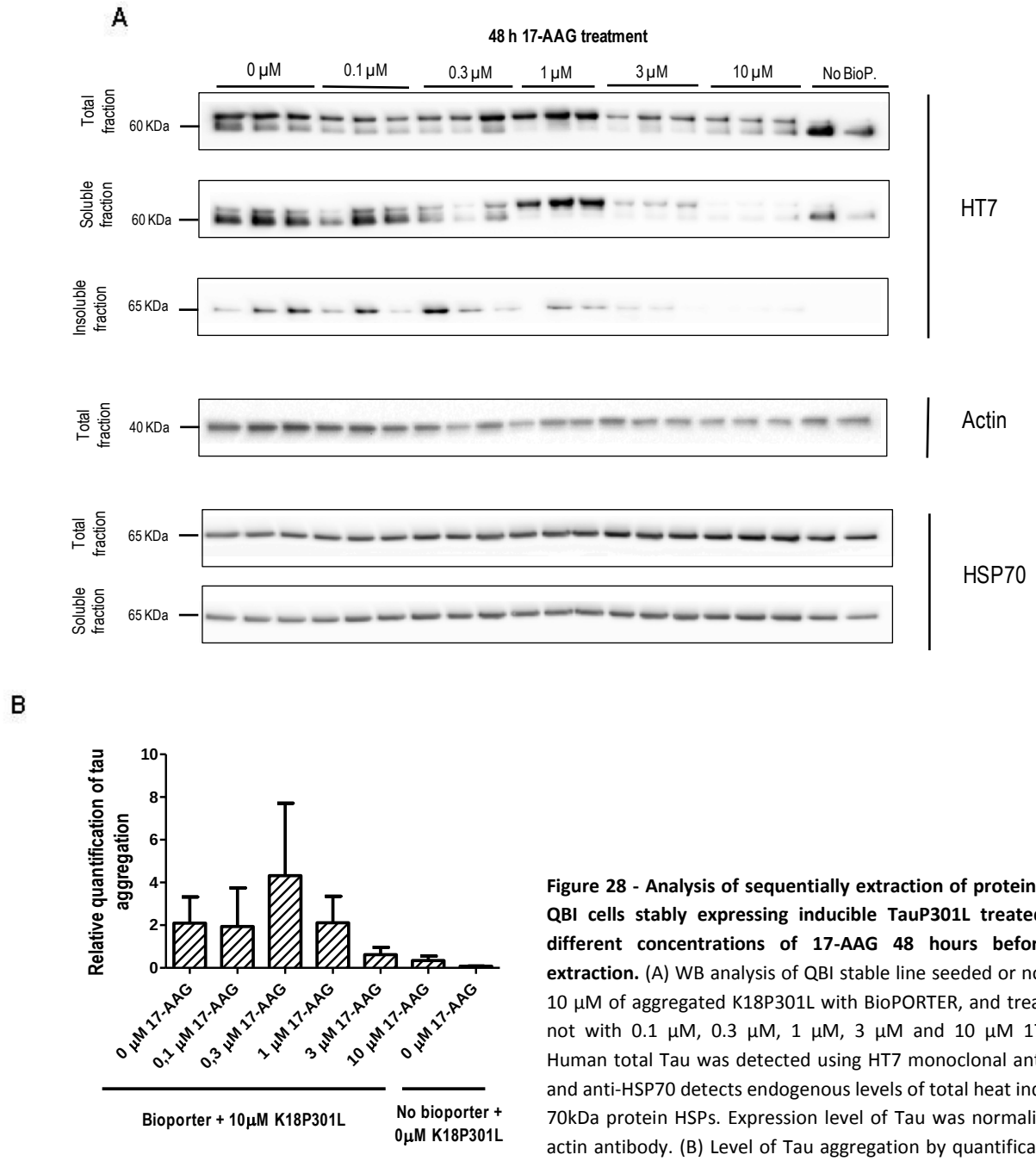

Figure 28 - Analysis of sequentially extraction of proteins from QBI cells stably expressing inducible TauP301L treated with different concentrations of 17-AAG 48 hours before the extraction. (A) WB analysis of QBI stable line seeded or not with 10 µM of aggregated K18P301L with BioPORTER, and treated or not with 0.1 µM, 0.3 µM, 1 µM, 3 µM and 10 µM 17-AAG. Human total Tau was detected using HT7 monoclonal antibody, and anti-HSP70 detects endogenous levels of total heat inducible 70kDa protein HSPs. Expression level of Tau was normalized by actin antibody. (B) Level of Tau aggregation by quantification of insoluble fraction band (normalized to actin), by western blot with HT7 antibody. N=3, average ± SD.

3.3. Development of assays for protein-protein interactions in living cells

3.3.1. BRET assay

In order to try to detect Tau-Tau interactions in living cells, we aimed to develop a BRET assay for monitoring transient protein-protein interactions in cells. Standard BRET system relies on the fusion of genetically encoded *Renilla* luciferase, which in presence of its bioluminogenic substrate acts as a resonance energy donor, and a fluorescent protein, which is a resonance energy acceptor. Currently BRET system emits light mostly in the green to yellow region of the visible spectrum (510-570 nm), rendering then suboptimal for imaging in living subjects. (Dragulescu-Andrasi, Chan, De, Massoud, & Gambhir, 2011; Savage, Wootten, Christopoulos, Sexton, & Furness, 2013).

Our lab used a BRET system, with better spectral properties. This assay uses an improved luciferase 150-fold brighter than *Renilla luciferase*, Nano-Luc luciferase (λ_{em}= 460nm) as donor, and HaloTag protein ($\lambda_{ex}/\lambda_{em}$ = 552/578nm) as the BRET acceptor. Nano-Luc is a small enzyme, of 19.1 KDa engineered for an optimal performance as a luminescent reporter. The luminescence reaction is ATP independent and designed to suppress background luminescence for maximal assay sensitivity. The HaloTag reporter protein is a monomeric protein, with 33 KDa, that is catalytically inactive, and it is derivative from a hydrolase, which forms a covalent bond with HaloTag ligands.

BRET proteins (Nano-Luc and HaloTag) were fused with full-length Tau2N4R with P301L mutation. Four different combinations to test this assay were tested, combining the four constructs made. These combinations could be with Nano-Luc either fused to the C- or N- terminus of Tau combined with Halotag either fused to the C- or N- terminus of another Tau molecule (Figure 29A). The constructs for the different fusion proteins were verified with a BsgI digest (Figure 29B). The size of the resulting DNA bands corresponded to the expected pattern of 5870 and 1110 bps for Nano-Luc-TauP301L (Figure 29B, lane 2), 6207 and 762 bps for TauP301L-Nano-Luc (Figure 29B, lane 3), 5702, 1110 and 571 bps for HaloTag-TauP301L (Figure 29B, lane 4) and 6180, 624 and 573 bps for TauP301L-HaloTag (Figure 29B, lane 5). The quality of the extracted DNA was acceptable, and the constructs were verified by sequencing, which reveled that the clones had no mutations. It was decided to use these plasmids further to co-transfect cells.

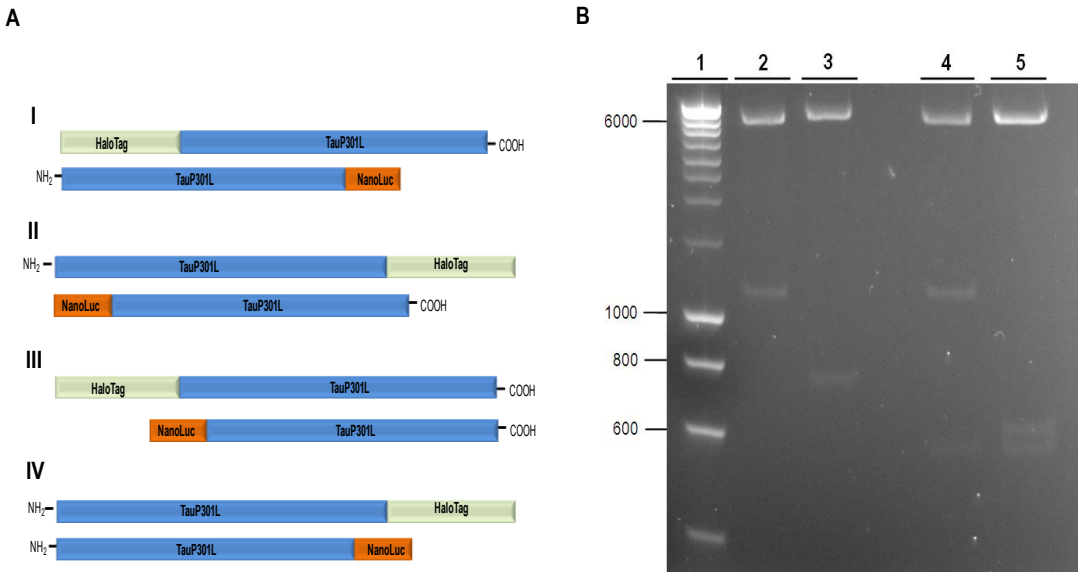

Figure 29 - Cloning of expression plasmids for different fusion proteins of Tau Nano-Luc or HaloTag. cDNA for Nano-Luc ™ luciferase or HaloTag® reporter protein was fused to the N- or C-terminus of the TauP301L. (A) Combinations: (I) HaloTag fused to the N-terminus of Tau and Nano-Luc fused to the C-terminus of Tau. (II) HaloTag fused to the C-terminus of Tau and Nano-Luc fused to the N-terminus of Tau (III) HaloTag fused to the N-terminus of Tau and Nano-Luc fused to the N-terminus of Tau. (IV) HaloTag fused to the C-terminus of Tau and Nano-Luc fused to the C-terminus of Tau. (B) BsgI control digestion of plasmid pcDNA4-TO MAPT-2N4R encoding Tau-Nano-Luc and -HaloTag fusion constructs. Samples were digested and run on a 2% e-gel. Lane 1 shows the Smart Ladder. Lane 2 show digested Nano-Luc-TauP301L. Lane 3 show digested TauP301L-Nano-Luc. Lane 4 show digested HaloTag-TauP301L. Lane 5 show digested TauP301L-HaloTag.

3.3.1.1. Quantification of Tau-Tau interactions in QBI seeding model

In order to understand if the BRET system developed by our group is functional, we made a positive control and a negative control with leucine zippers (LZs) constructs fused to Nano-Luc and Halo-tag proteins.

LZs are particularly strong interaction domains commonly frequent in transcription factors and have been shown to be functional in a heterologous context (Alber, 1992; Jérôme & Müller, 2001). This three dimensional motif is present in proteins, functioning as a dimerization domain and its presence produces adhesion forces in parallel α-helices. For this reason LZs are a good positive control.

Taking into account these characteristics, LZ was fused with C-terminal Nano-Luc and also LZ with C-terminal HaloTag (in a similar way as the schematic representation of the Tau fusion constructs). As a negative control we tested the combination of LZ-HaloTag with Nano-Luc-TauP301L. The optimal BRET signal is generally observed with the acceptor (HaloTag) species is in a molar excess to the donor (Nano-Luc species).

QBI 293 cells were co-transfected with different construct ratios of 1/1, 1/10, 1/100, and 1/1000 of HaloTag/ Nano-Luc (combining LZ/LZ or LZ/Tau) 48 hours before adding HaloTag TMR ligand. Upon

addition of NanoGlo (Nano-Luc substrate) luminescence was measured with band-pass filter 450 nm and with long pass filter 585 nm. To calculate BRET ratio this formula was used (see section 2.10 for more information):

$$BRET\ signal = \frac{[(average\ B) - (average\ A)]_{\text{LZ + LZ}}}{([(average\ B) - (average\ A))_{\text{LZ + Tau}}}$$

With LZ combination of constructs we observed a robust signal (Figure 30). The LZ-Tau combination resulted in no BRET signal (data not shown). We can conclude that BRET assay technically is working well, and that it can be used to detect interactions between proteins

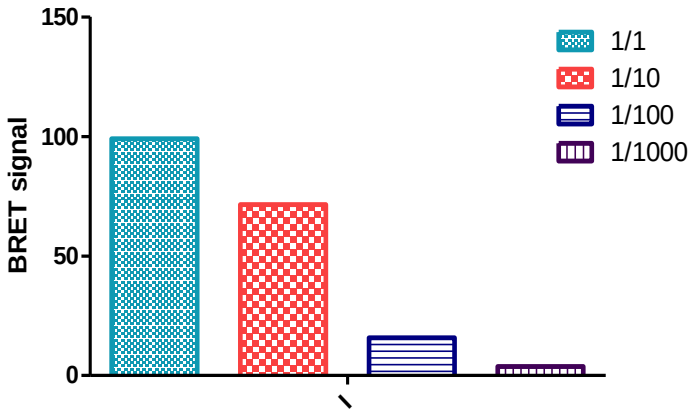

Figure 30 – BRET ratios measured in QBI cell cultures co-transfected with Leucine Zipper fused to Nano-Luc and HaloTag. Ratio was calculated with the signal of the positive control (LZs+LZs) over the negative control (LZs+Tau). 1/1, 1/10, 1/100 and 1/1000 corresponds to relative amounts of the plasmids co-transfected different dilutions, with acceptor species (HaloTag) in molar excess to the donor species (Nano-Luc).

Taking into account the previous results obtained with LZ constructs, different TauP301L-fusion constructs combinations were tested to determine the optimal ratio of energy donor to energy acceptor, in order to use the best one to measure the quantity of Tau aggregation in QBI seeding model.

For this, QBI cells were co-transfected with different constructs ratios 1/10, 1/30, and 1/100 of HaloTag/Nano-Luc fused to Tau2N4R-P301L (as described in topic 3.3.1). Cells were seeded with pre-aggregated fibrils 2 days after platting. The addition of HaloTag TMR ligand was done in the day after the cells were seeded with fibrils and in the day of measurement, NanoGlo substrate was added to the cells. The luminescence was measured with a band-pass filter of 450 nm and with a long pass filter of 585 nm. To calculate BRET ratio this formula was used (see section 2.10 for more information):

$$BRET\ signal = \frac{[(average\ B) - (average\ A)]_{\text{+ K18P301L}}}{([(average\ B) - (average\ A))_{\text{- K18P301L}}}$$

We could not obtain BRET signal in any construct combination tested, since as to considered BRET signal the ratio must be higher than 1 (Figure 31). It was expected that in this assay the more Tau protein is aggregating, the higher the BRET signal will be. The signal was slightly higher with N-terminal Nano-Luc with C-terminal HaloTag compared to others construct combinations, but this increase was not significant (Figure 31-IV). The results shown in Figure 31 are an average between the experiments performed. It was difficult to avoid variability of levels between cells and experiments, since in this kind of assay there is clear difference from plate to plate. In experiments with other constructs combinations, we could not detect any significant BRET signal under any conditions (different dilutions).

In order to discard the hypothesis that the problem of a lack of functioning of BRET assay is due to a lack of interaction between the fusion proteins, we tested the efficiency of aggregation of the different fusion proteins in QBI cells. For these a western blot analysis was performed on QBI cells expressing the different constructs and seeded with fibrils. HT7 antibody and a monoclonal Halo-tag antibody were used to detect the proteins in the blots. The fusion of donor and acceptor proteins with Tau did not lead to a significant change in aggregation kinetics in QBI seeding model, which was noticed by the absence of alteration in the intensity of bands present in insoluble fraction (data not shown).

Taking into account this data, we can conclude that with these constructs combinations, it is not possible to measure Tau aggregation in living cells. It may however be that the position of the donor relatively to the acceptor and the type of linker used has a crucial relevance for this assay. With a proper optimization of these aspects this technique could be a promising assay to use in the future.

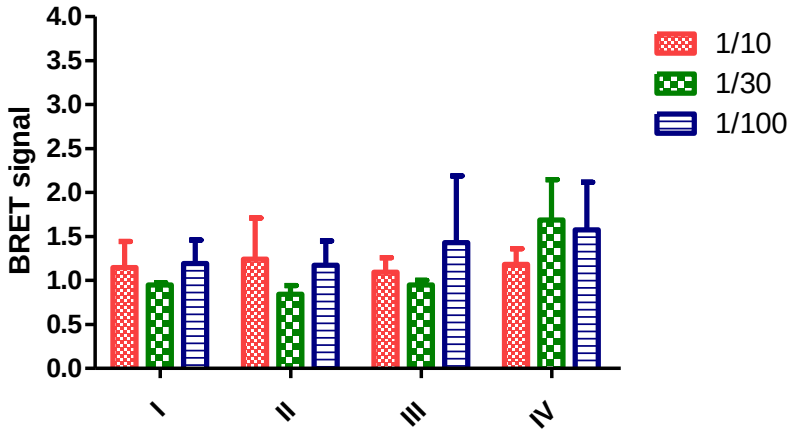

Figure 31 –Average of BRET ratios measured in QBI cell cultures transfected with different donor and acceptor combinations. QBI 293 cells were co-transfected with donor species - Nano-Luc fused to the N- or C-terminus of Tau2N4R-P301L isoform and with acceptor species - HaloTag also fused to the N- or C--terminus of Tau2N4R-P301L isoform. 1/10, 1/30, 1/100 corresponds to relative quantities of the transfected plasmids, with acceptor species (HaloTag) in molar excess to the donor species (Nano-Luc). QBI cells were also seeded or not with 10 µM pre-aggregated K18P301L (delivered to the cells with BioPORTER reagent). (I) Nano-Luc-TauP301L co-transfected with HaloTag-TauP301L. Average of 2 experiments is represented. (II) TauP301L-Nano-Luc co-transfected with TauP301L-HaloTag. Average of 4 experiments is depicted. (III) TauP301L-Nano-Luc co-transfected with HaloTag-TauP301L. Average of 3 experiments is presented. (IV) Nano-Luc-TauP301L co-transfected with TauP301L-HaloTag. Average of 4 experiments is presented. Error bars ± SD.

3.3.2. Venus split complementation assay

3.3.2.1. Qualitative analysis of Tau aggregation process in QBI seeding model

As an alternative to the BRET assay to measure aggregated Tau in living cells, we developed a split GFP complementation-based assay using QBI seeding model. This assay had been introduced to detect the aggregation state of proteins *in vitro*, consisting on the reassembly of a fluorescent protein from its two complementary nonfluorescencent fragments, where its association facilitated by interaction between two proteins fused to each fragment (Michnick, Ear, Manderson, Remy, & Stefan, 2007; Ohashi, Kiuchi, Shoji, Sampei, & Mizuno, 2012) [Figure 32].

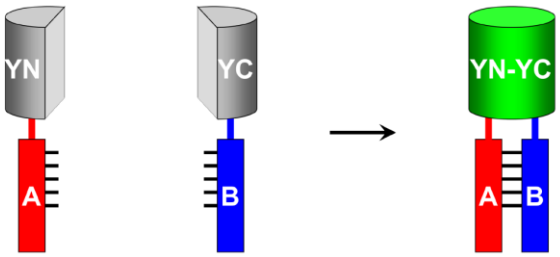

Figure 32- Schematic representation of Venus split complementation assay. Non-fluorescence fragments YN and YC are fused with two proteins (A and B). The interaction between proteins allows formation of a complex (Kerppola, 2008).

Our lab used a modified form of this assay with a Venus fused protein that is an improved in efficiency of yellow fluorescence protein. This protein contains a mutation that at 37°C greatly accelerates oxidation of the chromophore, the rate-limiting step of maturation (Cabantous, Terwilliger, & Waldo, 2005).

To examine qualitatively Tau aggregation in QBI seeding model, first, three different construct combinations were made. N- or C-terminal part of Venus was fused to the N- or C-terminus of full-length TauP301L (Figure 33A). QBI cells were co-transfected with different constructs that we made, and in the following day the cells were seeded or not with 10 µM pre-aggregated K18P301L fibrils delivered to the cell by BioPORTER reagent. We observed (Figure 33BII) a fluorescent signal in even the absence of K18P301L fibrils. It should be noted that no fluorescence signal was observed by co-expression of the Venus fragments by themselves which means that there was no spontaneous association between the N- and C-terminal parts of Venus (data not shown). A fluorescence signal was also observed (Figure 33BII) in presence of K18P301L fibrils there was however a redistribution of the localization of the signal in cells treated with pre-aggregating seeds.

Taking into account these data, they high background fluorescence in the absence of aggregation greatly reduced the usefulness of this assay.

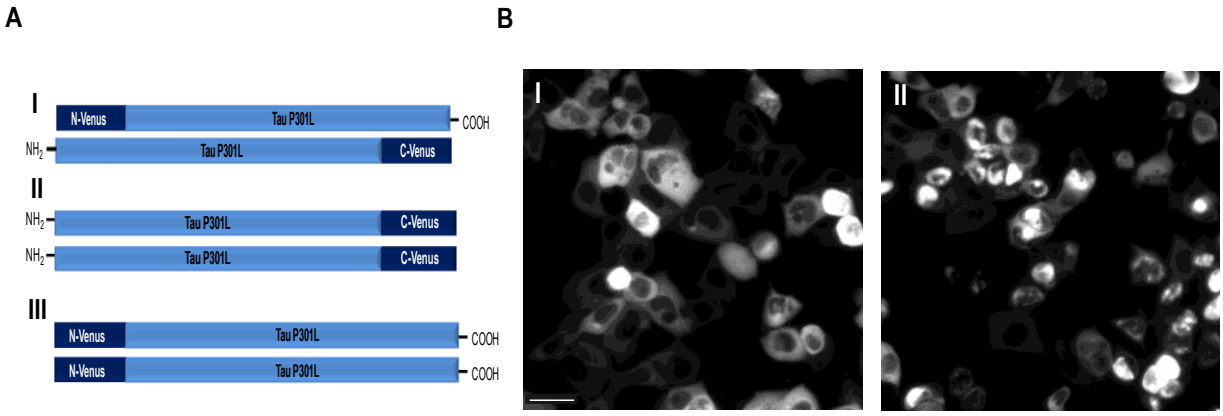

Figure 33 - Combinations of the N- or C-terminal part of Venus fused to the N- or C-terminus of TauP301L. The N- or C-terminal part of the Venus protein, a variant of yellow florescent protein, was fused to the N- or C-terminus of TauP301L. (A) Combinations: (I) N-terminal fragment of Venus fused to the C-terminus of TauP301L co-transfected with the C-terminal fragment of Venus fused to the N-terminus of TauP301L; (II) C-terminal fragment of Venus fused to the N-terminus of TauP301L co-transfected with the C-terminal fragment of Venus fused to the N-terminus of TauP301L; (III) N-terminal fragment of Venus fused to the C-terminus of TauP301L co-transfected with the N-terminal fragment of Venus fused to the C-terminus of TauP301L. (B) Fluorescence micrographs of QBI 293 cells expressing N-terminal fragment of Venus fused to the C-terminus of TauP301L co-transfected with the C-terminal fragment of Venus fused to the N-terminus of TauP301L; (I) not seeded with *in vitro* pre-aggregated K18P301L; and (II) seeded with *in vitro* pre-aggregated K18P301L. Images were acquired by a fluorescence microscopy with magnification of 20x. Scale bar: 450µM

In order to understand if the fluorescence signal obtained in the Figure above corresponds to spontaneous Tau aggregation in the QBI seeding model we made a constructs of Venus protein fused to Tau with two isoleucine to proline mutations in the MT-binding region. This mutation leads to an inefficiency of Tau aggregation, because proline interrupts the extended chain conformation necessary for ß-sheet interactions (von Bergen et al., 2001) .

N- or C- terminal part of Venus was fused with either the C- or N- terminus of K18/P301L/2P. We tested different combinations of constructs in the seeded the cells with pre-aggregated K18P301L fibrils delivered to the cell by BioPORTER reagent (Figure 34A). The double proline mutations did not reduce the basal fluorescent signal suggesting that this mutation did not block the interaction between these fusion proteins (Figure 34BI). However, the double proline did prevent the redistribution of the florescent signal (Figure 34BII). This suggests that the prolines interfered with aggregation in this model. The nature of the interaction between the fusion proteins in the absence of aggregation induction is not entirely clear from this data.

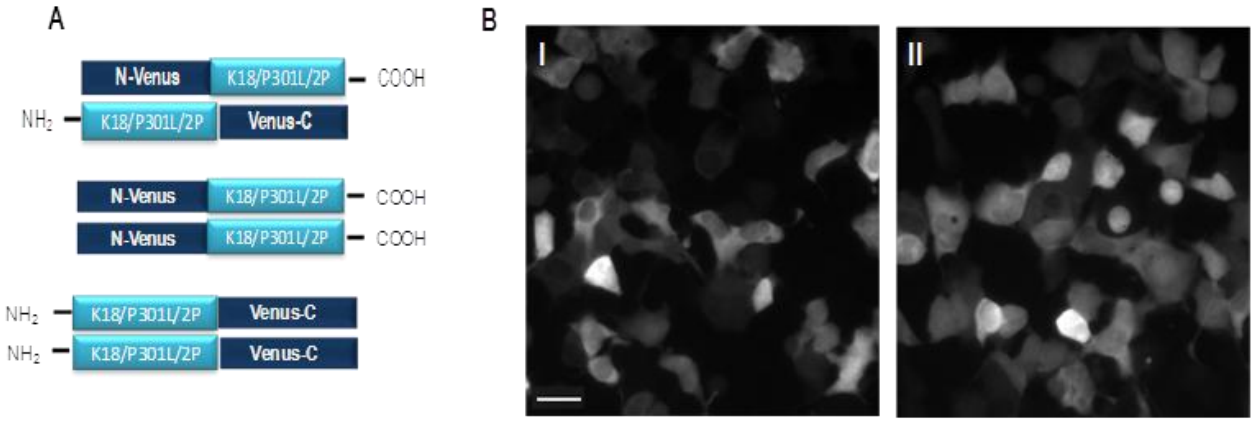

Figure 34 - Combinations of double proline Tau mutant construct with Venus expression constructs. Both of Venus constructs are fused with proline mutated constructs of Tau contains Iso-to-Pro substitution mutations at Iso277 and Iso308 in the hexapeptide motifs. All of the constructs were cloned in *E.coli* cells. A) Combinations: N-terminal fragment of Venus fused to C-terminus of K18/P301L/2P co-transfected with C-terminal fragment of Venus fused to the N-terminus of K18/P301L/2P; N-terminal fragment of Venus fused to C-terminus of K18/P301L/2P co-transfected with N-terminal fragment of Venus fused to the C-terminus of K18/P301L/2P; C-terminal fragment of Venus fused to N-terminus of K18/P301L/2P co-transfected with C-terminal fragment of Venus fused to the N-terminus of K18/P301L/2P. (B) Fluorescence micrographs of QBI 293 cells expressing N-terminal fragment of Venus fused to the C-terminus of K18/P301L/2P co-transfected with the C-terminal fragment of Venus fused to the N-terminus of K18/P301L/2P (I) not seeded with *in vitro* pre-aggregated K18P301L; and (II) seeded with *in vitro* pre-aggregated K18P301L. Images were acquired by a fluorescence microscopy with magnification of 20x. Scale bar: 450µM

To further study the nature of the interaction between the Tau-Venus fusion proteins in the absence of aggregation, constructs were made containing just MT-binding repeats. N- or C-terminus parts of Venus were fused to the N- or C-terminus of K18-P301L. Different combinations of constructs were co-transfected in QBI cells (Figure 35A). One day after transfection cells were seeded with or without pre-aggregated K18P301L fibrils delivered to the cells by BioPORTER reagent. Results obtained by fluorescence microscopy are shown in Figure 35B.

All the combinations of co-transfected K18P301L-Venus constructs showed a basal fluorescent signal similar to the signal obtained with full length TauP301L-Venus fusion proteins (Figure 35B). This suggests that also K18 fusion proteins showed spontaneous interactions. In addition, some cells showed a redistribution of the florescent signal reminiscent as described above even in cells not seeded with Tau fibrils (Figure 35BI, III). The signal redistribution is greatly enhanced after seeding with K18P301L fibrils to levels far greater than observed with full length Tau fusion protein (Figure 35BII, IV). This could be due to the stronger aggregation tendency of these shorter Tau fragments.

Analyzing the presented results, we can conclude that spontaneous aggregation in QBI seeding model occurs when they were co-transfected with these constructs, shown by the data obtained where we verified the presence of redistribution of signal in QBI cells none treated with pre-aggregated seeds. This means that truncated form K18-P301L increased the propensity to Tau aggregate in QBI cells.

Taking account the results previously showed in Figure 33B and the results of the Figure 35B we can observed that the percentage of QBI cells with spontaneous re-distribution of signal was significantly

higher for cells co-transfected with K18-P301L compared with cells co-transfected with full-length form of Tau. We can also conclude that spontaneous re-distribution of signal in presence or absent of fibril treatment was blocked with double-proline mutation.

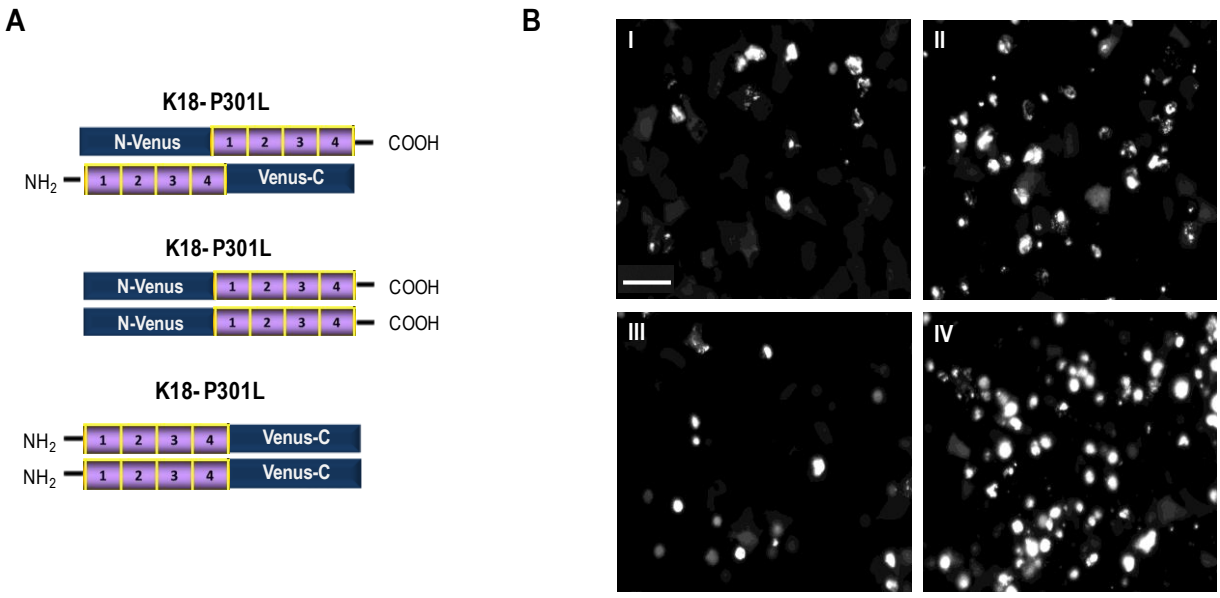

Figure 35 - Combinations of K18-P301L Tau mutant constructs with Venus expression constructs. Both constructs are fused with K18P301L truncated form of Tau containing only the four MT-binding repeats. All of the constructs were cloned in *E.coli* cells. (A) Combinations: N-terminal fragment of Venus fused to C-terminus of K18-P301L co-transfected with C-terminal fragment of Venus fused to the N-terminus of K18-P301L; N-terminal fragment of Venus fused to C-terminus of K18-P301L co-transfected with N-terminal fragment of Venus fused to the C-terminus of K18-P301L; C-terminal fragment of Venus fused to N-terminus of K18-P301L co-transfected with C-terminal fragment of Venus fused to the N-terminus of K18-P301L. (B) Fluorescence micrographs of QBI 293 cells expressing N-terminal fragment of Venus fused to the C-terminus of K18P301L co-transfected with the C-terminal fragment of Venus fused to the N-terminus of K18P301L (I) 24 hours of BioPORTER with sodium acetate treatment in QBI cells; (II) 24 hours of QBI cells seeded with BioPORTER+10 µM of *in vitro* pre-aggregated K18P301L. (III) 48 hours QBI cells treated with BioPORTER+sodium acetate; (IV) 48 hours of QBI cells seeded with BioPORTER+10 µM of *in vitro* pre-aggregated K18P301L. Images were acquired by a fluorescence microscopy with magnification of 20x. Scale bar: 450µM

Chapter 4 Discussion

Abnormal phosphorylation and mislocalization of Tau is considered an early hallmark of Tauopathies such as AD and precedes the aggregation process present in this kind of disease. However, the role of these changes in pathological conditions is still poorly understood. In an attempt to make advancements in understanding this, it is necessary to have a fast, flexible and robust test system. The first goal of the experimental work shown here was to optimize a consistent *in vitro* model of Tauopathy, in QBI cells and cortical primary rat neurons. During the years, there have been many significant efforts to produce cell-based models to mimic Tau aggregation, in a similar way to what is observed in Tauopathies, but without much success. One of the major obstacles is the high solubility of Tau and the fact that in solution it adopts a natively unfolded structure, which makes it difficult to reproduce aggregated structures in culture.

The model developed by Guo and Lee and adopted by our lab could be a promising model to mimic aggregation process in neuronal cells (Guo & Lee, 2011). Through the use of *in vitro* pre-aggregated fibrillized material, it was possible to accelerate the intracellular fibrillization of monomeric Tau, moving the process from the initial lag phase to elongation phase, since the fibrils assembly occurs by a nucleation-dependent mechanism which corresponds to a longer step (Guo & Lee, 2011). In concordance with the already described seeding model in QBI cells (Guo & Lee, 2011; Master thesis Sara Calafate 2012) a similar model was developed in cortical neurons. Also in these cells intracellular hTauP301L aggregation was nucleated through seeded with *in vitro* pre-aggregated fibrils. In these primary cortical neuronal cultures no spontaneous aggregation was observed. This means that the nucleation step is a fundamental step in the aggregation mechanism. The same conclusion was obtained with α-synuclein in SH-SY5Y cells, in which aggregation could be blocked with the use of small molecular compounds that inhibits ß-sheet formation (Nonaka et al., 2010).

During the optimization of the hTauP301L neuronal aggregation model, it was found that in cortical primary neurons it is possible to induce Tau aggregation by the simple addition of synthetic pre-aggregated fibrils to the neuronal cultures, without the presence of any delivery reagent. This is in contrast to what was described (Guo & Lee, 2011) and confirmed by our group in the QBI seeding model. When synthetic fibrils are applied directly to the medium of the QBI cells, intracellular Tau aggregation was induced in only a very small percentage of cells. This suggests that in neurons, the uptake of fibrillar Tau and seeding of normal Tau into pathological aggregates is much more efficient that in QBI cells. The uptake of *in vitro* pre-aggregated Tau fibrils has been shown to be regulated by non-receptor mediated endocytosis (Frost, Jacks, et al., 2009; Wu et al., 2013). Wu et al. suggested that in HeLa cells the internalized aggregates are transported via endosomal vesicles and trafficked through the endosomal pathway to lysosomes (Wu et al., 2013). This process can also occur in QBI cells, and without the presence of the BioPORTER delivery reagent, the cells can internalize a small quantity of aggregates in the same way that occurs in neurons. However, these aggregates can be forwarded to lysosomes and be immediately

degraded by autophagy-lyssomal system. If this occurs, there is no possible induction of aggregation by synthetic pre-aggregated fibrils in QBI cells without a delivery reagent. The use of the delivery reagent may increase the quantity of aggregated material taken up by the QBI cells, or it may alter the pathway by which the fibrils are taken up by the cells, which may protect the seeds from degradation.

It was observed in the hTauP301L neuronal model that the amount of hTauP301L aggregation is dependent on the amount of Tau mutant fibrils added to the system. This strongly suggests that an increase in uptake of *in vitro* pre-aggregated fibrils will trigger a higher level of intracellular hTauP301L aggregation. Eisenberg and Jucker demonstrated that if the transition of limitant step is exceeded, a higher concentration of the fibrils leads to an increase in aggregation (Eisenberg & Jucker, 2012). This data is also supported by the fact of Tau having amyloid fibril structure, and fibrils seeds are rich in cross-β-sheet secondary structure, that will facilitate aggregation of other proteins with this kind of structure (Lee, Lim, Masliah, & Lee, 2011).

During the optimization of the hTauP301L neuronal aggregation model it was not possible to demonstrate that recombinant K18P301L fibrils could induce WT Tau aggregation in cellular and neuronal systems. In cells transduced with hTauWT, a monomeric protein was detected in the total fraction similar to what was observed with cells transduced with hTauP301L. However, no WT Tau was found in the insoluble fraction after seeding the cells with fibrils. In addition, no increase in staining with AT8, a phospho-specific antibody, was seen after fibril seeding as was observed with TauP301L expressing neurons. This evidence is consistent with events that occur in FTDP-17 patients with the P301L mutation, since they do not present insoluble WT Tau deposition (Miyasaka et al., 2001). However it may be that WT does aggregate in this model, albeit at a much slower rate than Tau with the P301L mutation, a mutation that leads to an increased fibrilization propensity (Guo & Lee, 2011; Waxman & Giasson, 2011). In an attempt to verify this possibility, an experimental procedure to study the aggregation dynamic of hTauWT could be done, increasing the days of exposure to synthetic pre-aggregated fibrils in cultures expressing endogenous WT Tau. On the other hand, we could also study the aggregation process in cultures exposed to synthetic WT fibrils and expressing endogenous WT Tau.

One of the characteristics that has been associated with the Tau pathology in recent years is a temporal and spatial spread of NFT through the brain (Braak & Braak, 1991; Clavaguera et al., 2009). We observed that *in vitr*o pre-aggregated fibrils induced hTauP301L aggregation in a time dependent manner. It was observed that an increase in neuronal exposure length to pre-aggregated synthetic fibrils resulted in an increase in detection of hTauP301L aggregation. With an increase in exposure time to fibrillar material, a small increase in Tau aggregation, detected with HT7 antibody, was observed. The pre-tangle material, a soluble Tau form, can be identified by the AT8 antibody. However, the most imuno-reactivity achieved with this antibody is with the low migrating fraction/insoluble fraction as that this antibody is specific to phosphorylated epitopes Ser202 and Tyr205 (Augustinack et al., 2002; Braak & Del Tredici, 2011). So, with

this data we could not confirm an increase in phosphorylated Tau over time. However, it was possible to detect an increase in aggregated hTauP301L over time, since the aggregation process showed an exponential growth (DIV14 and 17) until the reaction reached an equilibrium phase, where the rate of fibrils growth was equal that of shrinkage (DIV20 and 22). The data presented here are supported by the amyloid fibrillation process (Lee et al., 2011). A hypothesis that could explain the increase in hTauP301L aggregation is the constitutively expression of transduction protein over time, in presence of synthetic fibrils. This may mean that a change in conformation of soluble Tau occurs induced by fibrillar material. However, it is not possible to determine the existence of spreading in these experimental procedures. This is because it is not noticeable in these kinds of neuronal cultures if the aggregated Tau spreading is from one cell to another or if each neuron uptakes the pre-aggregated fibrils. In order to overcome this problem and investigate if there is a spreading mechanism associated with the hTauP301L aggregation, microfluidic polydimethylsiloxane chambers could be used, since this kind of technique can allow to separate two chambers with different conditions, but keep dendrites and axons across both chambers, so the uptake and movement inside cells could be studied.

Neurodegeneration is closely associated with a neuronal loss in AD (Braak & Braak, 1997), although the mechanisms of Tau-mediated cell death are still under debate (Spires-Jones, Kopeikina, Koffie, De Calignon, & Hyman, 2011). In our hTauP301L neuronal aggregation model we could not correlate a decrease in neuronal viability over time with aggregation of hTauP301L. The initial increase in quantity of neurons from DIV0 to DIV3 observed in data could be explained by the loss of neurons in DIV0 due to washing steps that must be performed during the Immunocytochemistry protocol. All cortical neurons may not be adhered tightly to the plate 19 hours after plating, and with the washing steps some neurons may be removed. In primary cortical neurons there was no detection of any difference in cell viability in neurons that were transduced with TauP301L and seeded with *in vitro* pre-aggregated fibrils, compared to neurons neither transduced with TauP301L nor seeded with fibrils. The decrease in neuronal viability that occurs is related to the neuronal death process that happens to the neurons with an increase of days in culture. AD patients show an activation of inflammatory cells (Wyss-Coray, 2006), in agreement with this neuronal cultures also show an increase in non-neuronal cells, which may correlate with an increase in glial cells. This means that the aggregation process triggered by P301L Tau mutation and the presence of synthetic fibrils is not neurotoxic in cortical neurons.

In the P301L injected mice model developed by our group and described by Iba et al., with an intracellular injection of *in vitro* pre-aggregated fibrils (Iba et al., 2013), we detected no cell loss in the cortex. However, significant cell death was observed in the CA1 hipocampal region in the *in vivo* injection mouse model, observed with Nissl staining. Therefore, effects on neuronal viability in this model should be repeated using hippocampal cultures. With this knowledge it could be possible to have an increased bridge between the *in vitro* and the *in vivo* models.

Our study provides two models for the study of molecular mechanisms involved in Tau pathology, although the heterogeneity between cells (in primary cortical neurons as well in QBI cells) is obvious in all of the experiments performed with these models. This is however an evident problem for every attempt at optimizing a cellular model, since multiple mechanisms could often exist for a particular cellular behavior or activity. These mechanisms can also vary between individual cells, even within the same monoclonal population (Altschuler & Wu, 2010; Pelkmans, 2012). In a cellular model used to test compounds, the cell variability can be a problem as we would encounter extreme difficulties replicating the results, although these cellular differences may have no functional significance.

Mechanisms to avoid variability between cells will therefore need to be performed, for example we could increase the number of cultures being studied at the same time, which could be done by pooling repetitions with same conditions. In a primary culture it is also important to factor in the existence of other different brain cells within the culture, since the amount of protein being measured in the biochemical analysis may not all be from the neurons. A possibility to avoid this is to use for example a compound that partially inhibits astrocyte growth. The use of "housekeeping" proteins, such as actin, could be another problem in experiments performed with this model. This is because actin levels are often chose as reference in assays with the assumption that their variation in expression is small and/or biologically unimportant, but this may not be the case (Altschuler & Wu, 2010). The fact that actin is also not present in the insoluble fraction is another problem within this model.

Intracellular deposits of insoluble hyperphosphorylated Tau protein are one of the major pathogenic features associated with AD. Aberrant Tau aggregation may result in part from failure of chaperone-mediated protein ubiquitination and degradation (Waza et al., 2006). It has been shown that molecular chaperones are capable of reducing phosphorylated Tau and could prevent Tau-associated cellular toxicity (Petrucelli et al., 2004). Hsp90 is a major cellular chaperone which is evolved in the assembly of large complexes with a variety of co-chaperones, and its functions are to maintain protein quality control and assist in protein degradation. Tau is a client protein of this Hsp90 complex, so if the protein is in an abnormal or modified form, there may be recruitment of the CHIP protein, a co-chaperone with E3 activity, to the Hsp90-Tau complex, resulting the ubiquitination of Tau protein (Petrucelli et al., 2004; Salminen et al., 2011). Dickey et al. observed that CHIP can distinguish between Tau proteins phosphorylated at normal Ser residues and Ser/Thr phosphorylated Tau sites associated with pathological form of Tau protein and will then only bind to the aberrant proteins. This group also demonstrated that high-affinity Hsp90 binding complexes are present in AD patients samples, but not in control samples (Dickey et al., 2007). It was demonstrated that CHIP protein, in collaboration with Hsp90 complex, caused degradation of phosphorylated Tau. Inhibition of the Hsp90 complex promotes the selective degradation of phosphorylated Tau protein *in vivo* model of Tauopathy (Andorfer et al., 2003), indicating that the blockage of folding/refolding pathways promotes the degradation of phosphorylated Tau protein (Dickey,

Yue, et al., 2006; Dickey et al., 2007). This study demonstrates that Hsp90 inhibitors could provide a possible therapeutic strategy for AD, by the enhancement of Hsp90/CHIP mediated Tau phosphorylation.

To develop a way to induce the clearance of Tau aggregates, through the use of Hsp90 inhibitors, was one of aims of the work shown here. Previous work already developed in our group, with 17-DMAG, an Hsp90 inhibitor, showed that there was an active inhibition of the Hsp90 activity and a decrease in Tau aggregation (Master thesis Sara Calafate 2012). However, Dickey et al. showed an increased in toxicity for neurons treated with 17-DMAG compared to neurons treated with 17-AAG (Dickey, Dunmore, et al., 2006). Taking into account these conclusions, the effect of 17-AAG (Hsp90 inhibitor) was studied in the QBI seeding model, as well in the hTauP301L neuronal aggregation model. In the QBI seeding model it was detectable a decrease in Tau aggregation in cells treated with 17-AAG. This evident effect in soluble and insoluble aggregated Tau species, dependent on the concentration of inhibitor, clearly contradicted the results previously obtained by our group (Master thesis Sara Calafate 2012). However, in this model there was no visible activation of chaperone machinery, since the levels of Hsp70 reamined constant, not showing changes with treatment with Hsp90 inhibitor. This could be due to the fact that basal levels of Hsp70 expression in QBI cells are very high in conditions without treatment, so in case of cells treated with Hsp90 inhibitors there is no visible difference in the expression of Hsp70.

In the hTauP301L neuronal aggregation model, with 17-AAG treatment, as observed in QBI seeding model, there was also a dose dependent decrease in soluble Tau protein and an insoluble aggregated Tau. However it is evident an activation of chaperone machinery after neuronal treatment with 17-AAG inversely correlates with an increase in levels of Hsp70, as expected (Dickey et al., 2008). However, toxicity tests of some Hsp90 inhibitors made in our group on the hTauP301L neuronal aggregation model observed that toxic effects increased over time. The effects of Hsp90 inhibitors on Tau levels also correlate strongly with toxicity of this compound (data not shown). This fact makes this *in vitro* model inappropriate to test the Hsp90 inhibitors. Hsp90 inhibitors were also tested in the fibril injected P301L transgenic mouse model, but no positive results were achieved. We have also not tested the effects on the soluble and insoluble fractions in animals treated with one of the Hsp90 inhibitor. This was because the toxicity of these compounds was found to be too high, triggering extensive damage in the rat's organs. Taking this into account the Hsp90 inhibitor that showed less toxicity should be retested in a less aggressive mouse model of Tau aggregation.

Natural or herbal compounds could be potential candidates for the treatment of Tauopathies, such as AD. Ma et al. described that curcumin, a polyphenolic compound derived from the plant *Curcuma Long Lin,* reduced levels of soluble Tau dimers but not the levels of insoluble and monomeric phosphorylated Tau. This compound may act by increasing the levels of Hsp70, Hsp90 and HSC70 (Ma et al., 2013; Ringman et al., 2012). Our preliminary results with curcumin treatment in the hTauP301L neuronal aggregation model showed a decrease in levels of soluble and insoluble hTauP301L in cortical neurons exposed to this

compound for 48 hours, however there was no detection of any alteration in Hsp70 levels (data not shown). The ability of this compound to decrease Tau aggregation, and the role of Hsps still needs to be studied with a stronger effort.

It is necessary to try to find new strategies to increase protein turnover by, for example ubiquitin-proteossome system or/and by autophagy (Rubinsztein, 2006) and delay or inhibiting Tau aggregation by, for example, inhibitors that will have been effect in ß-sheet conformation. (Zheng et al., 2011; Zheng, Baghkhanian, & Nowick, 2013). Methylene blue has been shown to be an inhibitor of Tau aggregation *in vitro* (Taniguchi et al., 2005; Wischik et al., 1996) and *in vivo* (O'Leary et al., 2010). Congdon et al. demonstrated that methylene blue is capable of inducing autophagy in primary cortical neurons, in organotypic slice cultures and transgenic animals (JNLP3). This led to a decrease in levels of hyperphosphorylated soluble and insoluble Tau, as well in levels of aggregated Tau (Congdon et al., 2012). The reduction of phosphorylated Tau aggregation was also detected in another study using P301L Tau transgenic mice (Hosokawa et al., 2012). However several different mechanisms of action for this compound have been proposed. A study from Crowe et al. demonstrated that methylene blue has an effect on Hsp70 by inducing of Tau dimerization and these dimmers are excluded from the aggregation process (Crowe et al., 2013). This potential compound is in clinical trials in phase II with promising results in AD patients (Crowe et al., 2013). This evidence makes this compound a potential candidate for the inhibition of Tau fibrillization, and a possible lead compound to develop new potential compounds to treat AD.

Developing techniques to identify and analyze protein-protein interactions is extremely important to understanding various disease mechanisms and developing new therapeutic approaches. These interactions are present in many key events in cell processes, from division to adaption or response to extracellular signals, leading to biological effects. The establishment of an assay to quantitatively monitor Tau aggregate formation in living cells was one of the aims of the experimental project present here.

BRET system has several advantages compared with others methods. Since it is a homogenous assay, it could be performed in live cells as a fluorescence resonance energy transfer (FRET) assay, but with much higher sensitivity, that will permit monitoring interactions between proteins in an intact cellular context (Couturier & Deprez, 2012). We developed a BRET system with better spectral properties in an attempt to evaluate the Tau aggregation process in the QBI seeding model. To perform this technique, Nano-luc luciferase was used as a donor with the HaloTag protein, an affinity tag that can be covalently bound to molecules, being used as an acceptor. Our data with LZs indicates the maximal BRET signal that we could obtain in an optimal situation. This is because these structures work as a dimerization domain with their presence producing adhesion forces in parallel α-helices (Jérôme & Müller, 2001) which lead to an increased in proximity of constructs and an efficient transference of energy between donor and acceptor species. Building on the data obtained, this BRET system could be a promising assay to detect the

interaction between Tau proteins, in order to detect aggregation. The obtained signal from the BRET constructs fused with full-length Tau was expected to have a lower signal than the positive control, with LZ. The signal obtained from full-length Tau was indeed lower, but it was too low to be considered as a positive BRET signal, as to be considered BRET signal, the ratio must be above 1. Considering this, we could conclude that it is not possible to detect BRET signal with constructs using full-length form of Tau. This can be explained by the natively unfolded structure and a low content of secondary structure present in full-length form of Tau protein. These properties result in the presence of high fraction of basic hydrophilic amino acid residues, which resist the compact folding typical of most proteins (Jeganathan, Von Bergen, Mandelkow, & Mandelkow, 2008; Mukrasch et al., 2009). As such, these properties of Tau mean the constructs are not able to interact and transfer energy efficiently, even in presence of *in vitro* pre-aggregated fibrils to induce aggregation. Changing full-length TauP301L by Tau K18-P301L construct to fuse with Nano-Luc and HaloTag could be an hypothesis to better study this, since K18-P301L constructs have the same ß-structure of the full-length form of TauP301L but are a smaller size, just 129 aa, compared to the 441 aa of full length Tau (Jeganathan et al., 2008). This construct has a which could lead to a higher capacity of interaction and efficient energy transfer, and as a consequence, the detection of BRET signal.

As an alternative to BRET assay, to monitor Tau aggregate formation and evaluate how the process is modulated in living cells (Cabantous et al., 2005), we developed a variant of split GFP complementation assay, with Venus instead of GFP protein. This assay is extremely advantageous, especially due to its ease of use, and by the high sensitivity of the detection system (Kerppola, 2008; Pusch, Dissmeyer, & Schnittger, 2011). This relies on the fusion of two non-fluorescent halves of the functional Venus with the protein of interest, in our case Tau protein. In the study presented here, split Venus complementation with different Tau constructs was investigated in the QBI seeding model. Therefore full-length TauP301L exhibited complementation between the two halves of Venus, in the absence or presence of Tau aggregation induction, although the aggregation-resistant proline mutant also showed a fluorescence signal, but without signal re-distribution on cells. Nevertheless, the aggregation prone mutation, K18P301L, exhibited complementation efficiency with synthetic pre-aggregated fibrils treatment. However, there appears to be some complementation of the two halves of Venus without treatment with *in vitro* pre-aggregated fibrils that corresponds to a spontaneous Tau-Tau binding. This could be due to the formation of a dimeric complex of Tau. In order to exclude the possibility of a higher Venus complementation detection due to the proximity of Tau proteins which are bound to microtubules, QBI cells could be treated with a microtubule destabilizer, for example Nocodazole, to disrupt MT cytoskeleton and leave Tau unbound (Celik, Abdulreda, Maiguel, Li, & Moy, 2013). Venus halves could also be fused with full-length Tau with cysteine residues mutated, since these residues are essential for Tau assembly to the microtubules (Walker, Ullman, & Stultz, 2012).

Other methods to monitor protein misfolding/aggregation in living cells are in development and could be used in the future to detect Tau-Tau interactions The aggregation process could be monitored by assays using fluorescence reporter proteins, as folding reporter GFP fused to the C-terminus of a target protein, and the fluorescence intensity of cells expressing this reporter protein is directly proportional to correct folding of target protein (Waldo, Standish, Berendzen, & Terwilliger, 1999). Another assay using fluorescence reporter proteins is a FRET, in this assay the N- and C-termini of the target protein is tagged with each of the fluorescence proteins and the folding status could be determined by the FRET signal from the two proteins (Philipps, Hennecke, & Glockshuber, 2003). It is also possible to monitor protein aggregation using enzymatic activity assays, as complementation of split enzyme reporters, wherein two fragments that are fused to the N- or C- termini of the target protein will not be able to self-assemble, leading to a reduction of enzymatic activity, an example of this assay is a complementation with ß-galactosidase (Wigley, Stidham, Smith, Hunt, & Thomas, 2001).

Concluding Remarks

The search for an explanation for the pathology mediated by Tau and how alterations in this protein can trigger toxicity in the brain remains a major question for the scientific community. This present study provides two robust *in vitro* models, to study molecular mechanisms involved in Tau related pathology. The neuronal aggregation model has an advantage over the *in vivo* model due to the faster data generation and the easier manipulation. It is also better than the QBI seeding model due to the larger similarities with pathways that exist in the brain. Both models are however a strong and robust cellular system of Tau aggregation, showing key features of Tau associated disorders, and with an advantageous number of applications.

Our cellular Tauopathy models provide an invaluable platform to try to identify pathways involved in aggregation and in clearance of Tau aggregates, as well as new compound candidates. This could be applied, for example, in compound screening that prevents or delays Tau aggregation, to identify new targets by individual gene manipulation (over-expression or knocking-down). Lastly this could be used to validate targets and pathways already described with compounds and targets identified in other diseases related with aggregation or in diseases with similar pathways.

Chapter 5 References

Alber, T. (1992). Structure of the leucine zipper. *Current opinion in genetics & development*, *2*(2), 205–10.

Alonso, A. C., Zaidi, T., Grundke-Iqbal, I., & Iqbal, K. (1994). Role of abnormally phosphorylated tau in the breakdown of microtubules in Alzheimer disease. *Proceedings of the National Academy of Sciences of the United States of America*, *91*(12), 5562–6.

Altschuler, S. J., & Wu, L. F. (2010). Cellular heterogeneity□: when do differences make a difference□? *Cell*, *141*(4), 559–563.

Anckar, J., & Sistonen, L. (2007). Heat shock factor 1 as a coordinator of stress and developmental pathways. *Advances in experimental medicine and biology*, *594*, 78–88.

Andorfer, C., Kress, Y., Espinoza, M., De Silva, R., Tucker, K. L., Barde, Y.-A., Duff, K., et al. (2003). Hyperphosphorylation and aggregation of tau in mice expressing normal human tau isoforms. *Journal of neurochemistry*, *86*(3), 582–90.

Andrieux, A., Salin, P., Schweitzer, A., Bégou, M., Pachoud, B., Brun, P., Gory-Fauré, S., et al. (2006). Microtubule stabilizer ameliorates synaptic function and behavior in a mouse model for schizophrenia. *Biological psychiatry*, *60*(11), 1224–30.

Augustinack, J. C., Schneider, A., Mandelkow, E.-M., & Hyman, B. T. (2002). Specific tau phosphorylation sites correlate with severity of neuronal cytopathology in Alzheimer's disease. *Acta neuropathologica*, *103*(1), 26–35.

Avila, J, Santa-María, I., Pérez, M., Hernández, F., & Moreno, F. (2006). Tau phosphorylation, aggregation, and cell toxicity. *Journal of biomedicine & biotechnology*, *2006*(3), 74539.

Avila, Jesus, Lucas, J. J., Perez, M., & Hernandez, F. (2004). Role of tau protein in both physiological and pathological conditions. *Physiological reviews*, *84*(2), 361–84.

Bali, P., Pranpat, M., Bradner, J., Balasis, M., Fiskus, W., Guo, F., Rocha, K., et al. (2005). Inhibition of histone deacetylase 6 acetylates and disrupts the chaperone function of heat shock protein 90: a novel basis for antileukemia activity of histone deacetylase inhibitors. *The Journal of biological chemistry*, *280*(29), 26729–34.

Ballard, C., Gauthier, S., Corbett, A., Brayne, C., Aarsland, D., & Jones, E. (2011). Alzheimer's disease. *Lancet*, *377*(9770), 1019–31.

Bandyopadhyay, U., Kaushik, S., Varticovski, L., & Cuervo, A. M. (2008). The chaperone-mediated autophagy receptor organizes in dynamic protein complexes at the lysosomal membrane. *Molecular and cellular biology*, *28*(18), 5747–63.

Banz, V. M., Medová, M., Keogh, A., Furer, C., Zimmer, Y., Candinas, D., & Stroka, D. (2009). Hsp90 transcriptionally and post-translationally regulates the expression of NDRG1 and maintains the stability of its modifying kinase GSK3beta. *Biochimica et biophysica acta*, *1793*(10), 1597–603.

Barghorn, S., Zheng-Fischhöfer, Q., Ackmann, M., Biernat, J., Von Bergen, M., Mandelkow, E. M., & Mandelkow, E. (2000). Structure, microtubule interactions, and paired helical filament aggregation by tau mutants of frontotemporal dementias. *Biochemistry*, *39*(38), 11714–21.

Beere, H. M. (2004). "The stress of dying": the role of heat shock proteins in the regulation of apoptosis. *Journal of cell science*, *117*(Pt 13), 2641–51.

Berger, Z., Roder, H., Hanna, A., Carlson, A., Rangachari, V., Yue, M., Wszolek, Z., et al. (2007). Accumulation of pathological tau species and memory loss in a conditional model of tauopathy. *The Journal of neuroscience*, *27*(14), 3650–62.

Blennow, K., Leon, M. J. De, & Zetterberg, H. (2006). Alzheimer ’s disease. *The lancet*, *368*, 387–403.

Braak, H, & Braak, E. (1991). Demonstration of amyloid deposits and neurofibrillary changes in whole brain sections. *Brain pathology (Zurich, Switzerland)*, *1*(3), 213–6.

Braak, H, & Braak, E. (1997). Diagnostic criteria for neuropathologic assessment of Alzheimer’s disease. *Neurobiology of aging*, *18*(4 Suppl), S85–8.

Braak, Heiko, & Del Tredici, K. (2011). Alzheimer’s pathogenesis: is there neuron-to-neuron propagation? *Acta neuropathologica*, *121*(5), 589–95.

Brown, I. R. (2007). Heat shock proteins and protection of the nervous system. *Annals of the New York Academy of Sciences*, *1113*, 147–58.

Brunden, K. R., Trojanowski, J. Q., & Lee, V. M.-Y. (2008). Evidence that non-fibrillar tau causes pathology linked to neurodegeneration and behavioral impairments. *Journal of Alzheimer’s disease*, *14*(4), 393–9.

Brunden, K. R., Trojanowski, J. Q., & Lee, V. M.-Y. (2009). Advances in tau-focused drug discovery for Alzheimer’s disease and related tauopathies. *Nature reviews Drug Discov*, *8*(10), 783–93.

Brunden, K. R., Yao, Y., Potuzak, J. S., Ferrer, N. I., Ballatore, C., James, M. J., Hogan, A.-M. L., et al. (2011). The characterization of microtubule-stabilizing drugs as possible therapeutic agents for Alzheimer’s disease and related tauopathies. *Pharmacological research□: the official journal of the Italian Pharmacological Society*, *63*(4), 341–51.

Brunden, K. R., Zhang, B., Carroll, J., Yao, Y., Potuzak, J. S., Hogan, A.-M. L., Iba, M., et al. (2010). Epothilone D improves microtubule density, axonal integrity, and cognition in a transgenic mouse model of tauopathy. *The Journal of neuroscience□: the official journal of the Society for Neuroscience*, *30*(41), 13861–6.

Brunden, K., Trojanowski, J., & Lee, V. M.-Y. (2009a). Advances in tau-focused drug discovery for Alzheimer’s disease and related tauopathies. *Nature Reviews Drug Discovery*, *8*(10), 783–793.

Brunden, K., Trojanowski, J., & Lee, V. M.-Y. (2009b). Advances in tau-focused drug discovery for Alzheimer’s disease and related tauopathies. *Reviews Drug Discovery*, *8*(10), 783–793.

Buée, L., Bussière, T., Buée-Scherrer, V., Delacourte, A., & Hof, P. R. (2000). Tau protein isoforms, phosphorylation and role in neurodegenerative disorders. *Brain research reviews*, *33*(1), 95–130.

Bulbarelli, A., Lonati, E., Cazzaniga, E., Gregori, M., & Masserini, M. (2009). Pin1 affects Tau phosphorylation in response to Abeta oligomers. *Molecular and cellular neurosciences*, *42*(1), 75–80.

Cabantous, S., Terwilliger, T. C., & Waldo, G. S. (2005). Protein tagging and detection with engineered self-assembling fragments of green fluorescent protein. *Nature biotechnology*, *23*(1), 102–7.

Celik, E., Abdulreda, M. H., Maiguel, D., Li, J., & Moy, V. T. (2013). Rearrangement of microtubule network under biochemical and mechanical stimulations. *ELSEVIER Methods*, *60*(2), 195–201.

Chen, S., Li, B., Grundke-Iqbal, I., & Iqbal, K. (2008). I1PP2A affects tau phosphorylation via association with the catalytic subunit of protein phosphatase 2A. *The Journal of biological chemistry*, *283*(16), 10513–21.

Chirita, C., Necula, M., & Kuret, J. (2004). Ligand-dependent inhibition and reversal of tau filament formation. *Biochemistry*, *43*(10), 2879–87.

Cho, J.-H., & Johnson, G. V. W. (2004). Primed phosphorylation of tau at Thr231 by glycogen synthase kinase 3beta (GSK3beta) plays a critical role in regulating tau's ability to bind and stabilize microtubules. *Journal of neurochemistry*, *88*(2), 349–58.

Chung, S.-H. (2009). Aberrant phosphorylation in the pathogenesis of Alzheimer's disease. *BMB reports*, *42*(8), 467–74.

Clavaguera, F., Bolmont, T., Crowther, R. A., Abramowski, D., Frank, S., Probst, A., Fraser, G., et al. (2009). Transmission and spreading of tauopathy in transgenic mouse brain. *Nature cell biology*, *11*(7), 909–13.

Clavaguera, F., Bolmont, T., Crowther, R. A., Abramowski, D., Frank, S., Probst, A., Fraser, G., et al. (2010). Europe PMC Funders Group Transmission and spreading of tauopathy in transgenic mouse brain, *11*(7), 909–913.

Collinge, J., & Clarke, A. R. (2007). A general model of prion strains and their pathogenicity. *Science*, *318*(5852), 930–6.

Combadière, C., Raoul, W., Guillonneau, X., & Sennlaub, F. (2013). "Ccl2, Cx3cr1 and Ccl2/Cx3cr1 chemokine deficiencies are not sufficient to cause age-related retinal degeneration". *Experimental eye research*.

Congdon, E. E., Wu, J. W., Myeku, N., Figueroa, Y. H., Herman, M., Marinec, P. S., Gestwicki, J. E., et al. (2012). Methylthioninium chloride (methylene blue) induces autophagy and attenuates tauopathy in vitro and in vivo. *Autophagy*, *8*(4), 609–22.

Corder, E., Saunders, A., Strittmatter, W., Schmechel, D., Gaskell, P., Small, G., Roses, A., et al. (1993). Gene dose of apolipoprotein E type 4 allele and the risk of Alzheimer's disease in late onset families. *Science*, *261*, 921–923.

Couturier, C., & Deprez, B. (2012). Setting Up a Bioluminescence Resonance Energy Transfer High throughput Screening Assay to Search for Protein/Protein Interaction Inhibitors in Mammalian Cells. *Frontiers in endocrinology*, *3*(100).

Cowan, C. M., Quraishe, S., & Mudher, A. (2012). What is the pathological significance of tau oligomers? *Biochemical Society transactions*, *40*(4), 693–7.

Crowe, A., James, M. J., Lee, V. M.-Y., Smith, A. B., Trojanowski, J. Q., Ballatore, C., & Brunden, K. R. (2013). Aminothienopyridazines and methylene blue affect Tau fibrillization via cysteine oxidation. *The Journal of biological chemistry*, *288*(16), 11024–37.

David, D. C., Layfield, R., Serpell, L., Narain, Y., Goedert, M., & Spillantini, M. G. (2002). Proteasomal degradation of tau protein. *Journal of neurochemistry*, *83*(1), 176–85.

Dawson, H. N., Neurology, D., Box, P. O., Carolina, N., Cantillana, V., Vitek, M. P., Alexander, T. W., et al. (2010). Loss of Tau Elicits Axonal Degeneration in a Mouse Model of AD. *Neuroscience*, *169*(1), 516–531.

De Felice, F. G., Diana, W., Lambert, M. P., Fernandez, S. J., T Lacor, P., N, P., Bigio, E. H., et al. (2011). Alzheimer's disease-type neuronal tau hyperphosphorylation induced by Aβ oligomers, *29*(9), 1334–1347.

De Vrij, F. M. S., Fischer, D. F., Van Leeuwen, F. W., & Hol, E. M. (2004). Protein quality control in Alzheimer's disease by the ubiquitin proteasome system. *Progress in neurobiology*, *74*(5), 249–70.

De Yébenes, J. G., Sarasa, J. L., Daniel, S. E., & Lees, A. J. (1995). Familial progressive supranuclear palsy. Description of a pedigree and review of the literature. *Brain*, *118*, 1095–103.

Desplats, P., Lee, H., Bae, E., Patrick, C., Rockenstein, E., Crews, L., Spencer, B., et al. (2009). Inclusion formation and neuronal cell death through neuron-to-neuron transmission of alpha synuclein. *PNAS*, *106*(31).

Dickey, C. a, Koren, J., Zhang, Y.-J., Xu, Y.-F., Jinwal, U. K., Birnbaum, M. J., Monks, B., et al. (2008). Akt and CHIP coregulate tau degradation through coordinated interactions. *Proceedings of the National Academy of Sciences of the United States of America*, *105*(9), 3622–7.

Dickey, C. A., Dunmore, J., Lu, B., Wang, J.-W., Lee, W. C., Kamal, A., Burrows, F., et al. (2006). HSP induction mediates selective clearance of tau phosphorylated at proline-directed Ser/Thr sites but not KXGS (MARK) sites. *FASEB journal*, *20*(6), 753–5.

Dickey, C. A., Kamal, A., Lundgren, K., Klosak, N., Bailey, R. M., Dunmore, J., Ash, P., et al. (2007). The high-affinity HSP90-CHIP complex recognizes and selectively degrades phosphorylated tau client proteins. *Journal of Clinical Investigation*, *117*(3), 648–658.

Dickey, C. A., Yue, M., Lin, W.-L., Dickson, D. W., Dunmore, J. H., Lee, W. C., Zehr, C., et al. (2006). Deletion of the ubiquitin ligase CHIP leads to the accumulation, but not the aggregation, of both endogenous phospho- and caspase-3-cleaved tau species. *The Journal of neuroscience*, *26*(26), 6985–96.

Dickey, C.A., Patterson, C., Dickson, D., Petrucelli, L. (2007). Brain CHIP: removing the culprits in neurodegenerative disease. *Trends Mol. Med.*, *13*(1), 32–38.

Dickson, D. W., Rademakers, R., & Hutton, M. L. (2007). Progressive supranuclear palsy: pathology and genetics. *Brain pathology*, *17*(1), 74–82.

Dixit, R., Ross, J. L., Goldman, Y. E., & Holzbaur, E. L. F. (2008). Differential regulation of dynein and kinesin motor proteins by tau. *Science*, *319*(5866), 1086–9.

Dou, F., Netzer, W. J., Tanemura, K., Li, F., Hartl, F. U., Takashima, A., Gouras, G. K., et al. (2003). Chaperones increase association of tau protein with microtubules. *Proceedings of the National Academy of Sciences of the United States of America*, *100*(2), 721–6.

Dragulescu-Andrasi, A., Chan, C. T., De, A., Massoud, T. F., & Gambhir, S. S. (2011). Bioluminescence resonance energy transfer (BRET) imaging of protein-protein interactions within deep tissues of living subjects. *Proceedings of the National Academy of Sciences of the United States of America*, *108*(29), 12060–5.

Eisele, Y. S., Bolmont, T., Heikenwalder, M., Langer, F., Jacobson, L. H., Yan, Z.-X., Roth, K., et al. (2009). Induction of cerebral beta-amyloidosis: intracerebral versus systemic Abeta inoculation. *Proceedings of the National Academy of Sciences of the United States of America*, *106*(31), 12926–31.

Eisenberg, D., & Jucker, M. (2012). The amyloid state of proteins in human diseases. *Cell*, *148*(6), 1188–203.

Esch, F. S., Keim, P. S., Beattie, E. C., Blacher, R. W., Culwell, A. R., Oltersdorf, T., McClure, D., et al. (1990). Cleavage of amyloid beta peptide during constitutive processing of its precursor. *Science*, *248*(4959), 1122–4.

Ferri, C. P., Prince, M., Brayne, C., Brodaty, H., Fratiglioni, L., Ganguli, M., Hall, K., et al. (2005). Global prevalence of dementia: a Delphi consensus study. *Lancet*, *366*(9503), 2112–7.

Flach, K., Hilbrich, I., Schiffmann, A., Gärtner, U., Krüger, M., Leonhardt, M., Waschipky, H., et al. (2012). Tau oligomers impair artificial membrane integrity and cellular viability. *The Journal of biological chemistry*, *287*(52), 43223–33.

Foster, J. A., & Brown, I. R. (1997). Differential induction of heat shock mRNA in oligodendrocytes, microglia, and astrocytes following hyperthermia. *Brain research Molecular brain research*, *45*(2), 207–18.

Francisco, S. (2007). ALZHEIMER ' S DISEASE A New Take on Tau. *Science*, *316*.

Frost, B., Jacks, R. L., & Diamond, M. I. (2009). Propagation of tau misfolding from the outside to the inside of a cell. *The Journal of biological chemistry*, *284*(19), 12845–52.

Frost, B., Ollesch, J., Wille, H., & Diamond, M. I. (2009). Conformational diversity of wild-type Tau fibrils specified by templated conformation change. *The Journal of biological chemistry*, *284*(6), 3546–51.

Furukawa, K., Sopher, B. L., Rydel, R. E., Begley, J. G., Pham, D. G., Martin, G. M., Fox, M., et al. (1996). Increased activity-regulating and neuroprotective efficacy of alpha-secretase-derived secreted amyloid precursor protein conferred by a C-terminal heparin-binding domain. *Journal of neurochemistry*, *67*(5), 1882–96.

Galvan, V., Gorostiza, O. F., Banwait, S., Ataie, M., Logvinova, A. V, Sitaraman, S., Carlson, E., et al. (2006). Reversal of Alzheimer's-like pathology and behavior in human APP transgenic mice by mutation of Asp664. *Proceedings of the National Academy of Sciences of the United States of America*, *103*(18), 7130–5.

Gamblin, T C, King, M. E., Dawson, H., Vitek, M. P., Kuret, J., Berry, R. W., & Binder, L. I. (2000). In vitro polymerization of tau protein monitored by laser light scattering: method and application to the study of FTDP-17 mutants. *Biochemistry*, *39*(20), 6136–44.

Gamblin, T Chris, Chen, F., Zambrano, A., Abraha, A., Lagalwar, S., Guillozet, A. L., Lu, M., et al. (2003). Caspase cleavage of tau: linking amyloid and neurofibrillary tangles in Alzheimer's disease. *Proceedings of the National Academy of Sciences of the United States of America*, *100*(17), 10032–7.

Goedert, M, Jakes, R., Crowther, R. A., Six, J., Lübke, U., Vandermeeren, M., Cras, P., et al. (1993). The abnormal phosphorylation of tau protein at Ser-202 in Alzheimer disease recapitulates phosphorylation during development. *Proceedings of the National Academy of Sciences of the United States of America*, *90*(11), 5066–70.

Goedert, Michel, Clavaguera, F., & Tolnay, M. (2010). The propagation of prion-like protein inclusions in neurodegenerative diseases. *Trends in neurosciences*, *33*(7), 317–25.

Gong, C.-X., Liu, F., Grundke-Iqbal, I., & Iqbal, K. (2005). Post-translational modifications of tau protein in Alzheimer's disease. *Journal of neural transmission*, *112*(6), 813–38.

Goryunov, D., & Liem, R. K. H. (2007). CHIP-ping away at tau. *The Journal of clinical investigation*, *117*(3), 590–2.

Götz, J., Chen, F., Van Dorpe, J., & Nitsch, R. M. (2001). Formation of neurofibrillary tangles in P301l tau transgenic mice induced by Abeta 42 fibrils. *Science (New York, N.Y.)*, *293*(5534), 1491–5.

Götz, J., Probst, A., Spillantini, M. G., Schäfer, T., Jakes, R., Bürki, K., & Goedert, M. (1995). Somatodendritic localization and hyperphosphorylation of tau protein in transgenic mice expressing the longest human brain tau isoform. *The EMBO journal*, *14*(7), 1304–13.

Götz, J., Tolnay, M., Barmettler, R., Ferrari, A., Bürki, K., Goedert, M., Probst, A., et al. (2001). Human tau transgenic mice. Towards an animal model for neuro- and glialfibrillary lesion formation. *Advances in experimental medicine and biology*, *487*, 71–83.

Grover, A., Houlden, H., Baker, M., Adamson, J., Lewis, J., Prihar, G., Pickering-Brown, S., et al. (1999). 5' splice site mutations in tau associated with the inherited dementia FTDP-17 affect a stem-loop structure that regulates alternative splicing of exon 10. *The Journal of biological chemistry*, *274*(21), 15134–43.

Guo, J. L., & Lee, V. M.-Y. (2011). Seeding of normal Tau by pathological Tau conformers drives pathogenesis of Alzheimer-like tangles. *The Journal of biological chemistry*, *286*(17), 15317–31.

Haass, C., Kaether, C., Thinakaran, G., & Sisodia, S. (2012). Trafficking and Proteolytic Processing of APP. *Cold Spring Harbor perspectives in medicine*, *2*(5), 6270.

Haass, C., & Selkoe, D. J. (2007). Soluble protein oligomers in neurodegeneration: lessons from the Alzheimer's amyloid beta-peptide. *Nature reviews: Molecular cell biology*, *8*(2), 101–12.

Hamano, T., Gendron, T. F., Causevic, E., Yen, S.-H., Lin, W.-L., Isidoro, C., Deture, M., et al. (2008). Autophagic-lysosomal perturbation enhances tau aggregation in transfectants with induced wild-type tau expression. *The European journal of neuroscience*, *27*(5), 1119–30.

Hara, T., Nakamura, K., Matsui, M., Yamamoto, A., Nakahara, Y., Suzuki-Migishima, R., Yokoyama, M., et al. (2006). Suppression of basal autophagy in neural cells causes neurodegenerative disease in mice. *Nature*, *441*(7095), 885–9.

Hardy, J., & Selkoe, D. J. (2002). The amyloid hypothesis of Alzheimer's disease: progress and problems on the road to therapeutics. *Science*, *297*(5580), 353–6.

Hartl, F U. (1996). Molecular chaperones in cellular protein folding. *Nature*, *381*(6583), 571–9.

Hartl, F Ulrich, & Hayer-Hartl, M. (2009). Converging concepts of protein folding in vitro and in vivo. *Nature structural & molecular biology*, *16*(6), 574–81.

Hatakeyama, S., Matsumoto, M., Kamura, T., Murayama, M., Chui, D.-H., Planel, E., Takahashi, R., et al. (2004). U-box protein carboxyl terminus of Hsc70-interacting protein (CHIP) mediates poly-ubiquitylation preferentially on four-repeat Tau and is involved in neurodegeneration of tauopathy. *Journal of neurochemistry*, *91*(2), 299–307.

Himmelstein, D. S., Ward, S. M., Lancia, J. K., Patterson, K. R., & Binder, L. I. (2012). Tau as a therapeutic target in neurodegenerative disease. *Pharmacology & therapeutics*, *136*(1), 8–22.

Horiguchi, T., Uryu, K., Giasson, B. I., Ischiropoulos, H., LightFoot, R., Bellmann, C., Richter-Landsberg, C., et al. (2003). Nitration of tau protein is linked to neurodegeneration in tauopathies. *The American journal of pathology*, *163*(3), 1021–31.

Hosokawa, M., Arai, T., Masuda-Suzukake, M., Nonaka, T., Yamashita, M., Akiyama, H., & Hasegawa, M. (2012). Methylene blue reduced abnormal tau accumulation in P301L tau transgenic mice. *PloS one*, *7*(12).

Hurtado, D. E., Molina-Porcel, L., Iba, M., Aboagye, A. K., Paul, S. M., Trojanowski, J. Q., & Lee, V. M.-Y. (2010). A{beta} accelerates the spatiotemporal progression of tau pathology and augments tau amyloidosis in an Alzheimer mouse model. *The American journal of pathology*, *177*(4), 1977–88.

Hutton, M. (2001). Missense and splice site mutations in tau associated with FTDP-17: multiple pathogenic mechanisms. *Neurology*, *56*(11), S21–5.

Iba, M., Guo, J. L., Mcbride, J. D., Zhang, B., Trojanowski, J. Q., & Lee, V. M. (2013). Synthetic Tau Fibrils Mediate Transmission of Neurofibrillary Tangles in a Transgenic Mouse Model of Alzheimer's-like Tauopathy. *J Neurosci.*, *33*(3), 1024–1037.

Illenberger, S., Zheng-fischho, Q., Preuss, U., Stamer, K., Baumann, K., Trinczek, B., Biernat, J., et al. (1998). The Endogenous and Cell Cycle-dependent Phosphorylation of tau Protein in Living Cells : Implications for Alzheimer ’s Disease. *Molecular Biology of the Cell*, *9*(June), 1495–1512.

Ingram, E. M., & Spillantini, M. G. (2002). Tau gene mutations: dissecting the pathogenesis of FTDP-17. *Trends in molecular medicine*, *8*(12), 555–62.

Ittner, L. M., Ke, Y. D., Delerue, F., Bi, M., Gladbach, A., Van Eersel, J., Wölfing, H., et al. (2010). Dendritic function of tau mediates amyloid-beta toxicity in Alzheimer’s disease mouse models. *Cell*, *142*(3), 387–97.

Jackson, J. (2009). *World Alzheimer Report 2009 - THE GLOBAL ECONOMIC IMPACT OF DEMENTIA*. *Alzheimer’s Disease International, Alzheimer's Disease* (pp. 1–12).

Jaworski, T., Kügler, S., & Van Leuven, F. (2010). Modeling of tau-mediated synaptic and neuronal degeneration in Alzheimer’s disease. *International journal of Alzheimer’s disease*, *2010*.

Jeganathan, S., Von Bergen, M., Mandelkow, E.-M., & Mandelkow, E. (2008). The natively unfolded character of tau and its aggregation to Alzheimer-like paired helical filaments. *Biochemistry*, *47*(40), 10526–39.

Jellinger, K. a, & Popescu, B. O. (2012). Interaction between pathogenic proteins in neurodegenerative disorders. *Journal of cellular and molecular medicine*, *16*(6), 1166–83.

Jérôme, V., & Müller, R. (2001). A synthetic leucine zipper-based dimerization system for combining multiple promoter specificities. *Gene therapy*, *8*(9), 725–9.

Jinwal, U. K., Iii, J. K., Iii, J. C. O. L., Jones, J. R., Abisambra, J. F., & Dickey, C. A. (2010). Hsp70 ATPase Modulators as Therapeutics for Alzheimer’s and other Neurodegenerative Diseases. *Mol Cell Pharmacol*, *2*(2), 43–46.

Jung, H. H., Bremer, J., Streffer, J., Virdee, K., Spillantini, M. G., Crowther, R. A., Brugger, P., et al. (2012). Phenotypic variation of autosomal-dominant corticobasal degeneration. *European neurology*, *67*(3), 142–50.

Kamal, A., Boehm, M. F., & Burrows, F. J. (2004). Therapeutic and diagnostic implications of Hsp90 activation. *Trends in molecular medicine*, *10*(6), 283–90.

Kane, M. D., Lipinski, W. J., Callahan, M. J., Bian, F., Durham, R. A., Schwarz, R. D., Roher, A. E., et al. (2000). Evidence for seeding of beta -amyloid by intracerebral infusion of Alzheimer brain extracts in beta -amyloid precursor protein-transgenic mice. *The Journal of neuroscience*, *20*(10), 3606–11.

Kar, S., Fan, J., Smith, M. J., Goedert, M., & Amos, L. A. (2003). Repeat motifs of tau bind to the insides of microtubules in the absence of taxol. *The EMBO journal*, *22*(1), 70–7.

Keller, J. N., Hanni, K. B., & Markesbery, W. R. (2000). Impaired proteasome function in Alzheimer’s disease. *Journal of neurochemistry*, *75*(1), 436–9.

Kerppola, T. (2008). Bimolecular fluorescence complementation (BiFC) analysis as a probe of protein interactions in living cells. *Annual review of biophysics*, 465–487.

Kidd, M. (1963). Paired helical filaments in electron microscopy of Alzheimer’s disease. *Nature*, *197*, 192–3.

Kisselev, A. F., Callard, A., & Goldberg, A. L. (2006). Importance of the different proteolytic sites of the proteasome and the efficacy of inhibitors varies with the protein substrate. *The Journal of biological chemistry*, *281*(13), 8582–90.

Kolarova, M., García-Sierra, F., Bartos, A., Ricny, J., & Ripova, D. (2012). Structure and pathology of tau protein in Alzheimer disease. *International journal of Alzheimer’s disease*, *2012*, 13.

Komatsu, M., Waguri, S., Chiba, T., Murata, S., Iwata, J., Tanida, I., Ueno, T., et al. (2006). Loss of autophagy in the central nervous system causes neurodegeneration in mice. *Nature*, *441*(7095), 880–4.

Lachenal, G., Pernet-Gallay, K., Chivet, M., Hemming, F. J., Belly, A., Bodon, G., Blot, B., et al. (2011). Release of exosomes from differentiated neurons and its regulation by synaptic glutamatergic activity. *Molecular and cellular neurosciences*, *46*(2), 409–18.

LaFerla, F. M., Green, K. N., & Oddo, S. (2007). Intracellular amyloid-beta in Alzheimer's disease. *Nature reviews. Neuroscience*, *8*(7), 499–509.

Lambert, J.-C., & Amouyel, P. (2011). Genetics of Alzheimer's disease: new evidences for an old hypothesis? *Current opinion in genetics & development*, *21*(3), 295–301.

Lasagna-Reeves, C. A., Castillo-Carranza, D. L., Guerrero-Muoz, M. J., Jackson, G. R., & Kayed, R. (2010). Preparation and characterization of neurotoxic tau oligomers. *Biochemistry*, *49*(47), 10039–41.

Lasagna-Reeves, C. A., Castillo-Carranza, D. L., Sengupta, U., Clos, A. L., Jackson, G. R., & Kayed, R. (2011). Tau oligomers impair memory and induce synaptic and mitochondrial dysfunction in wild-type mice. *Molecular neurodegeneration*, *6*, 39.

Ledesma, M. D., Medina, M., & Avila, J. (1996). The in vitro formation of recombinant tau polymers: effect of phosphorylation and glycation. *Molecular and chemical neuropathology*, *27*(3), 249–58.

Lee, M. J., Lee, J. H., & Rubinsztein, D. C. (2013). Tau Degradation: The Ubiquitin-Proteasome System versus the Autophagy-Lysosome System. *Progress in neurobiology*.

Lee, S.-J., Desplats, P., Sigurdson, C., Tsigelny, I., & Masliah, E. (2010). Cell-to-cell transmission of non-prion protein aggregates. *Nature reviews. Neurology*, *6*(12), 702–6.

Lee, S.-J., Lim, H.-S., Masliah, E., & Lee, H.-J. (2011). Protein aggregate spreading in neurodegenerative diseases: Problems and perspectives. *Neuroscience research*, *70*(4), 339–48.

Lee, V. M., Goedert, M., & Trojanowski, J. Q. (2001). Neurodegenerative Tauopathies. *Annu. Rev. Neurosci*, *24*, 1121–159.

Lewis, J., McGowan, E., Rockwood, J., Melrose, H., Nacharaju, P., Van Slegtenhorst, M., Gwinn-Hardy, K., et al. (2000). Neurofibrillary tangles, amyotrophy and progressive motor disturbance in mice expressing mutant (P301L) tau protein. *Nature genetics*, *25*(4), 402–5.

Li, H.-L., Wang, H.-H., Liu, S.-J., Deng, Y.-Q., Zhang, Y.-J., Tian, Q., Wang, X.-C., et al. (2007). Phosphorylation of tau antagonizes apoptosis by stabilizing beta-catenin, a mechanism involved in Alzheimer's neurodegeneration. *Proceedings of the National Academy of Sciences of the United States of America*, *104*(9), 3591–6.

Lim, F., Hernández, F., Lucas, J. J., Gómez-Ramos, P., Morán, M. A., & Avila, J. (2001). FTDP-17 mutations in tau transgenic mice provoke lysosomal abnormalities and Tau filaments in forebrain. *Molecular and cellular neurosciences*, *18*(6), 702–14.

Lin, W.-L., Lewis, J., Yen, S.-H., Hutton, M., & Dickson, D. W. (2003). Ultrastructural neuronal pathology in transgenic mice expressing mutant (P301L) human tau. *Journal of neurocytology*, *32*(9), 1091–105.

Liu, F., Grundke-Iqbal, I., Iqbal, K., & Gong, C.-X. (2005). Contributions of protein phosphatases PP1, PP2A, PP2B and PP5 to the regulation of tau phosphorylation. *The European journal of neuroscience*, *22*(8), 1942–50.

López Salon, M., Morelli, L., Castaño, E. M., Soto, E. F., & Pasquini, J. M. (2000). Defective ubiquitination of cerebral proteins in Alzheimer's disease. *Journal of neuroscience research*, *62*(2), 302–10.

Lu, B. (2005). Understanding and treating neurodegeneration: insights from the flies. *Age (Dordrecht, Netherlands)*, *27*(3), 225–39.

Lu, Y., Ansar, S., & Michaelis, M. (2009). Neuroprotective activity and evaluation of Hsp90 inhibitors in an immortalized neuronal cell line. *Bioorg Med Chem.*, *17*(4), 1709–1715.

Luk, K. C., Song, C., O'Brien, P., Stieber, A., Branch, J. R., Brunden, K. R., Trojanowski, J. Q., et al. (2009). Exogenous alpha-synuclein fibrils seed the formation of Lewy body-like intracellular inclusions in cultured cells. *Proceedings of the National Academy of Sciences of the United States of America*, *106*(47), 20051–6.

Luo, W., Dou, F., Rodina, A., Chip, S., Kim, J., Zhao, Q., Moulick, K., et al. (2007). Roles of heat-shock protein 90 in maintaining and facilitating the neurodegenerative phenotype in tauopathies. *Proceedings of the National Academy of Sciences of the United States of America*, *104*(22), 9511–6.

Luo, W., Rodina, A., & Chiosis, G. (2008). Heat shock protein 90: translation from cancer to Alzheimer's disease treatment? *BMC neuroscience*, *9 Suppl 2*, S7.

Luo, W., Sun, W., Taldone, T., Rodina, A., & Chiosis, G. (2010). Heat shock protein 90 in neurodegenerative diseases. *Molecular neurodegeneration*, *5*, 24.

Ma, Q.-L., Zuo, X., Yang, F., Ubeda, O. J., Gant, D. J., Alaverdyan, M., Teng, E., et al. (2013). Curcumin suppresses soluble tau dimers and corrects molecular chaperone, synaptic, and behavioral deficits in aged human tau transgenic mice. *The Journal of biological chemistry*, *288*(6), 4056–65.

Maeda, S., Sahara, N., Saito, Y., Murayama, S., Ikai, A., & Takashima, A. (2006). Increased levels of granular tau oligomers: an early sign of brain aging and Alzheimer's disease. *Neuroscience research*, *54*(3), 197–201.

Mandelkow, E., Von Bergen, M., Biernat, J., & Mandelkow, E.-M. (2007). Structural principles of tau and the paired helical filaments of Alzheimer's disease. *Brain pathology (Zurich, Switzerland)*, *17*(1), 83–90.

Mandell, J. W., & Banker, G. A. (1996). A spatial gradient of tau protein phosphorylation in nascent axons. *The Journal of neuroscience*, *16*(18), 5727–40.

Martin, L., Latypova, X., & Terro, F. (2011). Post-translational modifications of tau protein: implications for Alzheimer's disease. *Neurochemistry international*, *58*(4), 458–71.

Matsuo, E. S., Shin, R. W., Billingsley, M. L., Van deVoorde, A., O'Connor, M., Trojanowski, J. Q., & Lee, V. M. (1994). Biopsy-derived adult human brain tau is phosphorylated at many of the same sites as Alzheimer's disease paired helical filament tau. *Neuron*, *13*(4), 989–1002.

Mattson, M. P. (1997). Cellular actions of beta-amyloid precursor protein and its soluble and fibrillogenic derivatives. *Physiological reviews*, *77*(4), 1081–132.

Mayer, M. P., & Bukau, B. (2005). Hsp70 chaperones: cellular functions and molecular mechanism. *Cellular and molecular life sciences*, *62*(6), 670–84.

Mendes, C. T., Mury, F. B., De Sá Moreira, E., Alberto, F. L., Forlenza, O. V., Dias-Neto, E., & Gattaz, W. F. (2009). Lithium reduces Gsk3b mRNA levels: implications for Alzheimer Disease. *European archives of psychiatry and clinical neuroscience*, *259*(1), 16–22.

Mendez, I., Viñuela, A., Astradsson, A., Mukhida, K., Hallett, P., Robertson, H., Tierney, T., et al. (2008). Dopamine neurons implanted into people with Parkinson's disease survive without pathology for 14 years. *Nature medicine*, *14*(5), 507–9.

Menéndez-González, M., Pérez-Pinera, P., Martínez-Rivera, M., Calatayud, M. T., & Blázquez Menes, B. (2005). APP processing and the APP-KPI domain involvement in the amyloid cascade. *Neuro-degenerative diseases*, *2*(6), 277–83.

Menzies, F. M., Ravikumar, B., & Rubinsztein, D. C. (2006). Protective roles for induction of autophagy in multiple proteinopathies. *Autophagy*, *2*(3), 224–5.

Meyer-Luehmann, M., Coomaraswamy, J., Bolmont, T., Kaeser, S., Schaefer, C., Kilger, E., Neuenschwander, A., et al. (2006). Exogenous induction of cerebral beta-amyloidogenesis is governed by agent and host. *Science (New York, N.Y.)*, *313*(5794), 1781–4.

Miyasaka, T., Morishima-Kawashima, M., Ravid, R., Kamphorst, W., Nagashima, K., & Ihara, Y. (2001). Selective deposition of mutant tau in the FTDP-17 brain affected by the P301L mutation. *Journal of neuropathology and experimental neurology*, *60*(9), 872–84.

Michnick, S. W., Ear, P. H., Manderson, E. N., Remy, I., & Stefan, E. (2007). Universal strategies in research and drug discovery based on protein-fragment complementation assays. *Nature reviews. Drug discovery*, *6*(7), 569–82.

Min, J.-N., Whaley, R. A., Sharpless, N. E., Lockyer, P., Portbury, A. L., & Patterson, C. (2008). CHIP deficiency decreases longevity, with accelerated aging phenotypes accompanied by altered protein quality control. *Molecular and cellular biology*, *28*(12), 4018–25.

Mondragón-Rodríguez, S., Basurto-Islas, G., Santa-Maria, I., Mena, R., Binder, L. I., Avila, J., Smith, M. A., et al. (2008). Cleavage and conformational changes of tau protein follow phosphorylation during Alzheimer's disease. *International journal of experimental pathology*, *89*(2), 81–90.

Morimoto, R. I., Kline, M. P., Bimston, D. N., & Cotto, J. J. (1997). The heat-shock response: regulation and function of heat-shock proteins and molecular chaperones. *Essays in biochemistry*, *32*, 17–29.

Morgan, K. (2011). The three new pathways leading to Alzheimer's disease. *Neuropathology and applied neurobiology*, *37*(4), 353–7.

Morris, J. C., Storandt, M., Miller, J. P., McKeel, D. W., Price, J. L., Rubin, E. H., & Berg, L. (2001). Mild cognitive impairment represents early-stage Alzheimer disease. *Archives of neurology*, *58*(3), 397–405.

Morris, M., Maeda, S., Vossel, K., & Mucke, L. (2011). The many faces of tau. *Neuron*, *70*(3), 410–26.

Muchowski, P. J., & Wacker, J. L. (2005). Modulation of neurodegeneration by molecular chaperones. *Nature reviews. Neuroscience*, *6*(1), 11–22.

Mukrasch, M. D., Bibow, S., Korukottu, J., Jeganathan, S., Biernat, J., Griesinger, C., Mandelkow, E., et al. (2009). Structural polymorphism of 441-residue tau at single residue resolution. *PLoS biology*, *7*(2), 0399–0414.

Murata, S., Minami, Y., Minami, M., Chiba, T., & Tanaka, K. (2001). CHIP is a chaperone-dependent E3 ligase that ubiquitylates unfolded protein. *EMBO reports*, *2*(12), 1133–8.

Nagai, T., Ibata, K., Park, E. S., Kubota, M., Mikoshiba, K., & Miyawaki, A. (2002). A variant of yellow fluorescent protein with fast and efficient maturation for cell-biological applications. *Nature biotechnology*, *20*(1), 87–90.

Neve, R. L., Harris, P., Kosik, K. S., Kurnit, D. M., & Donlon, T. A. (1986). Identification of cDNA clones for the human microtubule-associated protein tau and chromosomal localization of the genes for tau and microtubule-associated protein 2. *Brain research*, *387*(3), 271–80. R

Nixon, R. A., Wegiel, J., Kumar, A., Yu, W. H., Peterhoff, C., Cataldo, A., & Cuervo, A. M. (2005). Extensive involvement of autophagy in Alzheimer disease: an immuno-electron microscopy study. *Journal of neuropathology and experimental neurology*, *64*(2), 113–22.

Nonaka, T., Watanabe, S. T., Iwatsubo, T., & Hasegawa, M. (2010). Seeded aggregation and toxicity of {alpha}-synuclein and tau: cellular models of neurodegenerative diseases. *The Journal of biological chemistry*, *285*(45), 34885–98.

Nussbaum, R. L., & Ellis, C. E. (2003). Alzheimer's Disease and Parkinson's Disease. *New england journal of medicine*, *348*(14), 1356–1364.

O'Leary, J. C., Li, Q., Marinec, P., Blair, L. J., Congdon, E. E., Johnson, A. G., Jinwal, U. K., et al. (2010). Phenothiazine-mediated rescue of cognition in tau transgenic mice requires neuroprotection and reduced soluble tau burden. *Molecular neurodegeneration*, *5*, 45.

Ohashi, K., Kiuchi, T., Shoji, K., Sampei, K., & Mizuno, K. (2012). Visualization of cofilin-actin and Ras-Raf interactions by bimolecular fluorescence complementation assays using a new pair of split Venus fragments. *BioTechniques*, *52*(1), 45–50.

Pearl, L. H., & Prodromou, C. (2006). Structure and mechanism of the Hsp90 molecular chaperone machinery. *Annual review of biochemistry*, *75*, 271–94.

Pearl, L. H., Prodromou, C., & Workman, P. (2008). The Hsp90 molecular chaperone: an open and shut case for treatment. *The Biochemical journal*, *410*(3), 439–53.

Pedersen, J. T., & Heegaard, N. H. H. (2013). Analysis of Protein Aggregation in Neurodegenerative Disease. *Analytical chemistry*.

Pelkmans, L. (2012). Cell Biology. Using cell-to-cell variability--a new era in molecular biology. *Science (New York, N.Y.)*, *336*(6080), 425–6.

Petersen, R. C., & Morris, J. C. (2005). Mild cognitive impairment as a clinical entity and treatment target. *Archives of neurology*, *62*(7), 1160–3;

Petrucelli, L., Dickson, D., Kehoe, K., Taylor, J., Snyder, H., Grover, A., De Lucia, M., et al. (2004). CHIP and Hsp70 regulate tau ubiquitination, degradation and aggregation. *Human molecular genetics*, *13*(7), 703–14.

Phiel, C. J., Wilson, C. A., Lee, V. M.-Y., & Klein, P. S. (2003). GSK-3alpha regulates production of Alzheimer's disease amyloid-beta peptides. *Nature*, *423*(6938), 435–9.

Philipps, B., Hennecke, J., & Glockshuber, R. (2003). FRET-based in vivo screening for protein folding and increased protein stability. *Journal of molecular biology*, *327*(1), 239–49.

Piao, Y. S., Hayashi, S., Hasegawa, M., Wakabayashi, K., Yamada, M., Yoshimoto, M., Ishikawa, A., et al. (2001). Co-localization of alpha-synuclein and phosphorylated tau in neuronal and glial cytoplasmic inclusions in a patient with multiple system atrophy of long duration. *Acta neuropathologica*, *101*(3), 285–93.

Pirkkala, L., Nykänen, P., & Sistonen, L. (2001). Roles of the heat shock transcription factors in regulation of the heat shock response and beyond. *FASEB journal*, *15*(7), 1118–31.

Pusch, S., Dissmeyer, N., & Schnittger, A. (2011). Bimolecular-fluorescence complementation assay to monitor kinase-substrate interactions in vivo. *Methods in molecular biology*, *779*, 245–57.

Qiu, C., Kivipelto, M., & Strauss, E. (2009). Epidemiology of Alzheimer's disease: occurrence, determinants, and strategies toward intervention. *Dialogues Clin Neurosci*, *11*(2), 111–128.

Rana, A. Q., Ansari, H., & Siddiqui, I. (2012). The relationship between arm dystonia in corticobasal degeneration and handedness. *Journal of clinical neuroscience*, *19*(8), 1134–6.

Reitz C, Brayne C, M. R. (2011). Epidemiology of Alzheimer's disease. *Nat Rev Neurol.*, *7*(3), 137–152.

Reitz, C., Brayne, C., & Mayeux, R. (2011). Epidemiology of Alzheimer disease. *Nat Rev Neurol*, *7*(3), 137–152.

Ren, P.-H., Lauckner, J. E., Kachirskaia, I., Heuser, J. E., Melki, R., & Kopito, R. R. (2009). Cytoplasmic penetration and persistent infection of mammalian cells by polyglutamine aggregates. *Nature cell biology*, *11*(2), 219–25.

Reynolds, M. R., Reyes, J. F., Fu, Y., Bigio, E. H., Guillozet-Bongaarts, A. L., Berry, R. W., & Binder, L. I. (2006). Tau nitration occurs at tyrosine 29 in the fibrillar lesions of Alzheimer's disease and other tauopathies. *The Journal of neuroscience*, *26*(42), 10636–45.

Ringman, J. M., Frautschy, S. A., Teng, E., Begum, A. N., Bardens, J., Beigi, M., Gylys, K. H., et al. (2012). Oral curcumin for Alzheimer's disease: tolerability and efficacy in a 24-week randomized, double blind, placebo-controlled study. *Alzheimer's research & therapy*, *4*(5), 43.

Ritchie, K., & Lovestone, S. (2002). The dementias. *Lancet*, *360*(9347), 1759–66.

Roberson, E. D., Halabisky, B., Yoo, J. W., Yao, J., Chin, J., Yan, F., Wu, T., et al. (2011). Amyloid-β/Fyn–Induced Synaptic, Network, and Cognitive Impairments Depend on Tau Levels in Multiple Mouse Models of Alzheimer's Disease. *Neurobiology of Disease*, *31*(2), 700–11.

Roberson, E. D., Scearce-Levie, K., Palop, J. J., Yan, F., Cheng, I. H., Wu, T., Gerstein, H., et al. (2007). Reducing endogenous tau ameliorates amyloid beta-induced deficits in an Alzheimer's disease mouse model. *Science (New York, N.Y.)*, *316*(5825), 750–4

Robertson, L. A., Moya, K. L., & Breen, K. C. (2004). The potential role of tau protein O-glycosylation in Alzheimer's disease. *Journal of Alzheimer's disease*, *6*(5), 489–95.

Rossor, M. N. (2001). Pick's disease: a clinical overview. *Neurology*, *56*(11), S3–5.

Rubinsztein, D. C. (2006). The roles of intracellular protein-degradation pathways in neurodegeneration. *Nature*, *443*(7113), 780–6.

Sahara, N., Maeda, S., Yoshiike, Y., Mizoroki, T., Yamashita, S., Murayama, M., Park, J.-M., et al. (2007). Molecular chaperone-mediated tau protein metabolism counteracts the formation of granular tau oligomers in human brain. *Journal of neuroscience research*, *85*(14), 3098–108.

Salminen, A., Ojala, J., Kaarniranta, K., Hiltunen, M., & Soininen, H. (2011). Hsp90 regulates tau pathology through co-chaperone complexes in Alzheimer's disease. *Progress in neurobiology*, *93*(1), 99–110.

Savage, E. E., Wootten, D., Christopoulos, A., Sexton, P. M., & Furness, S. G. B. (2013). A simple method to generate stable cell lines for the analysis of transient protein-protein interactions. *BioTechniques*, *54*(4), 217–21.

Scheff, S. W., & Price, D. A. (2006). Alzheimer's disease-related alterations in synaptic density: Neocortex and hippocampus. *J Alzheimers Dis.*, *9*, 101–115.

Scheffa, S. W., Pricea, D. A., Schmitt, F. A., Scheff, M. A., & Mufson, E. J. (2011). Synaptic loss in the inferior temporal gyrus in mild cognitive impairment and Alzheimer's disease. *J Alzheimers Dis*, *24*(3), 547–557.

Selenica, M.-L., Jensen, H. S., Larsen, A. K., Pedersen, M. L., Helboe, L., Leist, M., & Lotharius, J. (2007). Efficacy of small-molecule glycogen synthase kinase-3 inhibitors in the postnatal rat model of tau hyperphosphorylation. *British journal of pharmacology*, *152*(6), 959–79.

Selkoe, D. J. (1998). The cell biology of beta-amyloid precursor protein and presenilin in Alzheimer's disease. *Trends in cell biology*, *8*(11), 447–53.

Sergeant, N., Bretteville, A., Hamdane, M., Caillet-Boudin, M.-L., Grognet, P., Bombois, S., Blum, D., et al. (2008). Biochemistry of Tau in Alzheimer's disease and related neurological disorders. *Expert review of proteomics*, *5*(2), 207–24.

Sergeant, N., Delacourte, A., & Buée, L. (2005). Tau protein as a differential biomarker of tauopathies. *Biochimica et biophysica acta*, *1739*(2-3), 179–97.

Shang, F., & Taylor, A. (2011). Ubiquitin-proteasome pathway and cellular responses to oxidative stress. *Free radical biology & medicine*, *51*(1), 5–16.

Shipton, O. A., Leitz, J. R., Dworzak, J., Acton, C. E. J., Tunbridge, E. M., Denk, F., Dawson, H. N., et al. (2011). Tau Protein Is Required for Amyloid β-Induced Impairment of Hippocampal Long-Term Potentiation. *J Neurosci.*, *31*(5), 1688–92.

Siegel, G. J., Albers, R. W., Brady, P. D. S. T., & Ph, D. (2006). Basic Neurochemistry MOLECULAR, CELLULAR AND MEDICAL ASPECTS (pp. 1–974).

Singer, S. M., Zainelli, G. M., Norlund, M. A., Lee, J. M., & Muma, N. A. (2002). Transglutaminase bonds in neurofibrillary tangles and paired helical filament tau early in Alzheimer's disease. *Neurochemistry international*, *40*(1), 17–30.

Snyder, E. M., Nong, Y., Almeida, C. G., Paul, S., Moran, T., Choi, E. Y., Nairn, A. C., et al. (2005). Regulation of NMDA receptor trafficking by amyloid-beta. *Nature neuroscience*, *8*(8), 1051–8.

Spires-Jones, T. L., Kopeikina, K. J., Koffie, R. M., De Calignon, A., & Hyman, B. T. (2011). Are tangles as toxic as they look? *Journal of molecular neuroscience : MN*, *45*(3), 438–44.

Stamer, K., Vogel, R., Thies, E., Mandelkow, E., & Mandelkow, E.-M. (2002). Tau blocks traffic of organelles, neurofilaments, and APP vesicles in neurons and enhances oxidative stress. *The Journal of cell biology*, *156*(6), 1051–63.

Supko, J. G., Hickman, R. L., Grever, M. R., & Malspeis, L. (1995). Preclinical pharmacologic evaluation of geldanamycin as an antitumor agent. *Cancer chemotherapy and pharmacology*, *36*(4), 305–15.

Takeda, N., Kishimoto, Y., & Yokota, O. (2012). Pick's disease. *Advances in experimental medicine and biology*, *724*, 300–16.

Taniguchi, S., Suzuki, N., Masuda, M., Hisanaga, S., Iwatsubo, T., Goedert, M., & Hasegawa, M. (2005). Inhibition of heparin-induced tau filament formation by phenothiazines, polyphenols, and porphyrins. *The Journal of biological chemistry*, *280*(9), 7614–23.

Tanzi, R. E., & Bertram, L. (2001). New Frontiers in Alzheimer 's Disease Genetics. *Neuron*, *32*(2), 181–184.

Tung, Y.-T., Wang, B.-J., Hu, M.-K., Hsu, W.-M., Lee, H., Huang, W.-P., & Liao, Y.-F. (2012). Autophagy: a double-edged sword in Alzheimer's disease. *Journal of biosciences*, *37*(1), 157–65.

Turturici, G., Sconzo, G., & Geraci, F. (2011). Hsp70 and its molecular role in nervous system diseases. *Biochemistry research international*, *2011*, 618127.

Vingtdeux, V., Sergeant, N., & Buée, L. (2012). Potential contribution of exosomes to the prion-like propagation of lesions in Alzheimer's disease. *Frontiers in physiology*, *3*(July), 229.

Virshup, D. M., & Shenolikar, S. (2009). From promiscuity to precision: protein phosphatases get a makeover. *Molecular cell*, *33*(5), 537–45.

Volpicelli-daley, L. A., Luk, K. C., Patel, T. P., Tanik, S. A., Dawn, M., Stieber, A., Meany, D. F., et al. (2012). Exogenous α-Synuclein Fibrils Induce Lewy Body Pathology Leading to Synaptic Dysfunction and Neuron Death. *Neuron*, *72*(1), 57–71.

Von Bergen, M, Barghorn, S., Li, L., Marx, a, Biernat, J., Mandelkow, E. M., & Mandelkow, E. (2001). Mutations of tau protein in frontotemporal dementia promote aggregation of paired helical filaments by enhancing local beta-structure. *The Journal of biological chemistry*, *276*(51), 48165–74.

Von Bergen, Martin, Barghorn, S., Müller, S. A., Pickhardt, M., Biernat, J., Mandelkow, E.-M., Davies, P., et al. (2006). The core of tau-paired helical filaments studied by scanning transmission electron microscopy and limited proteolysis. *Biochemistry*, *45*(20), 6446–57.

Waldo, G. S., Standish, B. M., Berendzen, J., & Terwilliger, T. C. (1999). Rapid protein-folding assay using green fluorescent protein. *Nature biotechnology*, *17*(7), 691–5.

Walker, S., Ullman, O., & Stultz, C. M. (2012). Using intramolecular disulfide bonds in tau protein to deduce structural features of aggregation-resistant conformations. *The Journal of biological chemistry*, *287*(12), 9591–600.

Wandinger, S. K., Richter, K., & Buchner, J. (2008). The Hsp90 chaperone machinery. *The Journal of biological chemistry*, *283*(27), 18473–7.

Wang, J.-Z., & Liu, F. (2008). Microtubule-associated protein tau in development, degeneration and protection of neurons. *Progress in neurobiology*, *85*(2), 148–75.

Wang, Y, Cui, J., Sun, X., & Zhang, Y. (2011). Tunneling-nanotube development in astrocytes depends on p53 activation. *Cell death and differentiation*, *18*(4), 732–42.

Wang, Yipeng, & Mandelkow, E. (2012). Degradation of tau protein by autophagy and proteasomal pathways. *Biochemical Society transactions*, *40*(4), 644–52.

Wang, Yipeng, Martinez-Vicente, M., Krüger, U., Kaushik, S., Wong, E., Mandelkow, E.-M., Cuervo, A. M., et al. (2009). Tau fragmentation, aggregation and clearance: the dual role of lysosomal processing. *Human molecular genetics*, *18*(21), 4153–70.

Waxman, E. a, & Giasson, B. I. (2011). Induction of intracellular tau aggregation is promoted by α-synuclein seeds and provides novel insights into the hyperphosphorylation of tau. *The Journal of neuroscience : the official journal of the Society for Neuroscience*, *31*(21), 7604–18.

Waza, M., Adachi, H., Katsuno, M., Minamiyama, M., Tanaka, F., Doyu, M., & Sobue, G. (2006). Modulation of Hsp90 function in neurodegenerative disorders: a molecular-targeted therapy against disease-causing protein. *Journal of molecular medicine*, *84*(8), 635–46.

Weingarten, M. D., Lockwood, A. H., Hwo, S. Y., & Kirschner, M. W. (1975). A protein factor essential for microtubule assembly. *Proceedings of the National Academy of Sciences of the United States of America*, *72*(5), 1858–62.

Wigley, W. C., Stidham, R. D., Smith, N. M., Hunt, J. F., & Thomas, P. J. (2001). Protein solubility and folding monitored in vivo by structural complementation of a genetic marker protein. *Nature biotechnology*, *19*(2), 131–6.

Wischik, C. M., Edwards, P. C., Lai, R. Y., Roth, M., & Harrington, C. R. (1996). Selective inhibition of Alzheimer disease-like tau aggregation by phenothiazines. *Proceedings of the National Academy of Sciences of the United States of America*, *93*(20), 11213–8.

Wu, J. W., Herman, M., Liu, L., Simoes, S., Acker, C. M., Figueroa, H., Steinberg, J. I., et al. (2013). Small misfolded Tau species are internalized via bulk endocytosis and anterogradely and retrogradely transported in neurons. *The Journal of biological chemistry*, *288*(3), 1856–70.

Wyss-Coray, T. (2006). Inflammation in Alzheimer disease: driving force, bystander or beneficial response? *Nature medicine*, *12*(9), 1005–15.

Yan, S. D., Chen, X., Schmidt, A. M., Brett, J., Godman, G., Zou, Y. S., Scott, C. W., et al. (1994). Glycated tau protein in Alzheimer disease: a mechanism for induction of oxidant stress. *Proceedings of the National Academy of Sciences of the United States of America*, *91*(16), 7787–91.

Yankner, B. a, Lu, T., & Loerch, P. (2008). The aging brain. *Annual review of pathology*, *3*, 41–66.

Yin, H., & Kuret, J. (2006). C-terminal truncation modulates both nucleation and extension phases of tau fibrillization. *FEBS letters*, *580*(1), 211–5.

Yorimitsu, T., & Klionsky, D. J. (2005). Autophagy: molecular machinery for self-eating. *Cell death and differentiation*, *12 Suppl 2*, 1542–52.

Young, J. C., Barral, J. M., & Ulrich Hartl, F. (2003). More than folding: localized functions of cytosolic chaperones. *Trends in Biochemical Sciences*, *28*(10), 541–547.

Yu, C.-H., Si, T., Wu, W.-H., Hu, J., Du, J.-T., Zhao, Y.-F., & Li, Y.-M. (2008). O-GlcNAcylation modulates the self-aggregation ability of the fourth microtubule-binding repeat of tau. *Biochemical and biophysical research communications*, *375*(1), 59–62.

Yuan, A., Kumar, A., Peterhoff, C., Duff, K., & Nixon, R. A. (2008). Axonal transport rates in vivo are unaffected by tau deletion or overexpression in mice. *The Journal of neuroscience*, *28*(7), 1682–7.

Yuzwa, S. A., Macauley, M. S., Heinonen, J. E., Shan, X., Dennis, R. J., He, Y., Whitworth, G. E., et al. (2008). A potent mechanism-inspired O-GlcNAcase inhibitor that blocks phosphorylation of tau in vivo. *Nature chemical biology*, *4*(8), 483–90.

Zhang, B., Maiti, A., Shively, S., Lakhani, F., McDonald-Jones, G., Bruce, J., Lee, E. B., et al. (2005). Microtubule-binding drugs offset tau sequestration by stabilizing microtubules and reversing fast axonal transport deficits in a tauopathy model. *Proceedings of the National Academy of Sciences of the United States of America*, *102*(1), 227–31.

Zhang, Y., Thompson, R., Zhang, H., & Xu, H. (2011). APP processing in Alzheimer's disease. *Molecular brain*, *4*(1), 3.

Zheng, H., & Koo, E. H. (2006). The amyloid precursor protein: beyond amyloid. *Molecular neurodegeneration*, *1*(5).

Zheng, J., Baghkhanian, A. M., & Nowick, J. S. (2013). A hydrophobic surface is essential to inhibit the aggregation of a tau-protein-derived hexapeptide. *Journal of the American Chemical Society*, *135*(18), 6846–52.

Zheng, J., Liu, C., Sawaya, M. R., Vadla, B., Khan, S., Woods, R. J., Eisenberg, D., et al. (2011). Macrocyclic β-sheet peptides that inhibit the aggregation of a tau-protein-derived hexapeptide. *Journal of the American Chemical Society*, *133*(9), 3144–57.